



UNIVERSITY OF THE
WITWATERSRAND,
JOHANNESBURG

**Substrate evaluation of the nitrile degrading enzymes from
Rhodococcus rhodochrous ATCC BAA 870**

Adelaide Mashweu (1715870)

A dissertation submitted to the Faculty of Science

University of the Witwatersrand

Johannesburg

In fulfilment for the requirements of the degree of Master of
Science

March 2020

Declaration

I declare that the work presented in this dissertation was carried out extensively by myself under the super-vision of Prof Dean Brady and Prof Moira Bode. It is submitted for the degree of Master of Science at University of the Witwatersrand, Johannesburg. It has not been submitted before for any degree or examination at any other university.



Adelaide Mashweu

Abstract

The focus of this research was the nitrile degrading enzymes nitrile hydratases (NHase) and whole cell nitrilases. NHases and whole cell nitrilases have not been as extensively applied in industry as they could be due to a number of reasons, including missing information relating to their substrate scope. Therefore, this research focussed on exploring the activity of both NHase and whole cell nitrilase towards a number of nitrile compounds. The Groebke-Blackburn-Bienaymé reaction (GBB) and Suzuki-Miyaura coupling reaction were employed to synthesize aromatic nitrile-bearing imidazo[1,2-*a*]pyridine and biaryl compounds respectively. These compounds were of varying sizes and the nitrile group was subjected to different electronic effects through incorporation of different substituents. Vinyl nitrile compounds were synthesized using the Morita-Baylis Hillman reaction (MBH), while simple nitrile compounds were purchased.

The synthesized nitrile-bearing imidazo[1,2-*a*]pyridine compounds were subjected to both NHase and whole cell nitrilase, however, these enzymes were inactive towards these compounds. NHase showed activity towards the biaryl compounds, however, there was complete loss of activity when the biaryl compounds had a 3,4-dimethoxy group as a substituent irrespective of its position relative to the nitrile group. There was also no activity when the 3,4-difluorophenyl group was in the *ortho*-position relative to the nitrile functional group. NHase also showed activity towards the MBH compounds, however, the rate of hydrolysis was slow in comparison with that of the biaryl compounds. NHase was inactive towards one MBH compound bearing a trimethoxyphenyl group as a substituent. Whole cell Nitrilase had no activity towards the MBH compounds and extending the time for hydrolysis resulted in no significant changes.

NHase demonstrated excellent activity towards the simple commercially available nitrile compounds, however, the rate of hydrolysis towards nitrile compounds bearing electron-withdrawing substituents was faster in comparison with those bearing electron-donating substituents.

Acknowledgements

Firstly I would like to thank God for His faithfulness, favour, love and grace for none of this would have been possible if it was not for Him.

Secondly I would like to thank my supervisors Prof Dean Brady and Prof Moira Bode for giving me this opportunity to work with them. I would like to also thank them for always sharing their knowledge with me and for giving me a project that I fell inlove with from Honours.

Thirdly I would like to thank my parents (Kgwaapa Barnabas and Christina Lebedi Mashweu) for their love and support and for believing in me you guys are the best parents one could ever ask for. To my confidants Kagiso and Kgothatso Mashweu you guys inspire me every day to be the better version of myself I love you to bits. To my aunt (Idah Riba) thank you for being a second mom and the big sister I never had.

To my lab mates Charles, Memory, Nompumelelo, Donald, Peter, Mudzuli, Phathu, Kamogelo, Fathima, Bianca, Khanani, Ntombi, Lesotho, Thabo, Wendy, Pious, Songz, Edward, Robin, Aaliyah, Lesotho, Idah thank you guys.

I would like to thank Refilwe, Eric and Thapelo for the Mass spectrometry services.

I would like to thank the Glass blower (Tapuwa) and the store keepers (Ntate Moloto and Baloi).

I would like to thank Varsha Chhiba for supplying us with enzymes.

I would also like to thank the DST/CSIR HCD interprogramme bursary for funding.

List of abbreviations

Arg	Arginine
DMSO	Dimethyl sulfoxide
DME	Dimethoxyethane
EM	Electron microscopy
IAN	Indole-3-acetonitrile
IAA	Indole-3-acetic acid
Cys	Cysteine
Cys-SO ₂ H	Cysteine-sulfinic acid
Cys-SOH	Cysteine-sulfenic acid
PHs	Petroleum Hydrocarbons
HIV	Human Immunodeficiency Virus
Glu	Glutamate
Lys	Lysine
GBB	Groebke-Blackburn-Bienaymé
MBH	Morita-Baylis-Hilman
NHase	Nitrile hydratase
H-NHase	High Molecular weight Nitrile hydratase
L-NHase	Low molecular weight Nitrile hydratase
PE	Pure Enzyme
Phe	Phenylalanine

Pd(PPh ₃) ₄	Tetrakis(triphenylphosphine)palladium
Thr	Threonine
Ser	Serine
Leu	Leucine
E factor	Environmental factor
HRMS	High resolution mass spectrometry
kDa	Kilo Dalton
NMR	Nuclear magnetic resonance
CSIR	Council for Scientific and Industrial Research
DEPT	Distortionless Enhancement by Polarization Transfer
HSQC	Heteronuclear single quantum correlation
TLC	Thin-layer chromatography
IR	Infrared
DMF	Dimethylformamide

Contents

Declaration.....	2
Abstract.....	3
Acknowledgements.....	4
List of abbreviations.....	5
Chapter 1.....	13
1. Introduction	13
1.1 Green chemistry.....	13
1.1.1 Biocatalysis.....	14
1.1.2 Industrial application of enzymes.....	15
1.2 Nitriles.....	16
1.2.1 Nitriles in nature	16
1.2.2 Synthetic nitriles	17
1.2.3 The removal of nitriles from the environment.....	18
1.3 Nitrile-degrading enzymes.....	18
1.3.1 NHase.....	19
1.3.1.1 Structure of NHase.....	19
1.3.1.2 Proposed catalytic mechanisms of NHases	21
1.3.1.3 Applications and limitations of NHase.....	24
1.3.1.4 Substrate preferences	25
1.3.2 Nitrilase.....	28
1.3.2.1 Nitrilase superfamily.....	29
1.3.2.2 Structure of nitrilase	29
1.3.2.3 Nitrilase mechanism	30
1.3.2.4 Nitrilase substrate specificity.....	34
1.3.2.5 Applications of nitrilase	34

1.3.2.6 Difficulties working with nitrilase	36
1.4 Project aims and objectives	36
Chapter 2.....	39
2.0 Results and Discussion	39
2.1 Synthesis of imidazo [1, 2 <i>a</i>] pyridines	39
2.1.1 Synthesis of imidazo[1,2- <i>a</i>]pyridine compounds bearing a nitrile functional group on the aromatic ring	41
2.1.2 Synthesis of imidazo[1,2- <i>a</i>]pyridines bearing an acyclic aliphatic group.....	44
2.1.3 Synthesis of imidazo[1,2- <i>a</i>]pyridines with nitrile on the pyridine ring	47
2.2 Synthesis of biaryl systems containing a nitrile functional group	49
2.3 Synthesis of Morita-Baylis-Hillman (MBH) derivatives.....	58
2.4 NHase and nitrilase activity	62
2.4.1 Standard Reaction.....	62
2.4.2 NHase and nitrilase activity towards imidazo[1,2- <i>a</i>]pyridine compounds bearing a nitrile functional group	63
2.4.3 NHase activity towards biaryl compounds bearing a nitrile functional group.....	67
2.4.4 NHase and nitrilase activity towards MBH compounds (56a-f) bearing a nitrile functional group.....	75
2.4.5 NHase activity towards a range of commercially available nitriles.....	78
2.4.6 Substrate preference of NHase	83
Chapter 3.....	84
3.0 Conclusions and future work	84
Chapter 4.....	86
4. Experimental procedures.....	86
4.1 General laboratory procedures	86
4.2 Experimental procedures.....	86

4.2.1 Groebke-Blackburn-Bienaymé multicomponent reaction general procedure.	87
4.2.1.1 Synthesis of 4-(3-(cyclohexylamino)imidazo[1,2- <i>a</i>]pyridin-2-yl)benzotrile ¹¹¹ (50a)	87
4.2.1.2 Synthesis of 3-(cyclohexylamino)-6-methylimidazo[1,2- <i>a</i>]pyridin-2- yl)benzotrile (50b).....	87
4.2.1.3 Synthesis of 4-(3-(cyclohexylamino)-5-methylimidazo[1,2- <i>a</i>]pyridin-2- yl)benzotrile (50c)	88
4.2.1.4 Synthesis of 4-(5-bromo-3-(cyclohexylamino)imidazo[1,2- <i>a</i>]pyridin-2- yl)benzotrile (50d).....	89
4.2.1.5 Synthesis of 4-(3-(Butylamino)imidazo[1,2- <i>a</i>]pyridin-2-yl)benzotrile (50e)	89
4.2.1.6 Synthesis of 4-(3-(isopropylamino)imidazo[1,2- <i>a</i>]pyridin-2-yl)benzotrile (50f)	90
4.2.1.7 Synthesis of 4-(3-(<i>tert</i> -butylamino)imidazo[1,2- <i>a</i>]pyridin-2-yl)benzotrile ⁹¹ (50h).....	90
4.2.1.8 Synthesis of 4-(3-(pentylamino)imidazo[1,2- <i>a</i>]pyridin-2-yl)benzotrile (50g)...	91
4.2.2 Groebke-Blackburn-Bienaymé multicomponent reaction with 2-cyano-6- aminopyridine as a starting material	91
4.2.2.1 Synthesis of 2-amino-6-cyanopyridine ⁹² (48e)	91
4.2.2.2 Synthesis of 3-(cyclohexylamino)-2-phenylimidazo[1,2- <i>a</i>]pyridine-5-carbonitrile (50i)	92
4.2.2.3 Synthesis of 2-(<i>sec</i> -butyl)-3-(cyclohexylamino)imidazo[1,2- <i>a</i>]pyridine-5- carbonitrile (50j)	92
4.2.3 Suzuki coupling reaction- general procedure	93
4.2.3.1 Synthesis of [1,1'-biphenyl]-4-carbonitrile ⁹⁴ (53a)	93
4.2.3.2 Synthesis of 4'-chloro-[1,1'-biphenyl]-4-carbonitrile ⁹⁸ (53b)	94
4.2.3.3 Synthesis of 3', 4'-dimethoxy-[1,1'-biphenyl]-4-carbonitrile ⁹⁷ (53c).....	94
4.2.3.4 Synthesis of 3',4'-difluoro-[1,1'-biphenyl]-4-carbonitrile ⁹⁵ (53d).....	94

4.2.3.5 Synthesis of 3-fluoro-[1,1'-biphenyl]-4-carbonitrile ⁹⁶ (53e).....	95
4.2.3.6 Synthesis of 3,3',4'-trifluoro-[1,1'-biphenyl]-4-carbonitrile (53f).....	95
4.2.3.7 Synthesis of 4'-chloro-3-fluoro-[1,1'-biphenyl]-4-carbonitrile (53g).....	96
4.2.3.8 Synthesis of 3-fluoro-3',4'-dimethoxy-[1,1'-biphenyl]-4-carbonitrile (53h).....	96
4.2.3.9 Synthesis of [1,1'-biphenyl]-3-carbonitrile ⁹⁹ (53i)	97
4.2.3.10 Synthesis of 3',4'-dimethoxy-[1,1'-biphenyl]-3-carbonitrile (53j)	97
4.2.3.11 Synthesis of 4'-chloro-[1,1'-biphenyl]-3-carbonitrile (53k)	98
4.2.3.12 Synthesis of 3',4'-difluoro-[1,1'-biphenyl]-3-carbonitrile (53l).....	98
4.2.3.13 Synthesis of 3',4,4'-trifluoro-[1,1'-biphenyl]-2-carbonitrile (53m).....	99
4.2.3.14 Synthesis of 4-fluoro-3',4'-dimethoxy-[1,1'-biphenyl]-2-carbonitrile (53n).....	99
4.2.3.15 Synthesis of 6-(4-chlorophenyl)picolinonitrile (53o).....	100
4.2.3.16 Synthesis of 6-(3,4-dimethoxyphenyl)picolinonitrile (53p).....	100
4.2.4 The Morita Baylis-Hillman reaction: general procedure	100
4.2.4.1 Synthesis of 2-(hydroxy(phenyl)methyl)acrylonitrile ¹⁰⁰ (56a).....	101
4.2.4.2 Synthesis of 2-((2-bromophenyl)(hydroxy)methyl)acrylonitrile ¹⁰¹ (56b).....	101
4.2.4.3 Synthesis of 2-(hydroxy(4-methoxyphenyl)methyl)acrylonitrile ³⁶ (56c).....	101
4.2.4.4 Synthesis of 2-((4-chlorophenyl)(hydroxy)methyl)acrylonitrile ¹⁰² (56d)	102
4.2.4.5 Synthesis of 2-((3-bromophenyl)(hydroxy)methyl)acrylonitrile (56e)	102
4.2.4.6 Synthesis of 2-(hydroxy(3,4,5-trimethoxyphenyl)methyl)acrylonitrile ¹⁰² (56f)	102
4.2.5 NHase biocatalysis reaction- general procedure.....	103
4.2.5.1 Synthesis of benzamide ¹⁰⁵ (38).....	103
4.2.5.2 Synthesis of [1,1'-biphenyl]-4-carboxamide ¹¹² (59a)	104
4.2.5.3 Synthesis of 3',4'-difluoro-[1,1'-biphenyl]-4-carboxamide (59d)	104
4.2.5.4 Synthesis of 4'-chloro-[1,1'-biphenyl]-4-carboxamide (59b).....	105
4.2.5.5 Synthesis of 4'-chloro-[1,1'-biphenyl]-4-carboxamide (59e).....	105
4.2.5.6 Synthesis of 3,3',4'-Trifluoro-[1,1'-biphenyl]-4-carboxamide (59f).....	106

4.2.5.7 Synthesis of 4'-Chloro-3-fluoro-[1,1'-biphenyl]-4-carboxamide (59g)	106
4.2.5.8 Synthesis of [1,1'-biphenyl]-3-carboxamide (59i).....	107
4.2.5.9 Synthesis of 3',4'-difluoro-[1,1'-biphenyl]-3-carboxamide (59l)	107
4.2.5.10 Synthesis of 4'-Chloro-[1,1'-biphenyl]-3-carboxamide (59k)	107
4.2.5.11 Synthesis of 6-(4-Chlorophenyl)picolinamide (59o)	108
4.2.5.12 Synthesis of 2-(Hydroxy(phenyl)methyl)acrylamide ¹¹⁰ (60a).....	108
4.2.5.13 Synthesis of 2-((2-Bromophenyl)(hydroxy)methyl)acrylamide (60b)	109
4.2.5.14 Synthesis of 2-(Hydroxy(4-methoxyphenyl)methyl)acrylamide ¹⁰⁹ (60c).....	109
4.2.5.15 Synthesis of 2-((4-Chlorophenyl)(hydroxy)methyl)acrylamide ¹⁰⁸ (60d).....	109
4.2.5.16 Synthesis of 4-Amino-2-bromopyrimidinecarboxamide (74).....	110
4.2.5.17 Synthesis of 2-hydroxybenzamide ¹¹³ (75)	110
4.2.5.18 Synthesis of 2-amino-5-bromobenzamide ¹¹⁴ (76).....	110
4.2.5.19 Synthesis of 3-bromo-4-methylbenzamide ¹¹⁵ (77).....	111
4.2.5.20 Synthesis of 4-methoxybenzamide ¹¹⁶ (78)	111
4.2.5.21 Synthesis of 2-fluoro-5-methylbenzamide (79).....	112
4.2.5.22 Synthesis of 4-bromo-2-fluorobenzamide ¹¹⁷ (80)	112
4.2.5.23 Synthesis of 2-bromo-5-fluorobenzamide (81)	113
4.2.5.24 Synthesis of 3-amino-4-Pyridinecarboxamide ¹¹⁸ (82)	113
4.2.5.25 Synthesis of 4-bromobenzamide ¹¹⁶ (83)	113
4.2.5.26 Synthesis of 3-bromobenzamide ¹¹⁶ (84)	114
4.2.5.27 Synthesis of 6-bromo-2-Pyridinecarboxamide (85).....	114
4.2.5.28 Synthesis of 2-aminobenzamide ¹¹⁹ (86)	115
4.2.6 Nitrilase biocatalytic reaction with whole cell nitrilases (A29 and A99)	115
4.2.6.1 Synthesis of benzoic acid by nitrilase ¹⁰⁴ (58).....	115
References	117
Appendix: ¹ H & ¹³ C NMR spectra	124

Chapter 1

1. Introduction

1.1 Green chemistry

Industrialization revolutionised the world economy, however in the 1940s there were already concerns regarding its impact on the environment.^{1,2} The production of chemicals generated waste, with the pharmaceutical industry being a significant contributor.³ In the 1980s there were concerns regarding the use of toxic reagents in the fine chemical industry.⁴ For example phloroglucinol (pharmaceutical intermediate) production from 2,4,6-trinitrotoluene (human carcinogen) generates chromium-containing waste.⁵ The plant was eventually forced to close when the costs of disposing waste made production uneconomical.⁵ The amounts of waste water and environmental pollutants generated through industrialization led to an appeal to industry to find new technologies for production.⁶

The impact that manufacturing industries have on the environment can be quantified using the E factor (Kg waste/ Kg product) which was introduced by Roger Sheldon.^{7,8} In 1992 he discovered that the pharmaceutical industry had the highest E factor (**Table 1**), as a result of the long and complex synthetic processes which are common.^{4,7-9} The resultant high E factor and low atom economy meant greater production of waste.⁷ The fine chemical and pharmaceutical industry were challenged by the results shown in **Table 1** to find new technologies of production that reduced the waste being generated.⁴ New processes that were cheaper, safer and produced less waste were being looked at as alternatives.^{10,11} Anastas and Warner developed the concept of “Green Chemistry” to promote greener and more sustainable chemical processes.^{7,12}

Table 1: Industrial E factors.^{4,8}

Industry Sector	Tonnage	E Factor (Kg waste/ Kg product)
Oil refining	$10^6 - 10^8$	< 0.1
Bulk chemicals	$10^4 - 10^6$	<1 - 5

Fine chemicals	$10^2 - 10^4$	5 to > 50
Pharmaceuticals	$10 - 10^3$	25 to > 100

Green chemistry has been described as a field that focuses at the molecular level to achieve sustainability.¹² This approach has been recommended to pharmaceutical industries in order to reduce waste production.⁷ Anastas and Warner have postulated 12 principles of green chemistry to assist in minimizing the production of waste and utilization of hazardous chemicals (**Figure 1**).^{1,12,13}

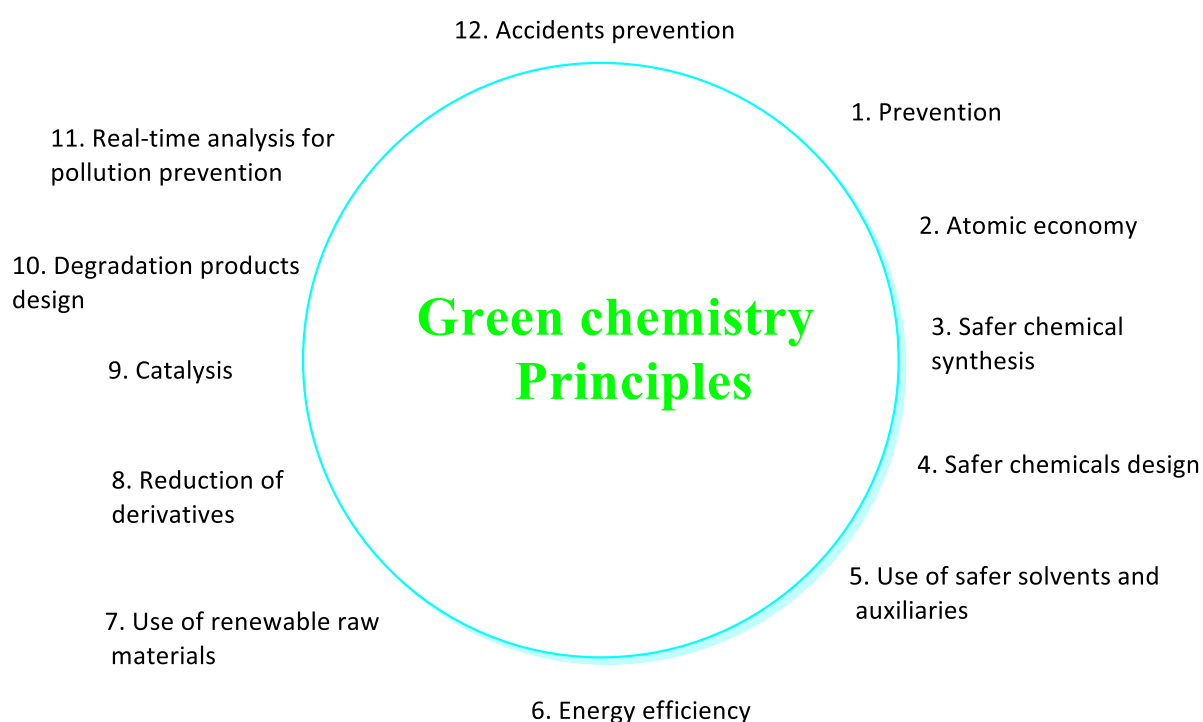


Figure 1: Twelve green chemistry principles.¹

Atom economy and the E factor are two green chemistry metrics that are used to measure the “greenness” of a reaction, and they have become a strategic focus in both industry and academia.^{4,14} Catalysis is an area of focus in minimizing waste production with biocatalysis being one of the best solutions to achieve “Green Chemistry”, as it offers a number of advantages over conventional chemical synthesis.^{1,7}

1.1.1 Biocatalysis

Bommarius has described Biocatalysis as the “generational term for the transformation of natural and non-natural compounds by enzymes”.^{11,15} Biocatalysis involves the application

of enzymes to catalyse chemical reactions.¹¹ This field of research has afforded the pharmaceutical industry an opportunity to transition from conventional chemical synthesis towards enzymatic reactions which offer sustainability, selectivity and are environmentally benign.¹¹ Enzymes are versatile as they are able to bio-transform a wide range of substrates that are structurally different from the substrates they have evolved to bio-transform in nature.^{11,16} The application of enzymes in chemical reactions has received interest due to its ability to reduce waste production and reduce the number of synthetic steps.^{17,18} It also offers regio-, chemo-, and enantio-selectivity which enables the pharmaceutical sector to achieve selectivity.^{17,18} Enzymes also improve reaction safety as they often function under mild conditions in comparison with the conventional chemical synthesis and avoid the use of toxic chemicals.^{7,18} Codexis and Novozymes offer enzyme engineering services and are commercial enzyme providers.⁷ The Presidential Green Chemistry Challenge Award recognises and encourages enzyme applications in chemistry.⁷

1.1.2 Industrial application of enzymes

Enzymes are nature's catalysts derived from renewable resources.¹⁹ Pure enzymes were discovered to be capable of producing non-natural compounds and they have been applied mainly in beverage processing, food and detergent production.²⁰ Enzymes in the textile industry have been acknowledged for replacing harsh chemicals previously being applied in the process.²¹ Enzymes have also been applied in the cosmetics, fine chemical and pharmaceutical sector for the production of chiral compounds.²² The PHs (petroleum hydrocarbons) are a source of energy, however, they are regarded as environmental pollutants when disposed of on land or in water due to spillages.²³ They are also difficult to degrade and enzymes from fungi and bacteria such as cytochrome P450 oxygenases have been used to assist with the degradation.²³

The industrial application of enzymes has frequently been hindered by high costs, enzyme instability, low catalytic efficiency, low solvent tolerance and a lack of the enzyme in a reusable form.^{10,11,16,24} These challenges may be overcome by screening for new enzymes and introducing mutations.^{10,16} In the 1980s and 1990s genetic engineering of enzymes allowed for an increase in their substrate scope, allowing for the bio-transformation of complex substrates.¹⁰ This allowed the more extensive application of enzymes in the manufacture of pharmaceutical intermediates and fine chemicals.¹⁰ However the

appropriate and well characterized enzyme in most cases is not readily available, therefore until recently enzymatic reactions are often considered only when the conventional methods are unable to achieve synthesis of a target compound.²⁴

1.2 Nitriles

1.2.1 Nitriles in nature

Nitriles are widespread in the environment; they are found in both prokaryotic and eukaryotic organisms.^{25,26} Nitriles are abundant in the plant kingdom, with 3-indoleacetonitrile and its derivatives (**1**) functioning as growth hormones (**Figure 2**).²⁷ Compounds **2** and **3** are plant metabolites with cyanoglycosides (**4**) serving as anti-herbivory agents.^{27,28} β -Cyano-L-alanine also functions as an anti-herbivory agent in some plants.²⁹ Nitriles in bacteria are produced by hydrogen cyanide synthase during bacterial growth or based on the level of nutrients.²⁹

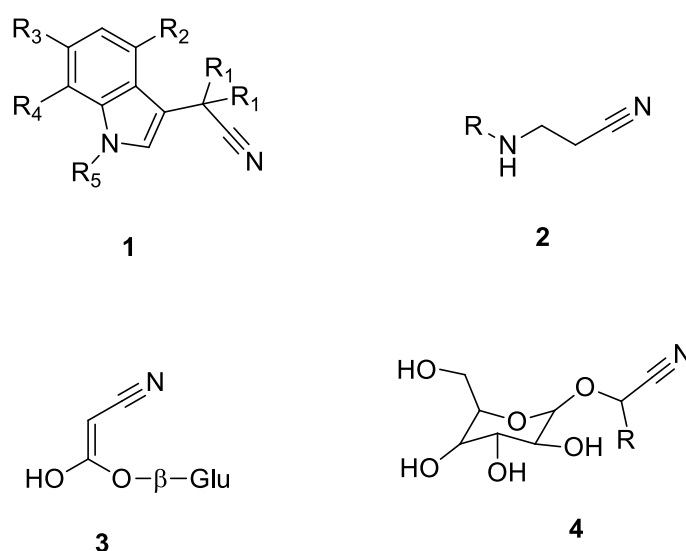


Figure 2: Nitriles found in plants.²⁸

Over 2000 plant species have been identified to contain cyanoglycosides which are the most widespread nitriles.^{26,28} During root exudation nitriles are also released, and as such they have contributed towards the evolution of microbes, which utilize nitriles as a source of carbon and nitrogen.²⁸ Hydrolytic enzymes are used by these microbes for the hydrolysis of the nitrile to a carboxylic acid and ammonia, which form part of their metabolite pool to synthesize the necessary elements.^{28,30}

1.2.2 Synthetic nitriles

Nitriles commonly feature as intermediates in the manufacture of plastics, fibres, pesticides, fine chemicals, amides, carboxylic acids, heterocyclic compounds and pharmaceuticals.^{25,28,31-33} The nitrile functional group is often vital for biological activity as observed in anti-HIV reverse transcriptase inhibitors (rilpivirine (**5**) and fosdevirine (**6**)) and in compounds used to treat cancer (**7**, **8** and **9**) while compound **10** (LR5 182) is used to treat cocaine addiction (**Figure 3**).^{26,34}

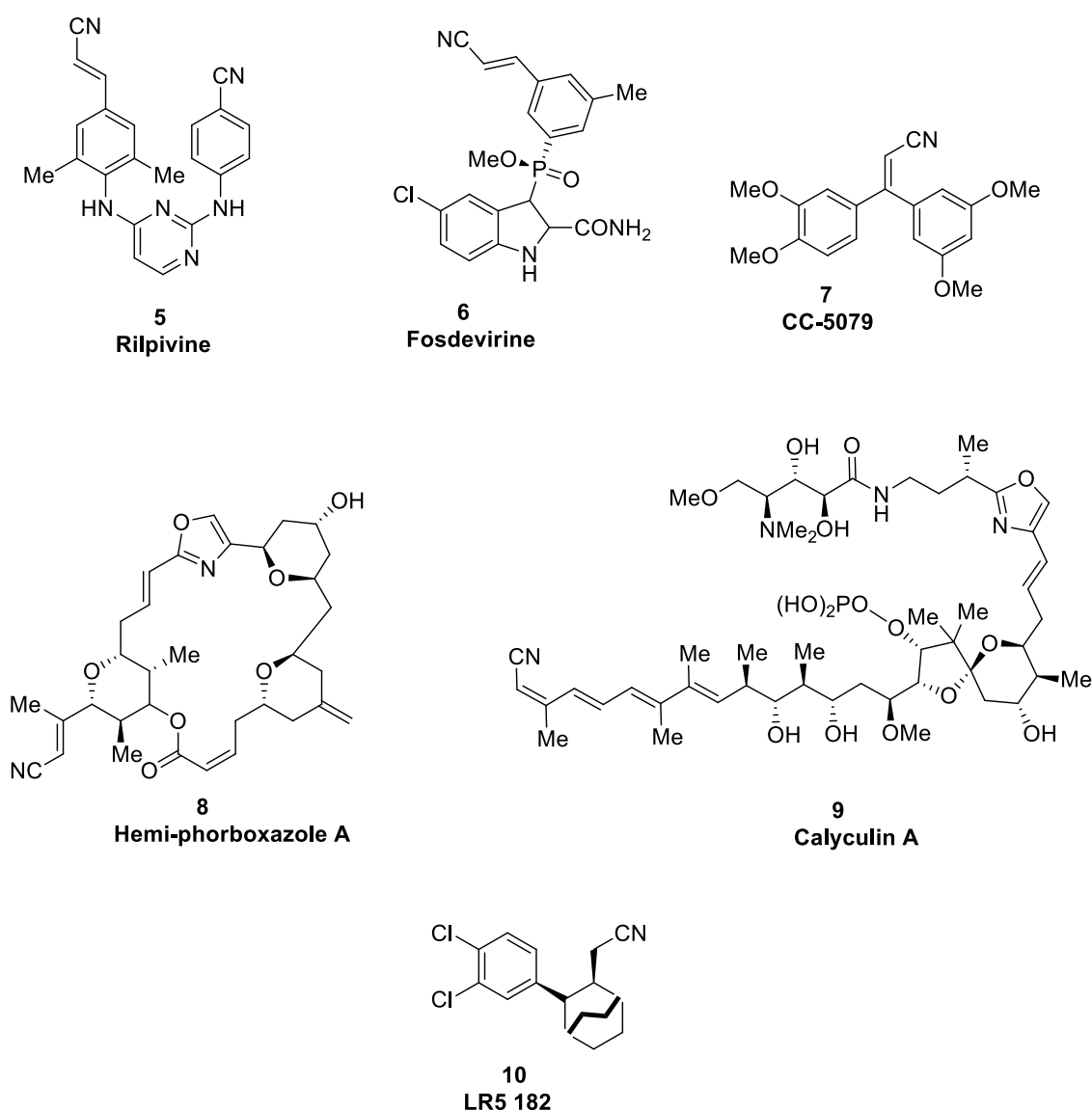


Figure 3: Nitrile group in pharmaceuticals.³⁴

Although nitriles are useful they can be toxic, carcinogenic and mutagenic and therefore may cause environmental problems.^{25,28,35} Acrylonitrile and pesticides (e.g. bromoxynil and

dichlobenil) are now being considered a threat to the environment.^{26,28} Nitrile-containing compounds have been found to form part of the chemical waste that is difficult for industries to dispose of.²⁸ It has also been found that in some instances industrial waste containing toxic nitriles is disposed of either into the sea, or pumped into deep pressure wells below the water table.²⁸

1.2.3 The removal of nitriles from the environment

Nitrile compounds can be eliminated from the environment using physical, chemical and biological methods.³⁵ The chemical hydrolysis of nitriles to their corresponding acids and amides is generally followed to remove the nitriles.^{25,31,32} The chemical hydrolysis, however, produces by-products and inorganic salts as waste.^{25,31,32,36} The microbial (biological) method of hydrolysis is the most widely accepted method due to its mild, low-cost and environmentally friendly characteristics.³⁵ Microorganisms can degrade nitriles by using them as a source of carbon and nitrogen for growth.²⁵ The microbial method of eliminating industrial waste containing toxic nitriles occurs through nitrile-degrading enzymes: nitrilase and nitrile hydratase (NHase).²⁵ The biotechnological potential of nitrile-degrading enzymes has led to isolation of nitrile-degrading bacteria and fungi.³⁷

1.3 Nitrile-degrading enzymes

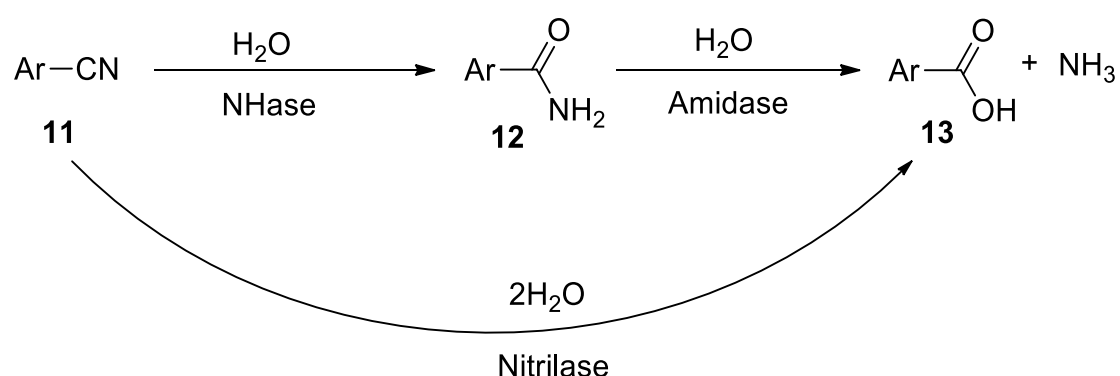
Rhodococcus rhodochrous is a gram-positive aerobic bacterium which is widely distributed in nature.³⁸⁻⁴⁰ Microbes from the *Rhodococcus* genus have varying enzymatic activities thus making them well-equipped for industrial applications.^{38,39} The hydrophobic outer cell wall of Rhodococcal microbes is resistant to a number of solvents and is therefore stable under industrial conditions.³⁹ *R. rhodochrous* has been applied in the industrial production of acrylamide.^{41,42}

R. rhodochrous strain J1 produces both a low and high molecular weight NHase.⁴² *R. rhodochrous* J1, *R. rhodochrous* LL 100-21 and *R. rhodochrous* PA-34 contain both nitrilase and NHase-amidase system.⁴³ These nitrile degrading enzymes can be selectively induced or selectively expressed to obtain the pure enzyme.⁴³ Rhodococcal nitrilase and NHase are the best characterized nitrile degrading enzymes.⁴⁴

A bacterium was isolated from Johannesburg (South Africa) soil samples by Brady *et al.* and was discovered to contain nitrile-degrading enzymes. The bacterium was submitted to the

ATCC culture collection and was designated strain BAA-870.⁴⁴ The BAA-870 strain expresses a single nitrilase (EC 3.5.5.1), as well as a low molecular weight nitrile hydratase (NHase, EC 4.2.1.84), that is associated with an amidase (EC 3.5.1.4).⁴⁴ Due to the strong bio-catalytic activity of NHase and amidase the microbe was observed as a potential biocatalyst.⁴⁴

NHase and nitrilase are responsible for the hydrolysis of nitriles to amides and carboxylic acids, respectively.⁴⁴ Amidase is responsible for the hydrolysis of amides to carboxylic acids as illustrated in **Scheme 1**.⁴⁴



Scheme 1: Nitrile hydrolysis by nitrile-degrading enzymes.⁴⁴

1.3.1 NHase

The first NHase was discovered by Asano *et al.* from an *Arthrobacter* sp. J-1, while the first structure of NHase was determined by Nelson and co-workers.^{28,43,45,46} The *Arthrobacter* sp. J-1 was later reclassified as *R. rhodochrous* J1.⁴³ The discovery of NHase had a high impact in academia and industry by offering synthesis of pure amides in higher yields in comparison with the conventional chemical processes.⁴³ NHases are commonly found in prokaryotes, however, they have recently been reported in a number of unicellular eukaryotes.^{43,47,48}

1.3.1.1 Structure of NHase

Purified NHase generally have molecular masses ranging from 54 to 530 kDa.⁴³ NHase consists of an α (26 kDa) and β (29 kDa) subunit and exists normally as an $\alpha\beta$ (46 kDa) heterodimer or $\alpha_2\beta_2$ (92kDa) heterotetramer.^{28,48-51} NHase functions as an $\alpha\beta$ subunit and fragmentation into individual subunits inactivates the enzyme.²⁸ The first structure of Fe-NHase (tetrameric $\alpha_2\beta_2$) was determined from *Brevibacterium* R 312.²⁸ Fe-NHase from *Rhodococcus* sp. R312 appears as a homotetramer ($\alpha\beta$) as shown in **Figure 4**.⁴⁴

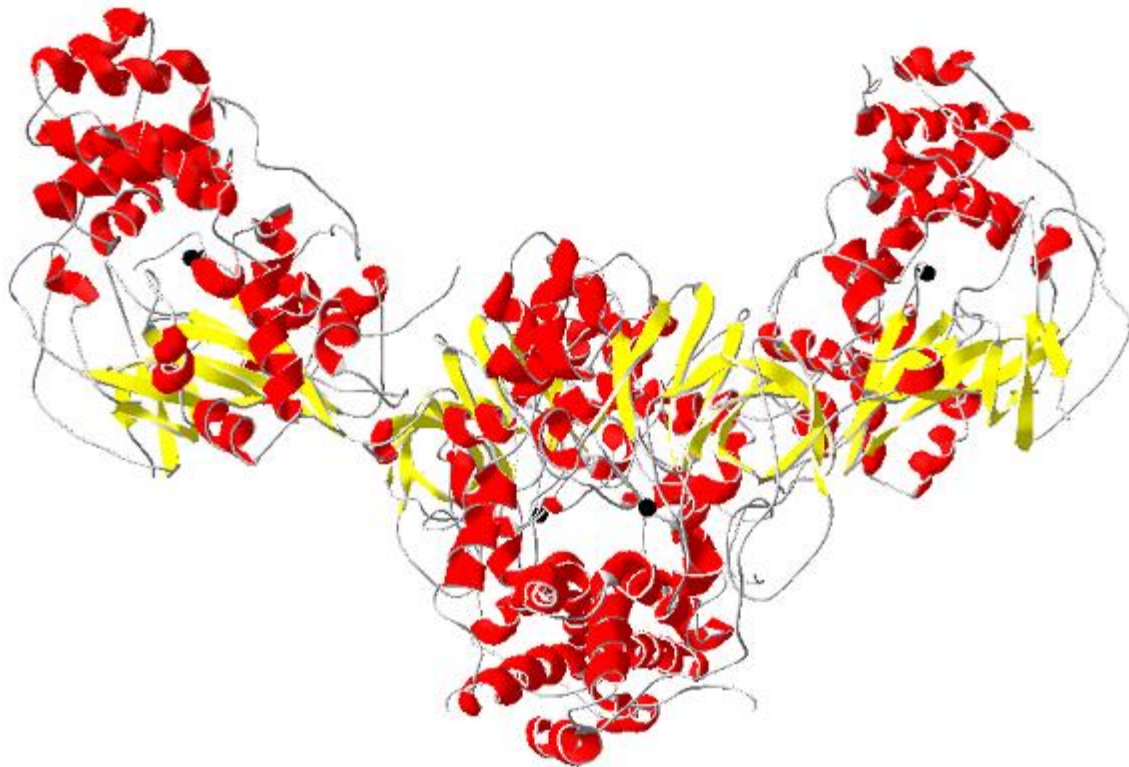


Figure 4: Structure of Fe-NHase from *Rhodococcus* sp. R312 (PDB - 1AHJ).⁴⁴

NHases contain either a low spin iron (Fe^{2+}) or a cobalt (Co^{2+}) metal ion at the catalytic centre, however, an unusual NHase containing Zn^{2+} from *Myrothecium verrucaria* fungus has also been discovered.^{28,43,44,52} Research has been carried out on simple models to understand the role of the metal ions in the hydrolysis of nitriles.²⁸ The metal ion at the catalytic centre is deeply buried at the interface of the α and β subunits.⁵⁰ The catalytic centre of NHases is highly conserved and has a distorted octahedral geometry (**Figure 5**).⁵³ Co^{2+} and Fe^{2+} ion-containing NHases have similar structures, however, it is not yet understood what causes them to incorporate either a Co^{2+} or an Fe^{2+} ion in the active site.⁴³ Substitution studies were carried out in which Fe^{2+} was substituted by Co^{2+} in a Fe-containing NHase from *Rhodococcus* sp. N-771.⁴³ A reduction in NHase activity was observed due to substitution of metal ions, indicating that the two types of NHases are specific in incorporating either a Co^{2+} or Fe^{2+} ion.⁴³

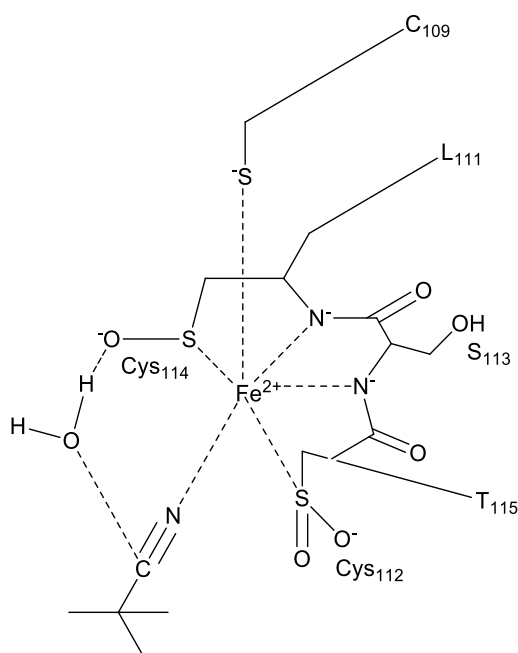


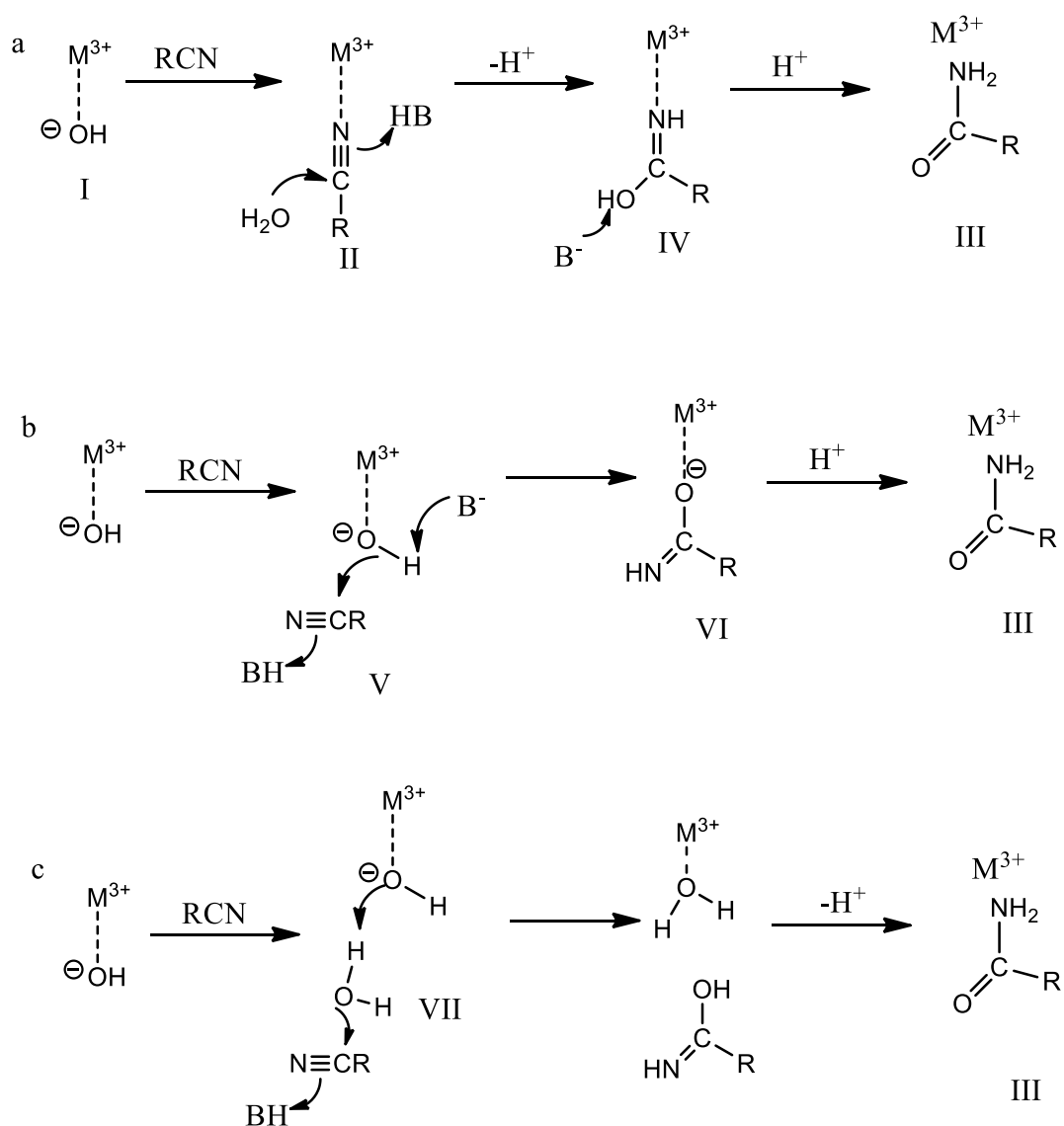
Figure 5: The catalytic centre of NHase.⁵³

The catalytic centre is composed of the following amino acids: Cys₁₀₉-Xxx-Leu₁₁₁-Cys₁₁₂-Ser₁₁₃-Cys₁₁₄ (Xxx is Ser in Fe-type NHase and Thr in Co-type NHase) which are found at the α subunit.⁵¹ The side chains of Cys₁₁₂ and Cys₁₁₄ are post translationally modified by oxidation to cysteine-sulfinic acid (Cys-SO₂H) and cysteine-sulfenic acid (Cys-SOH), respectively, although these modifications are not identified in a crystal structure at low resolution.^{48,53,54} This results in an unusual metal coordination geometry (claw-setting).^{48,53,54} The sixth position (trans to Cys₁₀₉) is available for substrate binding (**Figure 5**).⁵³ NHase's catalytic centre is buried in a protein scaffold, therefore for hydrolysis to occur the substrate must reach the interior, which is postulated to be 15 Å from one of the expected entrances for a Co-type NHase.^{43,55,56}

1.3.1.2 Proposed catalytic mechanisms of NHases

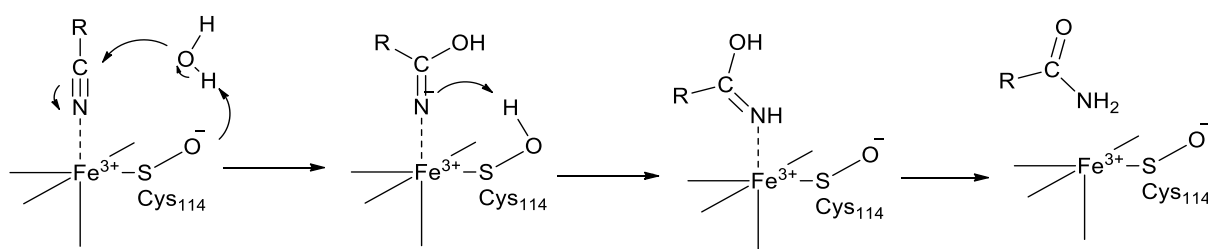
A number of NHase enzymatic mechanisms have been postulated through experimental and computational results, however, the mechanism remains debatable.⁵⁷ Nelson and co-workers have proposed three mechanisms for NHase as illustrated in **Scheme 2**.^{28,45} The first mechanism (**Scheme 2a**) suggests that the coordinated hydroxide (I) is displaced by a nitrile substrate (II) which coordinates to the metal ion followed by hydrolysis.²⁸ An amide (III) is formed through the metal bound iminol intermediate (IV).²⁸ This is known as the inner-sphere mechanism.²⁸ The direct binding of the nitrile nitrogen to the metal ion has been

proposed to increase the electrophilicity of the carbon atom, since the metal ion is proposed to function as a Lewis acid, thus facilitating the nucleophilic attack.^{28,45,52} The second mechanism, known as the outer-sphere mechanism (**Scheme 2b**), involves a nucleophilic attack by the metal-bound hydroxide on a nitrile substrate (V).^{28,57} This generates an iminolate bonded to the metal through oxygen (VI), which rearranges to an amide (III).²⁸ The third mechanism (**Scheme 2c**) proposes that the metal-bound hydroxide deprotonates a water molecule (VII).²⁸ The newly generated hydroxide carries out hydrolysis of the nitrile resulting in the generation of an amide (III).²⁸



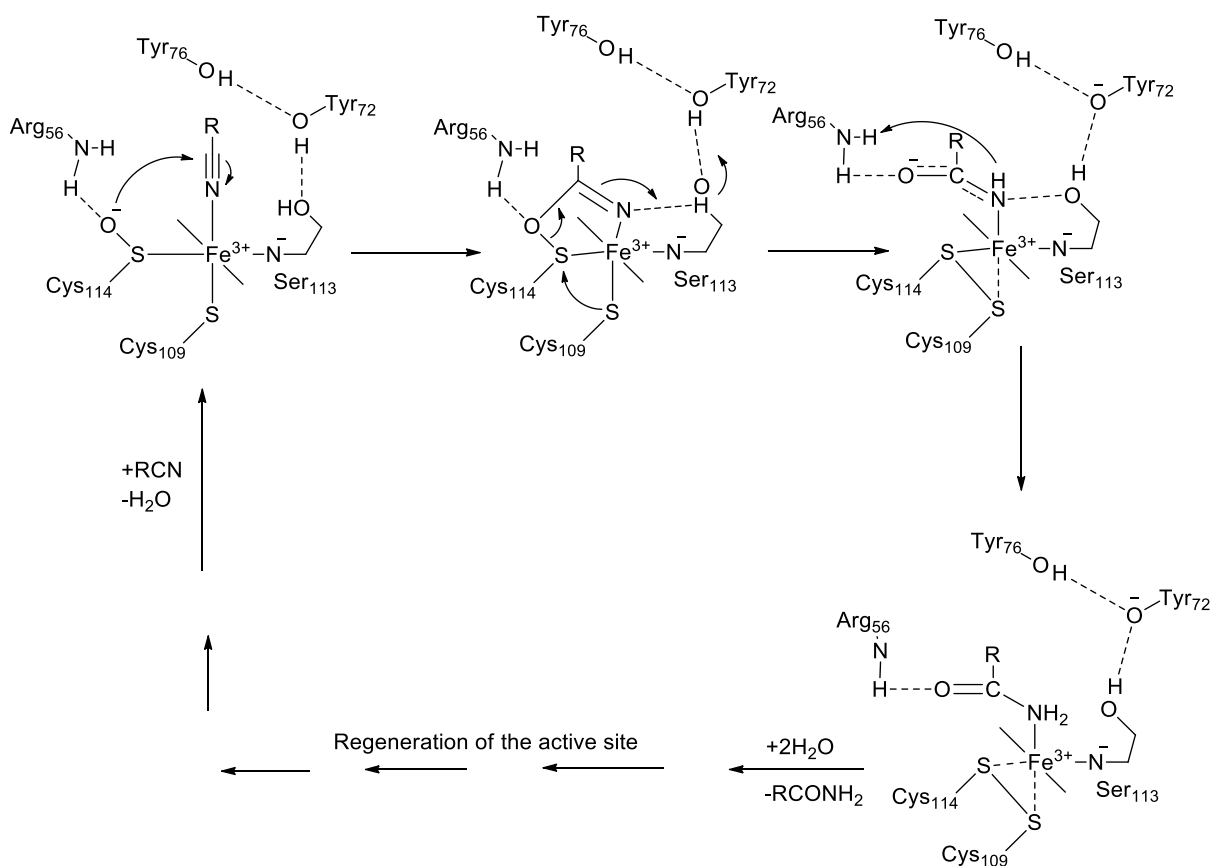
Scheme 2: Postulated enzymatic mechanisms for NHase.²⁸

MacDonald used quantum and molecular mechanics models to study the proposed nucleophilic water mechanism.⁵³ This study suggests that Cys-SO⁻₁₁₄ functions as a base by abstracting a proton from the water molecule as indicated in **Scheme 3**.⁵³ The ionized water molecule then functions as the new nucleophile attacking the nitrile carbon atom.⁵³ The attack is followed by protonation to form an iminol intermediate and tautomerization to form an amide.⁵³ This protonation where a proton attached to Cys-SOH₁₁₄ is transferred to the nitrogen atom of the nitrile regenerates the catalytic centre and leads to the release of an amide.⁵³



Scheme 3: MacDonal's proposed reaction mechanism for NHase.⁵³

A variation of the mechanism proposed by Hopmann suggests that Cys₁₁₄-SO⁻ acts as a nucleophile and attacks the nitrile carbon atom as indicated in **Scheme 4**.⁵⁷ A cyclic intermediate is generated through this nucleophilic attack, however this intermediate is destroyed by the formation of a disulfide bond between Cys₁₁₄ and Cys₁₀₉.⁵⁷ Upon formation of the disulfide bond an oxygen atom from the Cys₁₁₄ side chain is incorporated within the amide group.⁵⁷ The nitrogen atom of the nitrile abstracts a proton from the Arg₅₆ side chain, forming an iminol which is unstable thus resulting in the formation of an amide and regeneration of the catalytic centre.⁵⁷

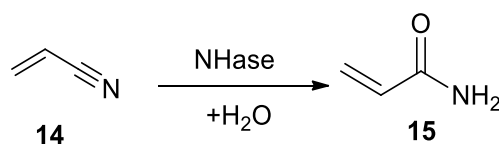


Scheme 4: Proposed reaction mechanism of NHase.⁵⁷

1.3.1.3 Applications and limitations of NHase

Acrylamide has in the past been synthesized using copper salts, however, toxic copper ions and unreacted acrylonitrile waste were generated in the process.⁵⁸ Amides can also be obtained through conventional synthesis at high temperatures under highly acidic or basic conditions.^{47,59} These conditions can often cause the amide to undergo a C-N hydrolysis resulting in formation of a carboxylic acid.⁴⁷

Unlike conventional chemical processes NHase is able to function in an aqueous solution (buffer), at lower temperatures and at physiological pH.^{18,47,60} NHase from *R. rhodochrous* J1 has been applied by Mitsubishi Rayon Corporation, for the industrial production of acrylamide in which 30,000 tons is produced every year.^{18,40,61} Senmin (AECI) from South Africa also applies this bio-catalytic process.³⁹ This was the first biotransformation to be applied in the petrochemical industry.^{18,40,61} Bunch (1998) and Mitsubishi Rayon Japan (2001) have reported that this biocatalytic process already accounted for approximately 25% of the world's total production of acrylamide (**Scheme 5**).⁴³



Scheme 5: NHase hydrolysis of acrylonitrile to acrylamide.⁵³

NHase offers a range of advantages, however, it is not extensively applied in industry due to substrate and product inhibition and the lack of a well characterized NHase, as well as poor stability.^{18,47,62} NHases are specific to the different kinds of nitriles they hydrolyse, therefore it is essential to understand how they select substrates, so that they can be genetically modified to be nonspecific, which will widen their industrial applications.⁵⁵ The solubility of nitriles in aqueous media can limit the activity of NHase, however, organic co-solvents can be used to assist with solubility.⁴⁷ NHase (Co-type) is robust to significant amounts of DMSO and methanol, therefore they can be used as co-solvents.⁴⁷ However, the majority of NHases are thermolabile and operate within the range 20 to 30 °C, with a few being able to operate at 40 °C, 50 °C and 60 °C.⁴³ NHase is able to function within a pH range of 6.5-8.5, however, loss of activity is observed when pH is decreased below 7.⁴³ It has been suggested that this loss might be due to denaturation/ modifications in the ionization of the active site residues or subunit dissociation.⁴³

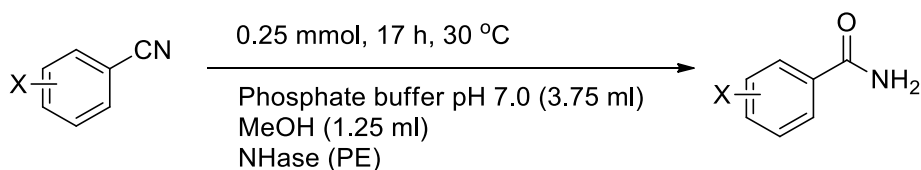
1.3.1.4 Substrate preferences

NHase from *P. chlororaphis* 323 and *Brevibacterium* R 321 contain an Fe²⁺ ion and have high activity towards aliphatic nitriles and low activity towards aromatic nitriles.^{59,63} *R. rhodochrous* J1 produces two types of Co²⁺ ion NHase: low molecular weight NHase (L-NHase) and high molecular weight NHase (H-NHase).⁴⁴ L-NHase has relatively higher activity towards aromatic and heterocyclic nitriles, while H-NHase has relatively higher activity towards aliphatic nitriles.^{43,59,63} NHase from *R. rhodochrous* ATCC BAA 870 is capable of hydrolysing a number of aliphatic and aromatic nitriles, and is structurally similar to the L-NHase.⁶⁴ Notably Co-type NHases are more stable and efficient with a wider substrate scope than the Fe-type NHase.^{28,58} NHases exhibit a broad substrate range, however, they have not been reported to convert any substrates other than nitriles.⁵⁴

It has been proposed that Co-NHase from *Pseudonocardia thermophile* JCM 3095 has a 7Å bottleneck entry channel to the active site, which could limit the hydrolysis of a range of

substrates due to steric hindrance.^{47,56} A study was carried out to investigate the effect of steric hindrance on the activity of pure NHase from *Rhododopseudomonas palustris* CGA009 (**Table 2**).⁴⁷ The results illustrate that the size of *ortho*-substituted groups on the nitrile compounds regulate the activity of NHase.⁴⁷ It was found that *ortho*-substituted methyl (**16**) and bromine (**17**) groups hinder the activity of NHase, however, *ortho*-substituted fluorine (**18**) and chlorine (**19**) do not hinder the activity.⁴⁷ The presence of a trifluoromethyl (**20**), methoxy (**21**) and an ester group (**22**) in the *ortho*-position inhibited activity of NHase. *Para*-substituted methyl (**23**), bromine (**24**), fluorine (**25**) and chlorine (**26**) groups did not hinder the activity of NHase as high amide yields were obtained (**Table 2**).⁴⁷ NHase was also active towards **27**, **28**, **29**, **30** and **31**, with compounds **29-31** carrying a ketone or an ester in the *para*-position.

Table 2: Pure NHase from *Rhododopseudomonas palustris* CGA009 activity towards a range of benzonitrile derivatives.⁴⁷

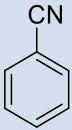
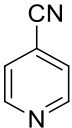
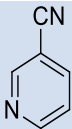
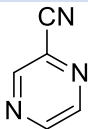
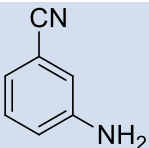


Entry	X	<i>ortho</i> -substituted compound	% Conversion	<i>para</i> -substituted compound	% Conversion
1	Me	16	17	23	>99.9
2	Br	17	5	24	>99
3	F	18	>99.9	25	>99.9
4	Cl	19	95	26	>99
5	CF ₃	20	5	27	>99.9
6	OMe	21	3	28	>99
7	COMe		-	29	>99
8	CO ₂ Me		-	30	98
9	CO ₂ Et	22	0	31	95

It was found that the β Phe37 residue of NHase from *P. thermophile* JCM 3095, was the cause of steric hindrance preventing substrates from interacting with the active site, thus limiting the number of substrates being hydrolysed based on their structure.^{43,65}

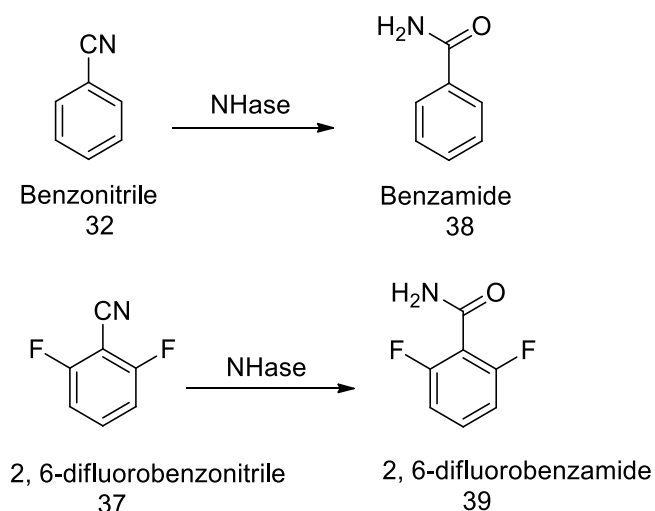
NHase from *Rhodococcus erythropolis* displayed good activity towards benzonitrile (**32**), 4-cyanopyridine (**33**), 3-cyanopyridine (**34**) and pyrazinonitrile (**35**) and was less active towards 3-amino-benzonitrile (**36**) (**Table 3**).⁴¹ The *meta*-substitution of benzonitrile with an amino group reduced the activity of NHase, and was suggested to be due to electron donating effects of the amino group.⁴¹ The *meta*-position on an aromatic nitrile has been known to affect the activity of NHase, as was observed with NHase from *Rhodococcus equi* A4.⁴¹

Table 3: Activity of NHase from *Rhodococcus erythropolis* towards a range of aromatic nitriles.⁴¹

Type of nitrile	Structure	Relative activity
Benzonitrile (32)		105
4-Cyanopyridine (33)		104
3-Cyanopyridine (34)		100
Pyrazinonitrile (35)		94
3-Aminobenzonitrile (36)		56

Bio-transformations of benzonitrile (**32**) and 2,6-difluorobenzonitrile (**37**) by NHase from *R. rhodochrous* J1 resulted in a higher yield of benzamide (**38**) as compared to 2,6-difluorobenzamide (**39**)(**Scheme 6**).⁶³ Mauger *et al.* suggested that the low yield of 2,6-

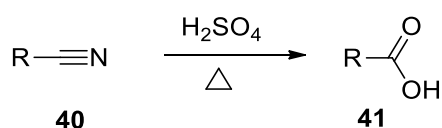
difluorobenzamide (**39**) is due to the two fluorine atoms which introduce some degree of steric hindrance, however, the small size of the fluorine atoms puts this in doubt.⁶³



Scheme 6: Hydrolysis of Benzonitrile and 2,6-difluorobenzonitrile by NHase from *Rhodococcus rhodochrous* J1

1.3.2 Nitrilase

Nitrilases are responsible for the direct hydrolysis of nitriles to carboxylic acids with the release of ammonia (**Scheme 1**).^{32,66} The conventional synthesis of carboxylic acids uses strong acids at high temperatures (**Scheme 7**), however, nitrilase operates under milder conditions.^{24,67}



Scheme 7: Traditional conventional synthesis of carboxylic acids.

Nitrilases are distributed within prokaryotes and eukaryotes, however, they are most commonly found in bacteria (prokaryotes).^{67,68} The first plant nitrilase was discovered in 1958 in barley and was found to catalyse the conversion of indole-3-acetonitrile (IAN) into the plant hormone indole-3-acetic acid (IAA).^{14,40,69} The first bacterial nitrilase to be discovered was ricinine nitrilase, from *Pseudomonas* which was discovered in 1964.^{14,29,69} Bacterial nitrilases were used to elucidate the hydrolytic mechanism, rather than to understand their role in nature.²⁹ The discovery of nitrilases has led to expression patterns being uncovered, thus providing clues in terms of their role in nature.²⁹

1.3.2.1 Nitrilase superfamily

Nitrilase enzymes belong to the nitrilase superfamily which is composed of 13 branches based on sequence identity and catalytic activity.⁶⁹ The nitrilase superfamily is composed of enzymes that hydrolyse the non-peptide C-N bond.^{29,69} Nitrilases, cyanide hydratases and cyanide dehydratase enzymes are structurally related and belong to the 1st branch of the superfamily.^{29,69} The remaining 12 branches have amidase, *N*-acyltransferase and carbamylase activity.⁷⁰ Interestingly, NHase does not belong to this superfamily.⁶⁹

The nitrilase superfamily has a characteristic protein structure with an α - β - β - α sandwich fold, that houses the catalytic triad (glutamic acid, lysine and cysteine) which is responsible for hydrolysis.^{29,71,72} The cysteine residue serves as a point of substrate attachment before hydrolysis.²⁹ Mutating the cysteine residue deactivates nitrilase activity, as observed in *Alcaligenes faecalis* JM3 and *Arabidopsis thaliana*.²⁹ The sulfhydryl group (cysteine) of nitrilase is essential for hydrolysis, thus nitrilases are referred to as thiol enzymes.²⁹

1.3.2.2 Structure of nitrilase

Nitrilase activity is activated depending on environmental conditions and substrate availability, thus they oligomerize to become the active form by forming spirals, as observed using negative stain electron microscopy.^{29,67} Nitrilases lack a metal cofactor and the active enzymes usually exist as homo-oligomers.⁴⁴ There are exceptions, the nitrilase from *Pyrococcus abyssi* exists as an inactive monomer and an active dimer ($\alpha\beta\beta\alpha$ - $\alpha\beta\beta\alpha$), while nitrilase from *R. rhodochrous* PA-34 exists as an active monomer ($\alpha\beta\beta\alpha$).^{29,37,67,73} The nitrilase from *R. rhodochrous* J1 exists as an inactive dimer and as an active decamer.⁷⁴ The preferred size of the oligomers is between 6-26 subunits.^{36,37} Nitrilase from *R. rhodochrous* ATCC BAA 870 forms fibres with a number of sizes as observed through the negative stain EM (**Figure 6**).⁷⁵

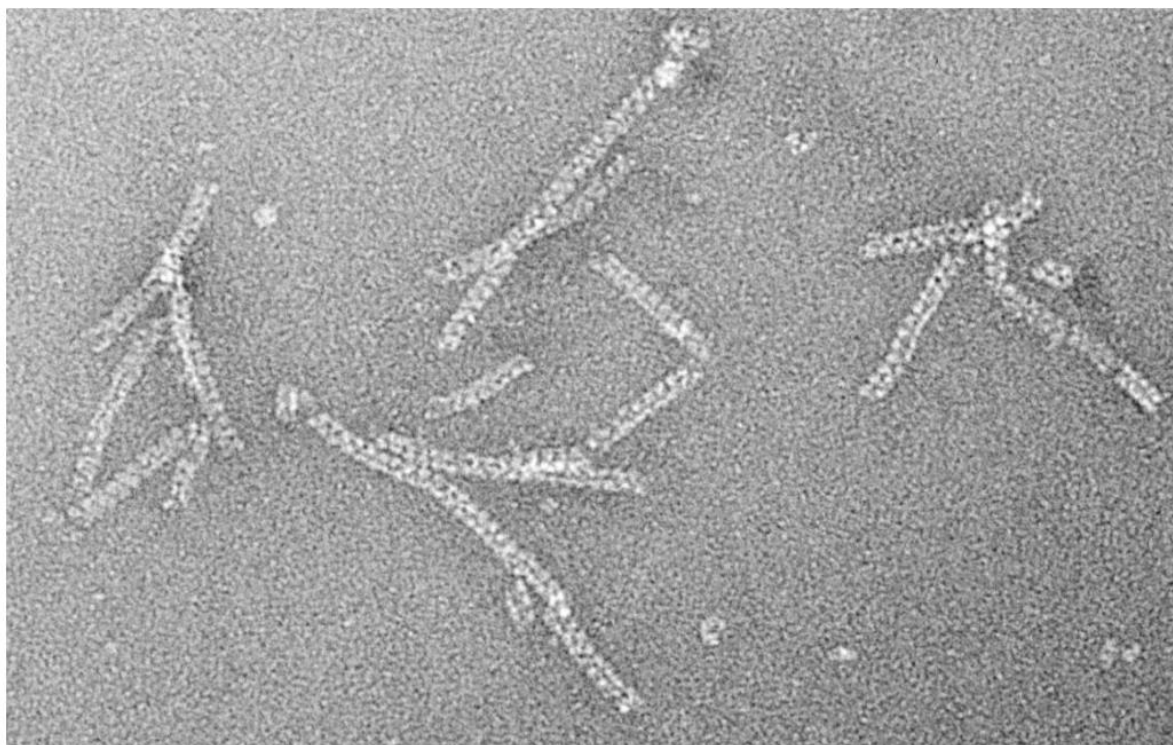


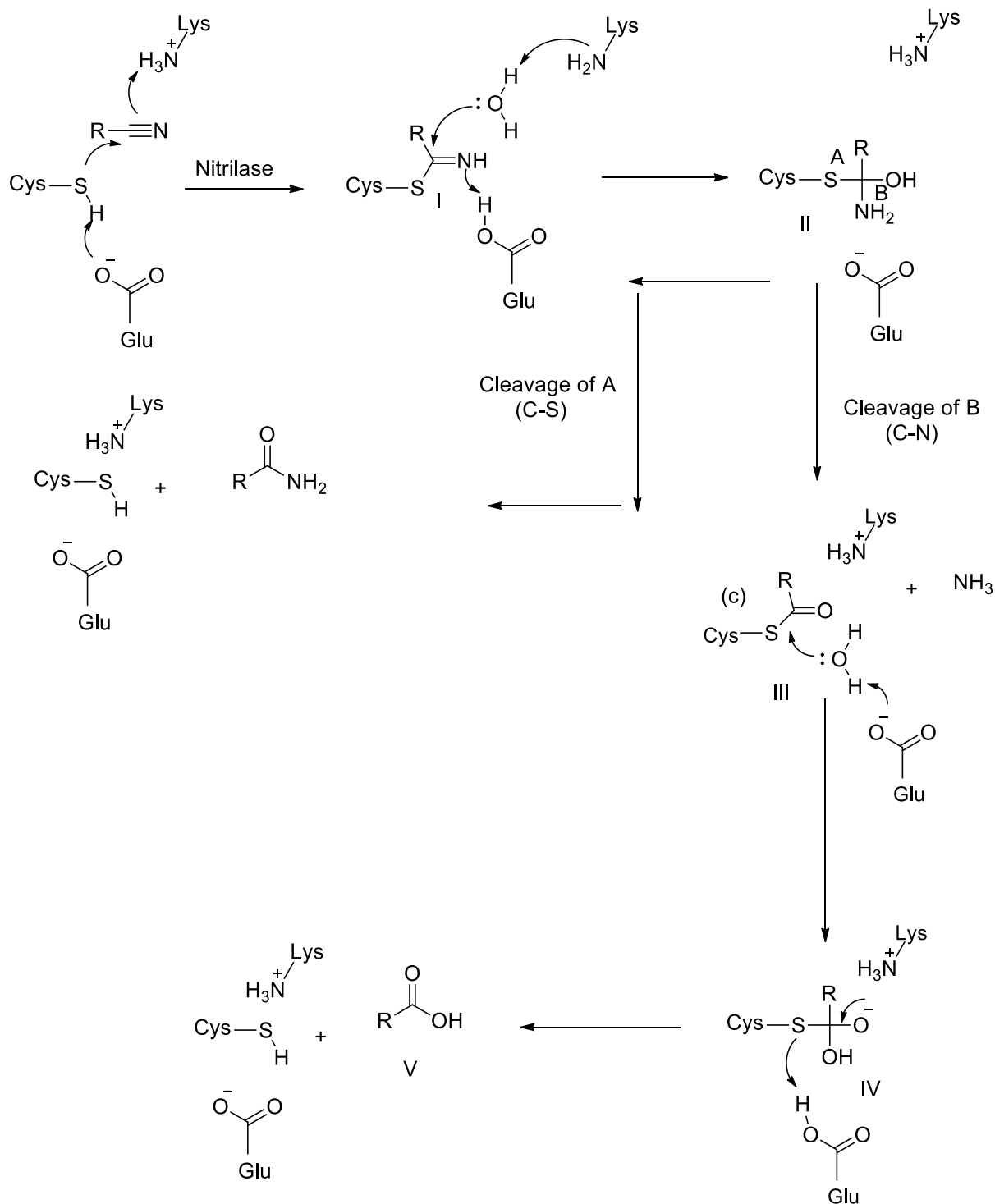
Figure 6: Nitrilase homo-oligomeric fibres from *R. rhodochrous* ATCC BAA 870.^{40,75}

The subunits of nitrilase from *R. rhodochrous* J1 aggregate in the presence of benzonitrile to form the active 410 kDa complex.^{32,37} The bigger the complex size of the active nitrilase the better the activity, as has been observed in Rhodococcal species.⁷⁴ It has been reported that nitrilase from *R. rhodochrous* ATCC BAA 870 is a 96% match to nitrilase from *R. rhodochrous* J1.⁷⁵ The nitrilase from *R. rhodochrous* J1 has been defined as the best characterized nitrilase.⁶⁷

1.3.2.3 Nitrilase mechanism

The proposed nitrilase mechanism shows that glutamate (base) activates the nucleophilic attack on the nitrile carbon atom by the sulfhydryl group (**Scheme 8**).³¹ This leads to the formation of a thioimidate (I).³¹ Lysine also acts as a base by activating the water molecule.³¹ This then attacks the imidate carbon atom leading to the formation of a tetrahedral intermediate (II) which spontaneously breaks down via cleavage at C-S or C-N bonds.³¹ The normal route for nitrilase involves cleavage of the C-N bond to produce the acyl enzyme intermediate (III) and ammonia.³¹ Glutamate activates the second hydrolysis which leads to another tetrahedral intermediate (IV).³¹ This intermediate spontaneously decomposes to give the carboxylic acid (V) and the enzyme.³¹ It has been found that the

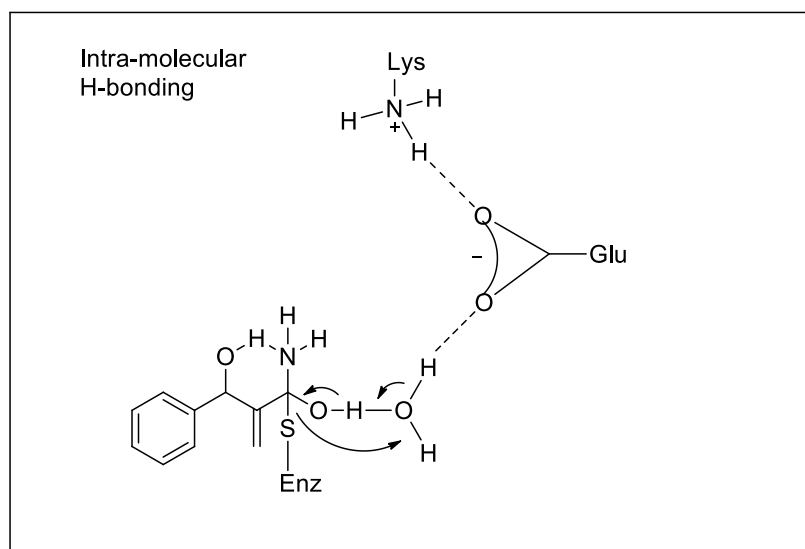
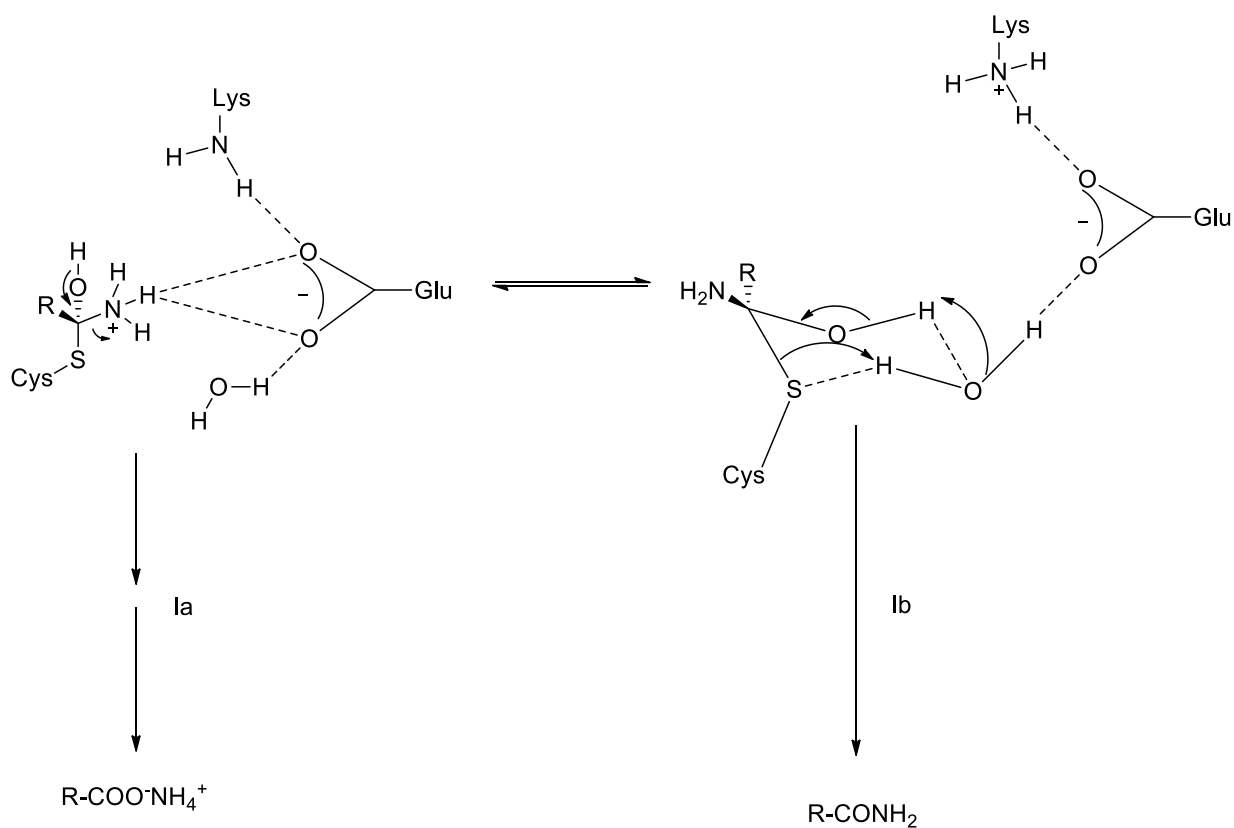
distance between the sulfhydryl group (cysteine) and the nitrile carbon atom of the substrate plays an important role in determining the catalytic activity of nitrilase.^{36,76}



Scheme 8: Proposed reaction mechanism of nitrilase.³¹

Under certain conditions, C-S bond cleavage occurs, giving rise to an amide product (**Scheme 8**).³¹ When the nitrogen atom of the tetrahedral intermediate contains a positive

charge stabilised by the Glu residue (path **IA**), ammonia is released to form the acid as illustrated in **Scheme 9**.³⁶ However, when the positive charge lies on the Lys residue, thiol elimination occurs to form an amide (path **IB**).³⁶ In the presence of an electron withdrawing group at the α -position of a nitrile substrate the intermediate in path **IA** is destabilized, therefore leading to the formation of an amide.³⁶ The quantity of the amide produced may be linked to the extent of destabilisation, through inductive effects at the α -position.³⁶ α -Methylene- β -hydroxy nitriles form hydrogen bonds with the amino moiety through the β -hydroxy group (**Scheme 9**), therefore this leads to increased formation of amides.³⁶ It has been suggested that steric hindrance can weaken the interactions between the charged nitrogen atom and Glu residue in both intermediates.³⁶



Scheme 9: Amide production by nitrilase.³⁶

Piotrowski *et al.* reported for the first time an amide-producing nitrilase from *Arabidopsis thaliana*, which can convert β -cyano-L-alanine to aspartic acid and asparagine (>60%).^{14,77} It has been discovered that the α -carbon configuration of substrates influences the ratio of acid/ amide being generated.¹⁴ Low temperature and increased pH favour amide formation

as opposed to acid formation.¹⁴ Electron-withdrawing substituents at the α -position tend to favour amide formation.^{14,31,36} Nitrilase from *R. rhodochrous* J1 is able to hydrolyse nitriles to carboxylic acids, without formation of amides.⁷⁸ Nitrilase from *Rhodococcus erythropolis* SET1 was able to hydrolyse β -hydroxynitriles lacking an α -substituent and acids were the major products, however, in the presence of an α -vinyl group amides were the major product.³⁶

1.3.2.4 Nitrilase substrate specificity

Nitrilases are classified based on their substrate specificities: aliphatic nitrilase, heterocyclic/aromatic nitrilase and arylacetonitrilases.²⁹ Aromatic nitrilases have been reported to be highly specific for aromatic nitriles.⁶⁷ Aliphatic nitrilases are capable of hydrolysing benzonitriles, however, at a slower rate compared to hydrolysing aliphatic nitriles.⁶⁷ The low molecular mass nitrilase from *R. rhodochrous* J1 is an aromatic nitrilase, in which an amino acid at position 142 is responsible for the substrate specificity.⁶⁹ Aromatic nitrilases from *R. rhodochrous* J1 and *Rhodococcus* NCIMB11216 are flexible as they are capable of hydrolysing acrylonitrile and propionitrile, respectively.⁶⁷ Nitrilase from *Klebsiella pneumoniae* sp. *Ozaenae* is, however, substrate specific.²⁹ Other nitrilases have a broader substrate scope, such as the nitrilase from *Bacillus pallidus* DAC 521, which hydrolyses aromatic, heterocyclic and aliphatic nitriles.²⁹ Nitrilases from fungal species have been found to belong mainly to the aromatic and arylacetonitrilases.⁷⁹

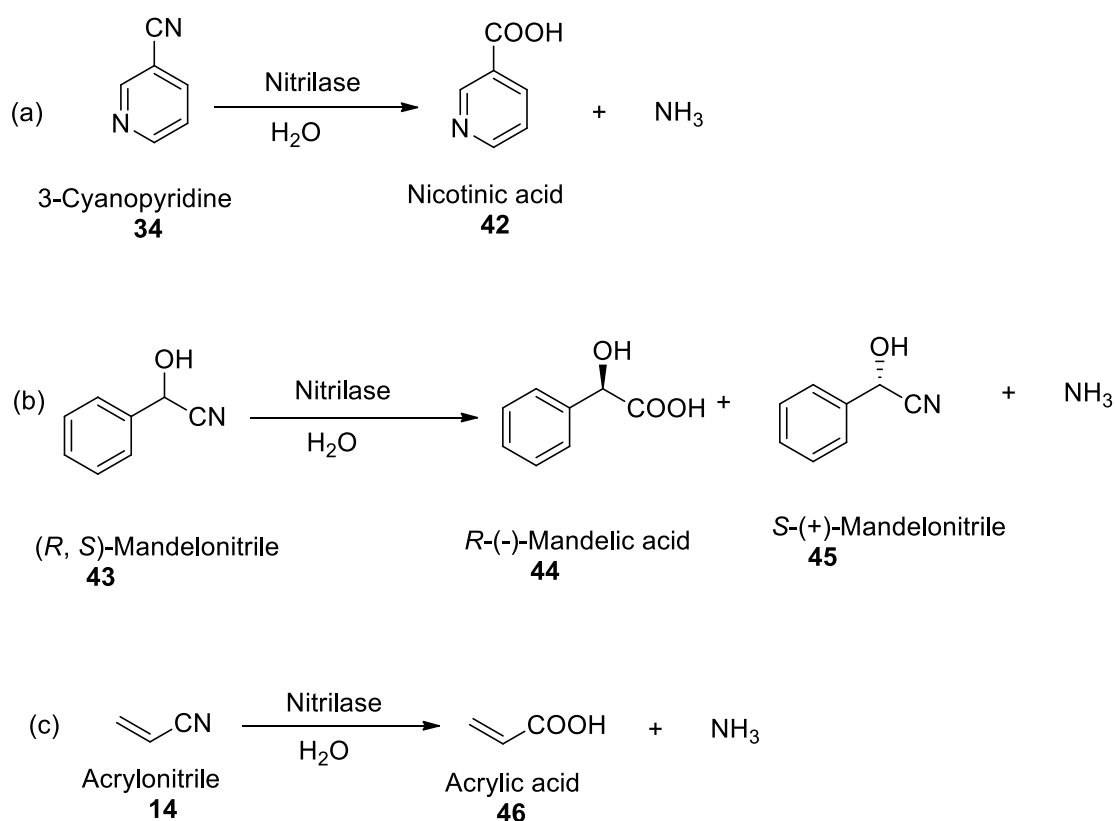
Nitrilases from *R. rhodochrous* J1 and *Rhodococcus* sp. ATCC 39484 prefer aromatic nitriles with *para* and *meta*-substituents (methyl and halogen group), however, they were inactive towards *ortho*-substituted substrates due to steric hindrance.³¹ Nitrilase from *Rhodococcus* NCIMB 11215 was active towards a substrate with fluorine atom in the *ortho*-position.³¹ *R. rhodochrous* K22 was the first strain found to express an aliphatic nitrilase.⁶⁹ Most nitrilases prefer aromatic nitriles as compared to aliphatic nitriles.³²

1.3.2.5 Applications of nitrilase

Nitrilases are of industrial importance due to their ease in hydrolysing nitriles to high-value carboxylic acids.^{79,80} Nitrilases possess enantio- and regio-selectivity, therefore they have

been applied in the pharmaceutical industry.⁶⁸ Nitrilases also have the potential of being applied in industry for bioremediation.¹⁴

Nitrilase, such as that from *R. rhodochrous* ATCC BAA 870 is considered a potential biocatalyst due to its ability to form stable enzyme complexes.⁷⁵ Nitrilase from *R. rhodochrous* J1 has been applied on an industrial scale due to its high hydrolytic activity.^{14,78} Conventional synthesis of nicotinic acid was achieved via ammoxidation and oxidation resulting in generation of by-products and inorganic salts.⁸¹ Synthesis of nicotinic acid by nitrilase was first introduced by Mathew *et al.* and since then it has received attention due to its high conversion rates and mild reaction conditions.^{81,82} Subsequently nitrilase has been applied in industry for the synthesis of nicotinic acid (Lonza) (**Scheme 10a**) and (*R*)-(-)-mandelic acid (**Scheme 10b**) (Mitsubishi rayon, BASF) therefore, it indicates that nitrilase is of great economic impact and further potential.^{14,83}



Scheme 10: Industrial applications of nitrilase.

Acrylic acid (**46**) and its derivatives are used in the textile industry and have been traditionally synthesised by oxidation of propylene which generates by-products together

with inorganic waste.¹⁴ The hydrolysis of acrylonitrile (**14**) to acrylic acid using nitrilase has been considered an appealing option (**Scheme 10c**).¹⁴

1.3.2.6 Difficulties working with nitrilase

A number of pure nitrilases have demonstrated high enantio-selectivity towards compounds of commercial interest, however, pure nitrilases have some drawbacks such as poor stability under industrial conditions, difficulty in separation from the product, and low reusability which limit its applications.⁶⁸ Nitrilases are intracellular enzymes that are sensitive to the outside environment, hence purification of nitrilases is more challenging than for extracellular enzymes.¹⁴ The application of whole cells has some disadvantages because they are able to use low molecular weight aliphatic nitriles and nitrile-containing hydroxyl or amino groups as a source of carbon for their growth thus resulting in low acid yields.⁸⁴

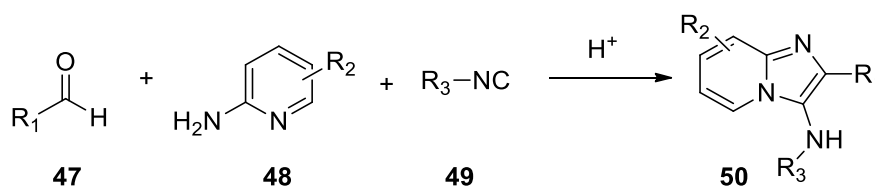
Nitrile degrading enzymes (nitrilase and NHase) are not as extensively applied in industry in comparison with enzymes such as proteases, lipases and amylases.⁴⁴ One of the challenges is that the nitrilase activity is low when compared to conventional synthetic methodologies.¹⁴ The screening of nitrilase-producing strains is still on-going to identify those with greater potential.¹⁴ The substrate scope of nitrilases is narrow, therefore widening the scope would be beneficial for its industrial application.¹⁴ Nitrilase stability should be improved by isolating stable wild-type strains or by engineering the target strain towards desired stability.¹⁴ Nitrilases are inactive at higher temperatures, with nitrilase activity from *R. rhodochrous* J1 decreasing to 7% when incubated at 50 °C for 1 hr.⁶⁶ Nitrilases from mesophilic sources have a narrow substrate scope and low thermal and solvent stability as compared to nitrilase from thermophilic sources.^{14,85} The lack of a proper crystal structure for nitrilase and loss of activity after storage also pose challenges to its industrial application.⁶⁹

1.4 Project aims and objectives

Nitrile degrading enzymes are not as extensively applied in industry as they could be, because they are not yet well understood in terms of their potential and limitations; therefore the aim of this project is to investigate factors which affect the activity of the NHase and nitrilase through substrate profiling. The aim is to test simple commercially available nitriles as well as complex nitriles prepared using a number of different synthetic

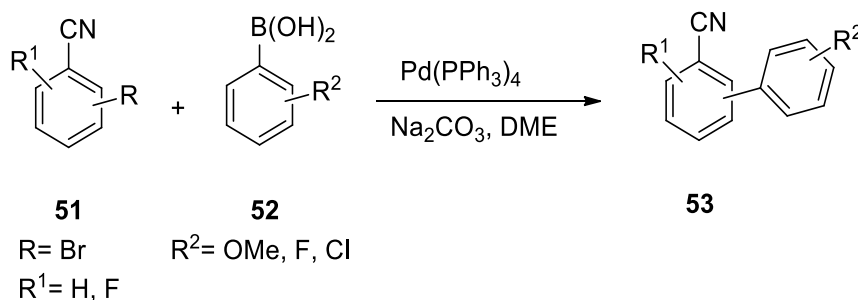
methodologies. In particular, the effect of electron density and steric factors on the activity of NHase and nitrilase will be examined.

The synthetic plan is to firstly use the Groebke-Blackburn-Bienaymé reaction for the preparation of imidazo[1,2-*a*]pyridines bearing a nitrile functional group as illustrated in **Scheme 11**. Reaction of an aldehyde (**47**), 2-aminopyridine (**48**) and isocyanide (**49**) will give rise to imidazo[1,2-*a*]pyridines (**50**).



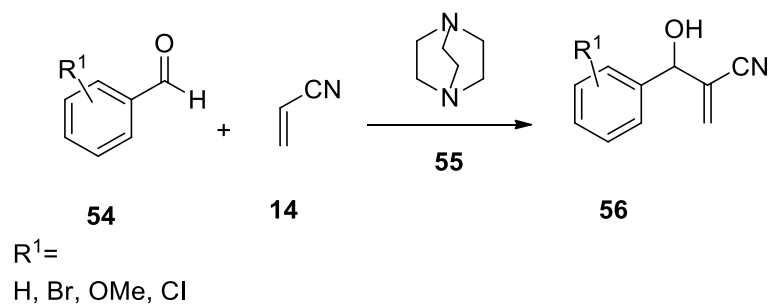
Scheme 11: Groebke-Blackburn-Bienaymé reaction scheme.

Secondly, simple biaryl systems bearing a nitrile group will be synthesized through the Suzuki-Miyaura coupling reaction (**Scheme 12**). In this reaction, a bromobenzonitrile derivative (**51**) will be reacted with boronic acids (**52**) to give the desired biaryl compounds (**53**)



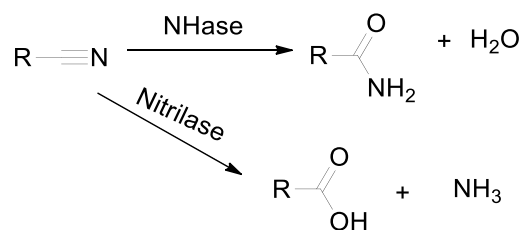
Scheme 12: Suzuki-Miyaura coupling reaction.

Thirdly, vinyl nitriles will be synthesized by using the Morita-Baylis Hillman reaction (**Scheme 13**) where benzaldehyde derivatives (**54**) and acrylonitrile (**14**) will be reacted in the presence of DABCO (**55**) to give MBH adducts (**56**).



Scheme 13: Morita-Baylis Hillman reaction.

After synthesis of the nitrile-containing compounds they will be subjected to NHase and nitrilase enzymes (**Scheme 14**) and activity of the enzymes towards the substrates will be monitored by TLC (thin layer chromatography). Products will be isolated and identified by spectroscopic techniques.



Scheme 14: NHase/ nitrilase reactions.

After testing the synthesized compounds and commercially available nitriles, conclusions will be drawn on the substrates favoured by the enzymes tested.

Chapter 2

2.0 Results and Discussion

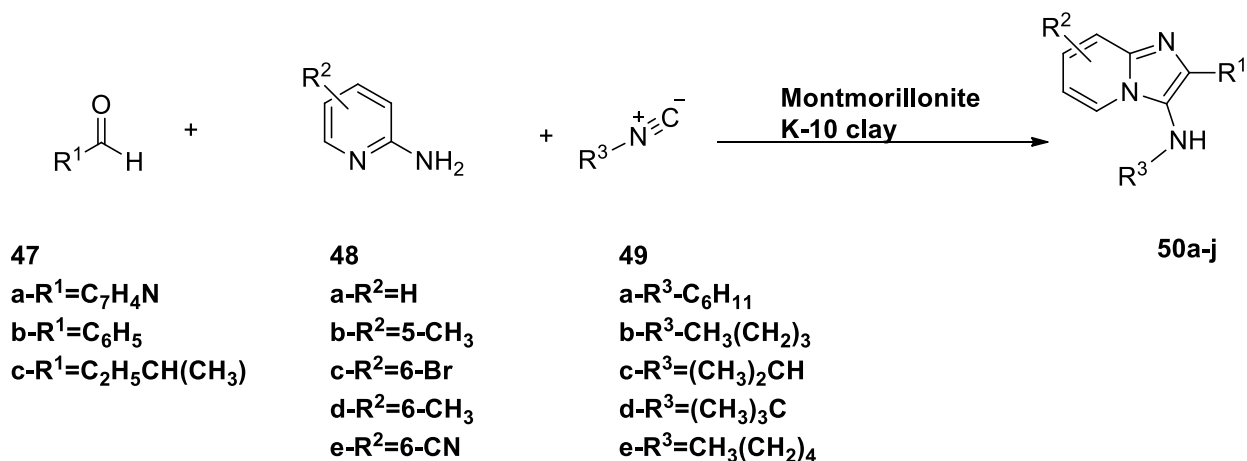
The overall aim of the project was to undertake substrate profiling of the NHase and nitrilase from *R. rhodochrous* ATCC BAA 870. Two effects were investigated: steric bulk and electronic effects. This was done by subjecting various nitrile compounds to NHase and nitrilase and observing the activity in order to fully understand the effect that electron density and steric hindrance have on the enzyme's activity. Both the NHase and nitrilase were tested in order to establish similarities and differences in activity between these two nitrile-degrading enzymes.

Firstly, there was a need to explore the cavity sizes of the enzymes through establishing if they can accommodate bulky nitrile compounds in the active site. This necessitated the synthesis of different nitriles with varying bulk and various substitution patterns. Secondly, the activity of the enzymes towards nitriles of different electron densities needed to be tested. This required synthesis of nitrile compounds with electron-withdrawing and electron-donating substituents.

Synthesis of three different types of compounds was undertaken: imidazo[1,2-*a*]pyridines using the Groebke-Blackburn-Bienaymé (GBB) reaction, biaryl compounds using the Suzuki-Miyaura coupling reaction and finally Morita-Baylis Hillman adducts.

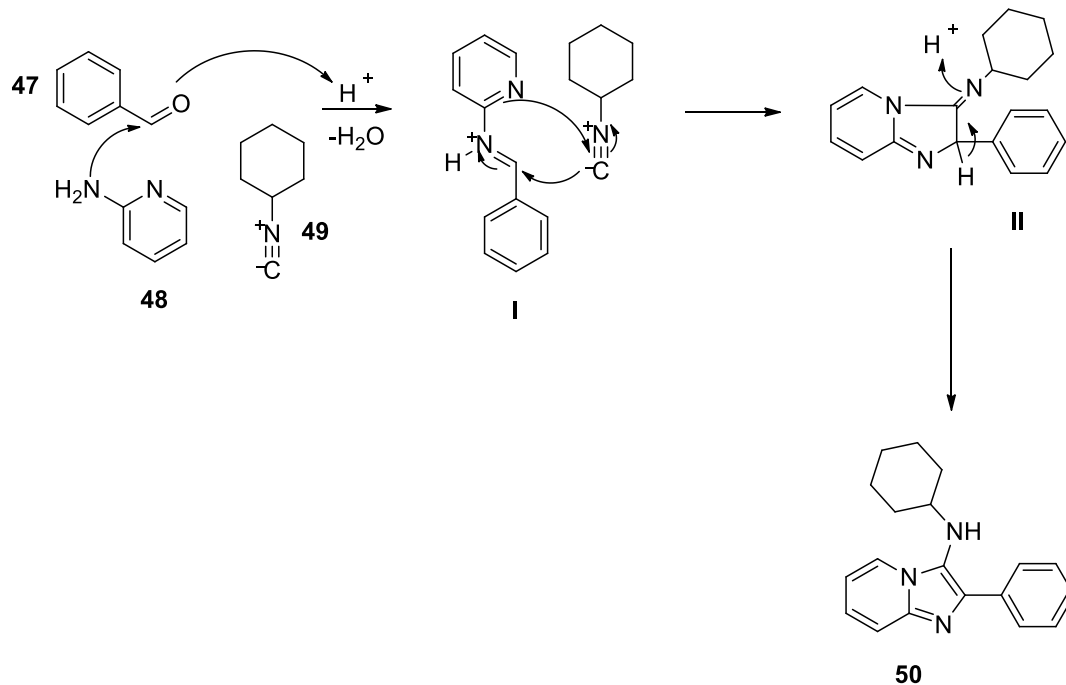
2.1 Synthesis of imidazo [1, 2*a*] pyridines

Synthesis of imidazo[1,2-*a*]pyridines (**50**) involves a reaction between an aldehyde (**47**), isocyanide (**49**) and a 2-aminopyridine (**48**) in the presence of montmorillonite K-10 clay (**Scheme 15**).



Scheme 15: The GBB reaction.

The GBB reaction is initiated via a condensation reaction of an aldehyde (**47**) and 2-aminopyridine (**48**) to give an imine derivative (**I**, **Scheme 16**). A [4+1] (non-concerted) cycloaddition between the protonated imine (**I**) and the isocyanide (**49**) occurs to form an intermediate **II**.^{86,87} The intermediate (**II**) undergoes prototropic shift [1, 3-H shift] to generate the imidazo[1,2-*a*]pyridine (**50**).⁸⁷



Scheme 16: Groebke-Blackburn-Bienaymé reaction mechanism.^{86,87}

2.1.1 Synthesis of imidazo[1,2-*a*]pyridine compounds bearing a nitrile functional group on the aromatic ring

The compounds as indicated in **Figure 7** were synthesized by using different 2-aminopyridine derivatives **48a-d** while the aldehyde (4-formylbenzonitrile **47a**) and the isocyanide (cyclohexyl isocyanide **49a**) were not varied.

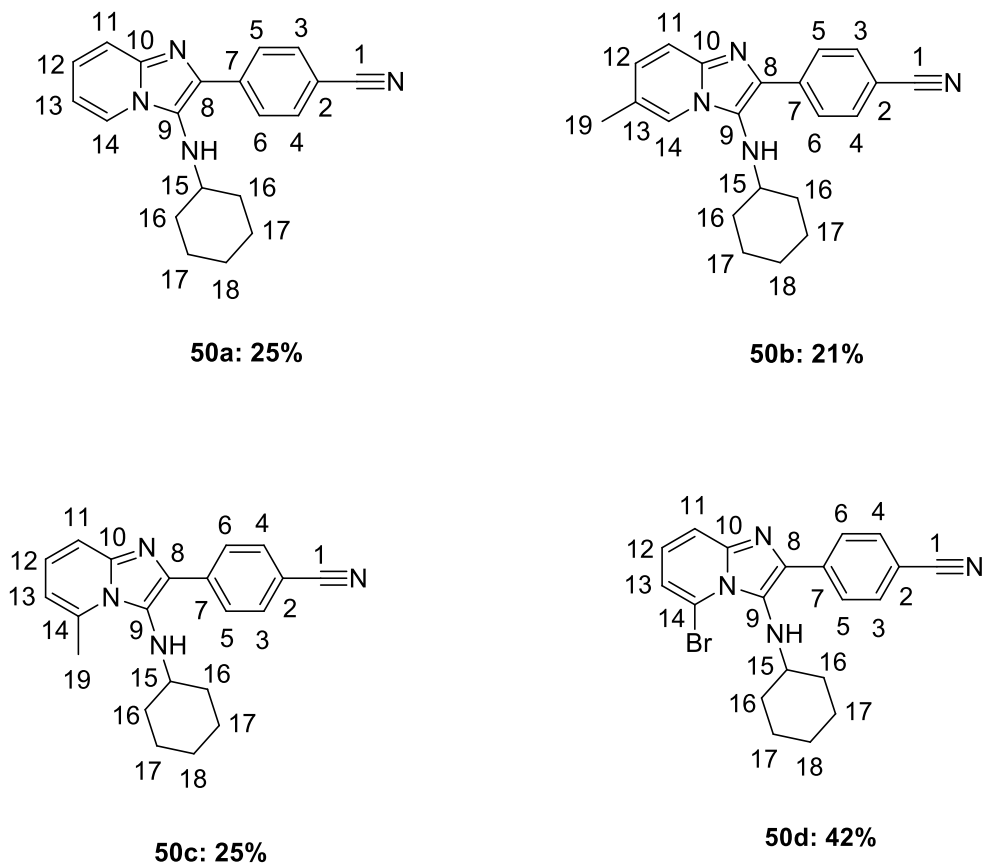


Figure 7: Imidazo[1,2-*a*]pyridines **50a-d** synthesized by variation of 2-aminopyridine derivatives and their isolated yields.

The GBB reaction was performed in 1,4-dioxane in the presence of montmorillonite K-10 clay. Purification of the products (**50a-d**) was challenging as the products co-eluted with the unreacted isocyanide (**49a**) and aldehyde (**47a**) during column chromatography. This challenge was overcome by using flash chromatography eluting with 5 - 15% ethyl acetate/hexane to afford the products. The GBB reaction was low yielding with yields ranging between 21% and 42% (**Figure 7**).

The GBB reaction uses a Lewis or Brønsted acid catalyst to initiate the reaction by increasing the rate of imine formation, however, even in the absence of a catalyst the reaction can still sometimes proceed, depending on the nature of the reagents.⁸⁸ Clay is known to function as a Lewis acid and a Brønsted acid and as such the K-10 clay was incorporated into the reaction to function as a catalyst.^{89,90}

It has been reported that electron rich aldehydes and isocyanides result in low yields being obtained.⁸⁸ Electron-withdrawing substituents on 2-aminopyridine, especially halogens, were previously observed to increase the yield of imidazo[1,2-*a*]pyridines.⁸⁸ This was found to be true for **50d** which has a bromine substituent on the 2-aminopyridine and was synthesized in 42% yield, the highest yield obtained of the 4 compounds prepared. Low yields have also generally been observed for benzaldehydes bearing electron-withdrawing substituents.⁸⁸ The nitrile group is electron withdrawing and this may explain the low yields being obtained for these compounds (**50a-d**).

The imidazo[1,2-*a*]pyridine formation was confirmed by the presence of NH signals for the synthesized compounds (**Table 4**) which did not correlate with ¹³C signals in the HSQC spectra. The signal for H-15 appears close to the NH signal in all the synthesized compounds, with the NH group always being more downfield. However, for compound **50b**, H-15 and the NH group overlap and therefore the signal integrates for 2 protons at δ 3.10 - 2.90. The presence of a signal in the ¹³C NMR spectra ranging between δ 139.8 - 139.1 for C-7 also confirmed formation of the imidazo[1,2-*a*]pyridine. The signal for C-7 always appears downfield when compared to the signal for C-8 in all the synthesized compounds. C-10 is the most deshielded carbon signal in the synthesized imidazo[1,2-*a*]pyridines due to the two adjacent nitrogen atoms, therefore it appears downfield at chemical shifts ranging between δ 144.4 and δ 141.1 as expected.

Table 4: Selected ¹H and ¹³C NMR chemical shifts for compounds **50a-d**.

	H-15	NH	H-3 & H-4	H-5 & H-6	C-7	C-8	C-10	C-1
50a	δ 2.97-2.92 (m, 1H),	δ 3.08 (br s, 1H)	δ 7.75-7.65 (m, 2H)	δ 8.32-8.18 (m, 2H)	δ 139.1	δ 134.5	δ 141.9	δ 119.2

50b		δ 3.10- 2.90 (m, 2H)	δ 7.77- 7.63 (m, 2H)	δ 8.40- 8.15 (m, 2H)	δ 139.3	δ 134.6	δ 141.1	δ 119.3
50c	δ 2.82- 2.72 (m, 1H)	δ 3.07 (s, 1H)	δ 7.78 – 7.63 (m, 2H)	δ 8.26 – 8.11 (m, 2H)	δ 139.8	δ 137.1	δ 143.7	δ 119.3
50d	δ 2.96- 2.86 (m, 1H)	δ 3.72 (d, $J =$ 4.0 Hz, 1H)	δ 7.73 – 7.66 (m, 2H)	δ 8.50 – 8.41 (m, 2H)	δ 139.1	δ 137.2	δ 144.4	δ 119.3

Due to symmetry the protons at H-3 and H-4 are equivalent and hence give one signal. The same is true for protons at H-5 and H-6. The signals for H-3 and H-4 all appear as multiplets as do the signals for H-5 and H-6. It was expected that the signals for H-3 and H-4 and that of H-5 and H-6 should appear as a doublet because each pair is chemically equivalent and only couples with one neighbour. However, the signals appear as multiplets because the protons are magnetically inequivalent, which is as a result of the protons at H-3 and H-4 and those at H-5 and H-6 having a different coupling relationship with the neighbouring proton. The nitrile functional group for the synthesized compounds appears within the range of δ 119.3-119.2, which is as expected for a nitrile signal in ^{13}C NMR spectroscopy. Compounds **50b**, **50c** and **50d** are reported for the first time here.

IR spectroscopy confirmed the presence of a nitrile and an NH functional group in the synthesized compounds (**Table 5**). The presence of a nitrile group was confirmed by the appearance of strong peaks ranging between 2218 cm^{-1} and 2224 cm^{-1} . The presence of an NH group in the compounds was confirmed by the appearance of peaks between 3236 cm^{-1} and 3368 cm^{-1} .

Table 5: Selected IR spectroscopic signals for compounds **50a-d**.

	50a	50b	50c	50d
CN (cm^{-1})	2220 (s)	2219 (s)	2224 (s)	2218 (s)
NH (cm^{-1})	3306 (w)	3236 (s)	3343 (br w)	3368 (s)

* S-strong, W-weak, br-broad

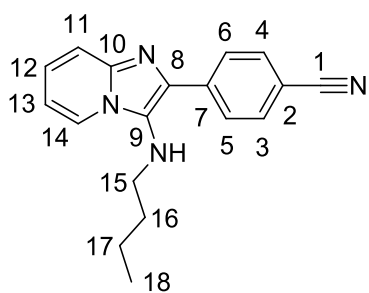
HRMS (m/z) results for **50b-d** further confirmed formation of the products as the masses obtained were as expected (**Table 6**).

Table 6: HRMS results from compounds **50b-d**.

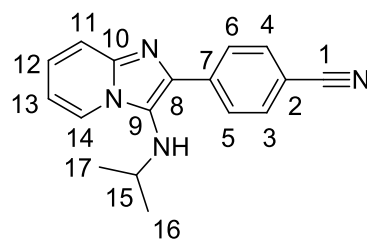
	50b	50c	50d
Expected mass (M + H)⁺	331.1917	331.1917	395.0866
Found mass (M + H)⁺	331.1920	331.1922	395.0868

2.1.2 Synthesis of imidazo[1,2-*a*]pyridines bearing an acyclic aliphatic group

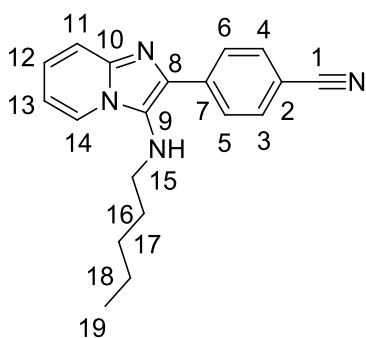
The second group of compounds synthesized had acyclic aliphatic groups in place of the cyclohexyl group. The acyclic aliphatic groups were varied by using long (1-pentyl and butyl) and short (isopropyl and *tert*-butyl) chains (**Figure 8**). Compounds **50e**, **50f** and **50g** are reported here for the first time. Compound **50h** was previously reported by *Shivhare et al.*, and the characterized peaks obtained from ¹H and ¹³C NMR spectroscopy correspond with those previously obtained.⁹¹



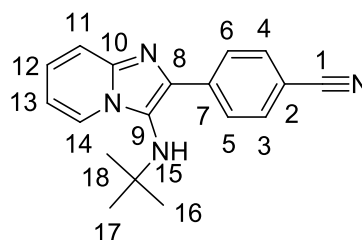
50e: 17%



50f: 22%



50g: 35%



50h: 17%

Figure 8: Synthesized nitrile-bearing imidazo[1,2-*a*]pyridine **50e-h** from the acyclic aliphatic series and their isolated yields.

The preparations of nitrile-bearing imidazo[1,2-*a*]pyridines with an acyclic aliphatic chain were low yielding, with the yield ranging between 17-35% (**Figure 8**). Formation of the compounds was confirmed by the appearance of the NH signal in the ^1H NMR spectra of the synthesized compounds (**Table 7**). The NH signals were identified by being the only protons not showing correlations in the HSQC spectra. The NH signal from **50e** overlaps with the signal for H-15 at δ 3.11-3.02 and integrates for 3 protons, as expected.

The signals for H-3 and H-4 appear at δ 7.69 for **50e** as doublets while the signals for these protons for **50f**, **50g** and **50h** appear as multiplets (**Table 7**). They appear as multiplets due to the effect of magnetic inequivalence as discussed previously. The signal for H-5 and H-6 also appears as a doublet at δ 8.18 for **50e** while the signals for **50f**, **50g** and **50h** appear as multiplets. The nitrile functional group appears at δ 119.2 for all the compounds in the ^{13}C NMR spectra.

Table 7: Selected chemical shifts from ^1H and ^{13}C NMR spectra for compounds **50e-h**.

	NH	H-3 & H-4	H-5 & H-6	C-7	C-8	C-10	CN
50e	δ 3.11-3.02 (m, 3H)	δ 7.69 (d, $J = 8.2$ Hz, 2H)	δ 8.18 (d, $J = 8.2$ Hz, 2H)	δ 139.1	δ 133.8	δ 141.9	δ 119.2
50f	δ 3.07 (d, $J =$ 4.5 Hz, 1H)	δ 7.77-7.63 (m, 2H)	δ 8.32-8.18 (m, 2H)	δ 139.1	δ 134.9	δ 142.0	δ 119.2
50g	δ 3.12-3.10 (m, 1H)	δ 7.73-7.65 (m, 2H)	δ 8.29-8.13 (m, 2H)	δ 139.1	δ 133.8	δ 141.9	δ 119.2
50h	δ 3.02 (s, 1H)	δ 7.82-7.63 (m, 2H)	δ 8.28-8.03 (m, 2H)	δ 140.0	δ 137.5	δ 142.5	δ 119.2

The ^{13}C NMR spectroscopic signal for C-7 appears at δ 139.1 for **50e**, **50f** and **50g** while it appears at δ 140.0 for **50h**. The signal for C-8 appears between δ 133.8 and δ 137.5. The same pattern for **50a-d** is also observed for **50e**, **50f**, **50g** and **50h** in which the signal for C-7 appears downfield as compared to the signal for C-8. The C-10 signal for compounds **50e-h** bearing an acyclic aliphatic group is similar to those bearing a cyclohexyl group (**50a**, **50b**, **50c** and **50d**) as they both appear downfield compared to the other signals.

The peaks from the IR spectra further confirmed the presence of a nitrile group and an NH functional group in the synthesized compounds (**Table 8**). The presence of strong peaks between 2217 cm^{-1} and 2221 cm^{-1} for **50e-g** and a weak peak at 2224 cm^{-1} for **50h** confirmed the presence of a nitrile group in the compounds. The presence of an NH functional group in the compounds was confirmed by the presence of peaks ranging between 3232 cm^{-1} and 3310 cm^{-1} . Results from HRMS were as expected.

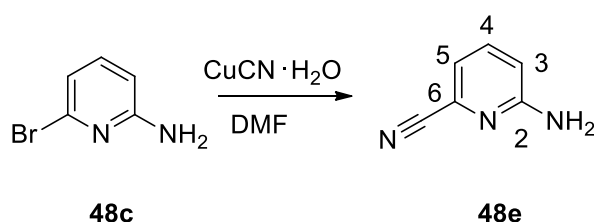
Table 8: IR spectroscopic peaks for the synthesized imidazo[1,2-*a*]pyridines bearing an acyclic aliphatic group.

	50e	50f	50g	50h
NH(cm^{-1})	3310 (s)	3245 (s)	3232 (s)	3280 (w)
CN(cm^{-1})	2217 (s)	2220 (s)	2221 (s)	2224 (w)

*S-strong, W-weak

2.1.3 Synthesis of imidazo[1,2-*a*]pyridines with nitrile on the pyridine ring

In order to change the position of the nitrile group, cyanation was done on 2-amino-6-bromopyridine (**48c**) to form 2-amino-6-cyanopyridine (**48e**) (**Scheme 17**) which will serve as a new starting material replacing 2-aminopyridine in the GBB reaction. This reaction was allowed to react overnight but was very low yielding with only 5% of the product being obtained. TLC analysis of the reaction mixture showed only one spot which appeared as a fluorescent blue colour under the UV lamp. This spot was identified as 2-amino-6-cyanopyridine (**48e**).



Scheme 17: Cyanation of 2-bromo-6-aminopyridine.

The low yield of the 2-amino-6-cyanopyridine (**48e**) and the inability to trace 2-amino-6-bromopyridine (**48c**) in the organic layer indicates that either or both 2-amino-6-bromopyridine and 2-amino-6-cyanopyridine might be complexing with the copper from CuCN.H₂O and migrating to the aqueous layer during the liquid-liquid extraction (ethyl acetate/ water). The aqueous layer was, however, not analyzed by TLC to verify this. Perhaps a different catalyst needs to be used to replace CuCN.H₂O and observe how that affects the yields obtained.

The synthesis of 2-amino-6-cyanopyridine (**48e**) was confirmed by the presence of a signal at δ 118.0 in the ¹³C NMR spectrum corresponding to the nitrile group, indicating that cyanation was successful. The ¹H NMR spectrum showed a signal at δ 7.51 appearing as a doublet of doublets with a coupling constant of $J = 8.6, 7.1$ Hz indicating its coupling to 2 *ortho* protons. This was assigned as H-4, which couples to H-3 and H-5. The signals at δ 7.02 and δ 6.71 were assigned as protons H-5 and H-3, respectively, as assisted by the HMBC spectra. A broad signal at δ 6.55 integrating for 2 protons was assigned as protons from the NH₂ group. The proton at H-4 is directly bonded to the carbon at δ 137.9 as observed from the HSQC spectrum. The protons appearing at δ 7.02 and δ 6.71 are directly bonded to the carbons appearing at δ 117.1 and δ 113.1, respectively, as observed from the HSQC

spectrum. Compound **48e** has been reported before in the literature by *Bode et al.*, and the characteristic signals reported from the ^1H NMR spectrum are similar to the signals obtained here.⁹²

Compound **48e** was used in the GBB reaction to synthesize the novel modified nitrile-bearing imidazo[1,2-*a*]pyridine compounds **50i** and **50j** (**Figure 9**) which were synthesized in low yields.

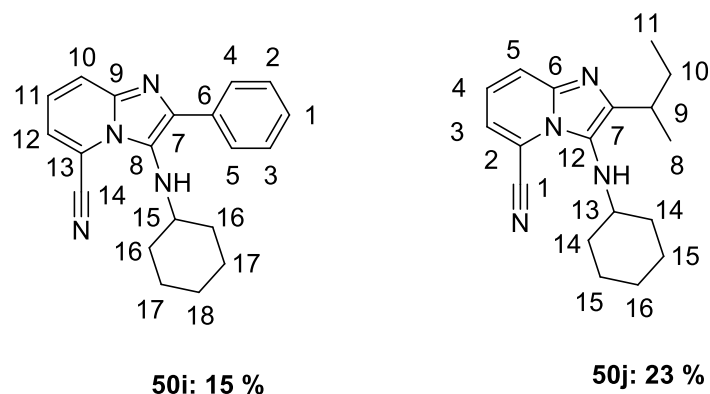


Figure 9: Modified nitrile bearing imidazo[1,2-*a*]pyridine compounds and their isolated yields.

Formation of the compounds was confirmed by the presence of an NH signal in the ^1H NMR spectrum at δ 3.37 as a doublet for **50i** and δ 2.93-2.88 which occurs as a multiplet for **50j**. The presence of a signal for C-7 at δ 133.4 in the ^{13}C NMR spectrum for **50i** and δ 141.3 for **50j** also confirmed formation of the compounds. The nitrile functional group appears at δ 114.3 for **50j** and δ 114.2 for **50i** (**Table 9**).

Table 9: ^1H and ^{13}C chemical shifts for modified nitrile-bearing imidazo[1,2-*a*]pyridine compounds **50i-j**.

	NH	CN	C-7
50i	δ 3.37 (d, $J = 4.9$ Hz, 1H)	δ 114.2	δ 133.4
50j	δ 2.93-2.88 (m, 1H)	δ 114.3	δ 141.3

The HRMS results for these compounds were as expected (**Table 10**).

Table 10: HRMS (m/z) results for the novel modified imidazo[1,2-*a*]pyridines (**50i-j**).

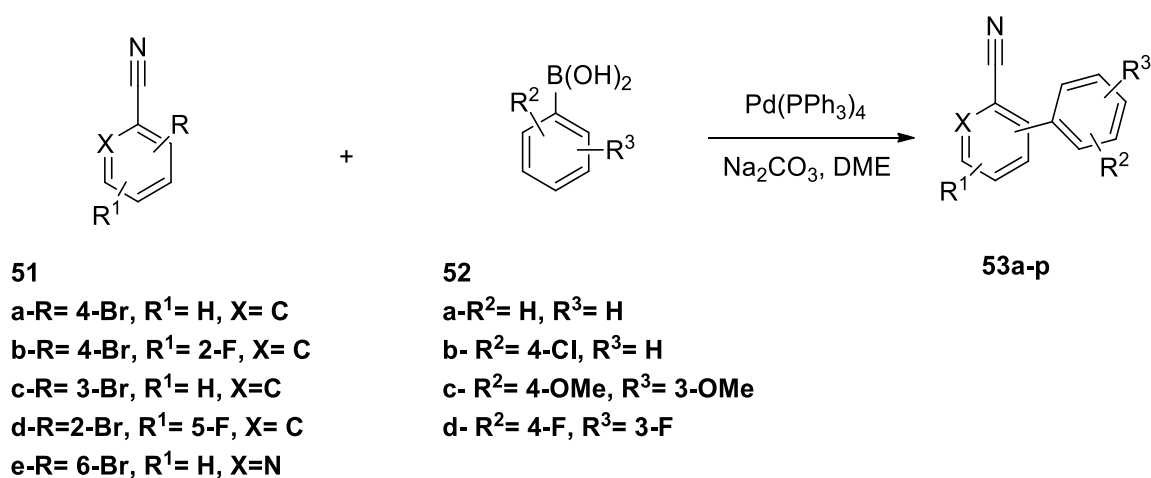
	50i	50j
Expected mass (M + H)⁺	317.1761	297.2074
Found mass (M + H)⁺:	317.1764	297.2077

IR spectroscopy confirmed the presence of an NH functional group by the presence of a weak signal at 3376 cm⁻¹ for **50i** and 3333 cm⁻¹ for **50j**. The presence of the nitrile group was confirmed by the appearance of a weak signal at 2216 cm⁻¹ for **50i** and 2219 cm⁻¹ for **50j**.

The GBB reaction was used to successfully synthesize **50i** and **50j**, however, they were prone to decomposition. After using flash chromatography to isolate the product only one spot corresponding to the product was observed, however when spotted the following day multiple spots were observed. In order to slow the rate of decomposition the compounds were kept in the dark in a -18 °C freezer.

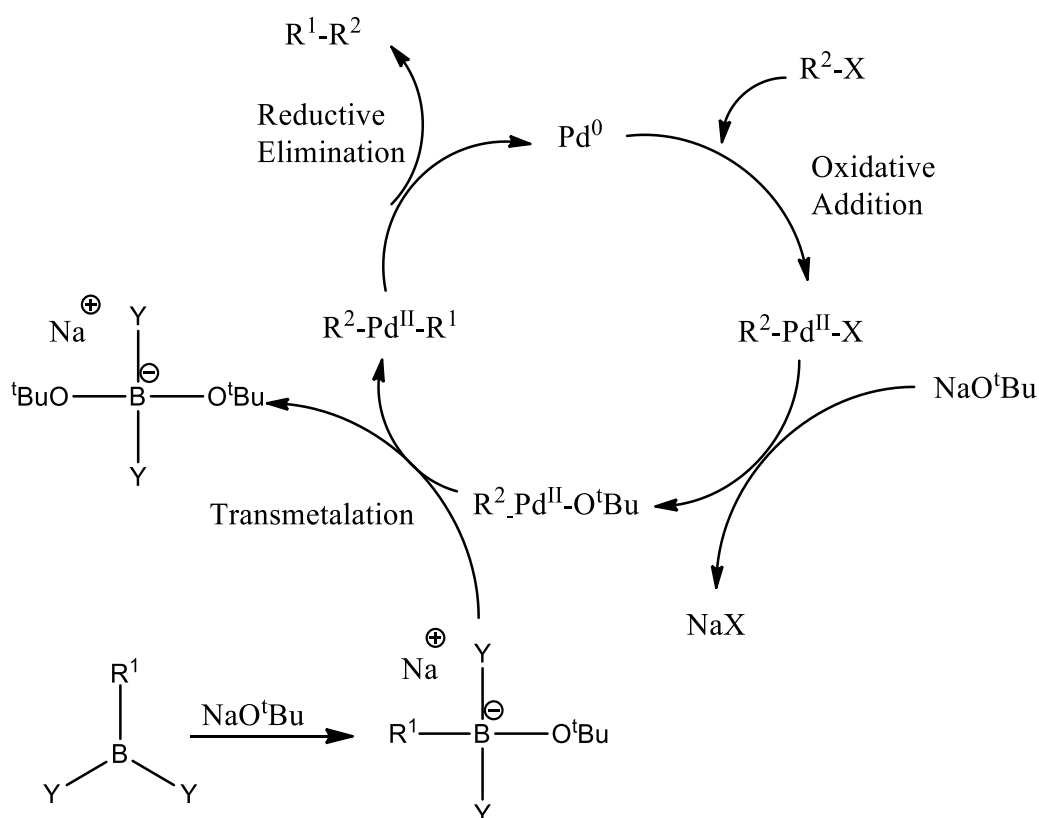
2.2 Synthesis of biaryl systems containing a nitrile functional group

The Suzuki-Miyaura coupling reaction was employed to synthesize nitrile-bearing simple biaryl compounds (**53**) (**Scheme 18**). The reaction was catalyzed by Pd(PPh₃)₄ which was freshly prepared in our laboratory. Pd(PPh₃)₄ is prone to decomposition if left open and exposed to sunlight for long durations. It turns from yellow to an orange colour indicating decomposition, however, it can still be used although it has to be used in larger quantities for catalysis to occur. Therefore, immediately after preparation it was placed in a vial that was covered with a foil and stored in the dark in a -18 °C freezer to avoid decomposition.



Scheme 18: Suzuki-Miyaura coupling reaction.

The Suzuki-Miyaura coupling reaction is initiated by Pd being in an oxidation state of "0". Pd (II) species need to be reduced *in situ* to an oxidation state of "0" for catalysis to occur, however, Pd(PPh₃)₄ is already in an oxidation state of "0" since PPh₃ are neutral ligands.⁹³ The Suzuki-Miyaura coupling reaction mechanism is illustrated in **Scheme 19**. The reaction was high-yielding, however, during purification there was co-elution of the product (**53**) with the unreacted benzonitrile derivatives (**51**) and boronic acids (**52**). Using a low polarity solvent system this challenge was overcome. The identity of the synthesized compounds was confirmed using NMR and IR spectroscopy and mass spectrometry.



Scheme 19: Suzuki-Miyaura coupling reaction mechanism.

4-Bromobenzonitrile (**51a**) was reacted with a variety of boronic acids (**52**) to give rise to compounds **53a-d**, while for compounds **53e-h** 2-fluoro-4-bromobenzonitrile (**51b**) and various boronic acids were used as starting materials.

The Suzuki-Miyaura coupling reaction for the synthesis of biaryl compounds (**53a-h**) bearing a nitrile group gave moderate to high yields ranging between 55-98% (**Figure 10**).

Compounds **53a-e** have been reported before in the literature.⁹⁴⁻⁹⁸ The characteristic signals for ¹H and ¹³C NMR spectroscopy reported in literature for **53a-e** are similar to the signals obtained here.

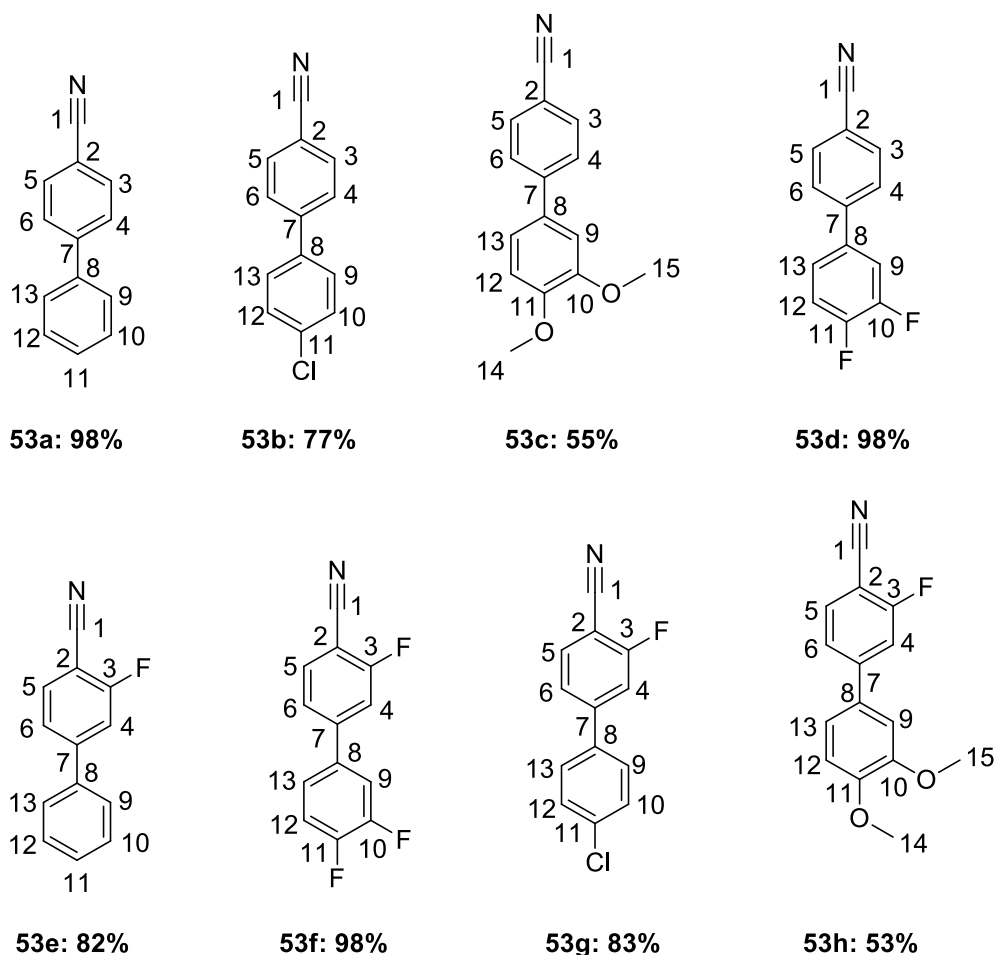


Figure 10: Synthesized biaryl nitrile compounds **53a-h** and their isolated yields.

Formation of these compounds was confirmed by the presence of signals for C-7 and C-8 in the ¹³C NMR spectra. The signal for C-7 appears between δ 143.5 and δ 148.6 for the synthesized biaryl compounds. The C-7 signal for **53d**, **53e**, **53f**, **53g** and **53h** appears as a doublet in the ¹³C NMR spectrum due to the presence of fluorine in the compounds. The C-7 signal for compound **53d** has a coupling constant (J_{CF}) of 1.7 Hz which is a $^4J_{CF}$ coupling because the fluorine atom at C-10 is 4 bonds away from C-7. Compounds **53e**, **53f**, **53g** and **53h** have a coupling constant range between $J = 7.6$ - 8.2 Hz indicating a $^3J_{CF}$ coupling since C-7 is 3 bonds away from the fluorine atom at C-3. The signal for C-8 appears between δ 130.7 and δ 139.1 (**Table 11**) for the prepared biaryl compounds. The C-8 signal for compounds **53e**, **53g** and **53h** appear as doublets due to the presence of a fluorine atom in

the compounds. The C-8 signals for **53e**, **53g** and **53h** have a coupling constant range between $J = 1.8$ - 2.1 Hz, indicating a $^4J_{CF}$ coupling since it is 4 bonds away from the fluorine atom at C-3. The C-8 signal for **53d** appears as a doublet of doublets due to the influence of the 2 fluorine atoms and has a coupling constant of $J_{CF} = 5.9, 3.9$ Hz, indicating it has a $^4J_{CF}$ and $^3J_{CF}$ coupling since it is 3 bonds away from the fluorine atom at C-10 and 4 bonds away from the fluorine atom at C-11. The C-8 signal for **53f** appears as a doublet of doublets of doublets due to the presence of the 3 fluorine atoms in the compound. It has coupling constants (J_{CF}) of 6.1, 4.0, 2.1 Hz since it is 3 bonds away from the fluorine atom at C-10 and 4 bonds away from the fluorine atom at C-11 and C-3.

The protons at H-3, 4, 5 and 6 for **53a** overlap into one signal and appear at $\delta 7.71$ in the 1H NMR spectra. For compound **53c** the protons at H-3, 4, 5 and 6 overlap into one signal and appear as a multiplet at $\delta 7.73$ - 7.62 . For compound **53b** and **53d** only H-3 and H-5 overlap into one signal at $\delta 7.68$ - 7.62 and $\delta 7.76$ - 7.71 respectively.

Table 11: Selected 1H and ^{13}C NMR chemical shifts for the synthesized bi-aryl nitrile compounds (**53a-h**).

	H-3 & H-4	C-7	C-8	C-10 & C-12	CN
53a	$\delta 7.71$ (2xd, $J = 8.4, 8.3$ Hz, 4H)	$\delta 145.6$	$\delta 139.1$	$\delta 127.2$	$\delta 118.9$
53b	$\delta 7.68$ - 7.62 (m, 2H)	$\delta 144.7$	$\delta 137.9$	$\delta 128.8$	$\delta 119.1$
53c	$\delta 7.73$ - 7.62 (m, 4H)	$\delta 145.4$	$\delta 131.9$	$\delta 149.8$ & 149.5	$\delta 119.0$
53d	$\delta 7.76$ - 7.71 (m, 2H)	$\delta 143.5$ (d, $J_{CF} = 1.7$ Hz)	$\delta 136.3$ (dd, $J_{CF} = 5.9, 3.9$ Hz)	$\delta 150.8$ & 150.7 (dd, $J_{CF} = 250.5, 12.6$ Hz & dd, $J_{CF} = 251.5, 12.5$ Hz)	$\delta 118.6$
53e	$\delta 7.67$ (dd, $J = 8.1, 6.7$ Hz, 1H)	$\delta 148.6$ (d, $J = 8.1$ Hz)	$\delta 137.9$ (d, $J = 2.0$ Hz)	$\delta 129.25$	$\delta 114.1$
53f	$\delta 7.71$ (dd, $J =$	$\delta 146.3$ (d, J_{CF}	$\delta 135.1$ (ddd,	$\delta 151.1$ & 150.8	$\delta 113.8$

	8.1, 6.6 Hz, 1H)	= 7.6 Hz	$J_{CF} = 6.1, 4.0,$ 2.1 Hz)	(dd, $J_{CF} = 250.7,$ 11.1 Hz & dd, $J_{CF} = 244.8, 7.7$ Hz)	
53g	δ 7.69 (dd, $J =$ 8.1, 6.6 Hz, 1H)	δ 147.2 (d, J_{CF} = 8.2 Hz	δ 136.4 (d, J_{CF} = 1.8 Hz)	δ 129.5	δ 113.9
53h	δ 7.64 (t, $J =$ 7.1 Hz, 1H)	δ 148.3 (d, J_{CF} = 8.2 Hz)	δ 130.7 (d, J_{CF} = 2.1 Hz)	δ 150.3 & 149.5	δ 114.22

A single signal is observed for C-10 and C-12 in the ^{13}C NMR spectra for compounds **53a**, **53b**, **53e** and **53g** as expected due to symmetry. The signals appear between δ 127.2 and δ 129.5. The signals for C-10 and C-11 appear at δ 149.8 and δ 149.5 for **53c** and δ 150.3 and δ 149.5 for **53h**, however, it has not been clearly established which signal belongs to C-10 and which to C-11. The signals for C-10 and C-11 appear at δ 150.8 and δ 150.7 for **53d** and at δ 151.1 and δ 150.8 for **53f**. The signals for C-10 and C-11 for **53d** appear as doublets of doublets with coupling constants of $J_{CF} = 250.5, 12.6$ Hz and $J_{CF} = 251.5, 12.5$ Hz, while the signals for **53f** appears as a doublet of doublets with coupling constants of $J_{CF} = 250.7, 11.1$ Hz and $J_{CF} = 244.8, 7.7$ Hz.

The nitrile functional groups appear at δ 118.9 for **53a**, δ 119.1 for **53b**, δ 119.0 for **53c** and δ 118.6 for **53d**, however, the nitrile signal for compounds with a fluorine atom *ortho* to the nitrile group appear upfield at δ 114.1 for **53e**, δ 113.8 for **53f**, δ 113.9 for **53g** and δ 114.22 for **53h** (Table 11). Fluorine has dual characteristics as it can donate electron density by resonance and withdraw electron density by induction. The decrease in the chemical shift of a nitrile signal in the presence of a fluorine atom in the *ortho* position (**53e-h**) indicates that fluorine donates electron density by resonance to the nitrile group in the *ortho* position, hence it appears upfield in comparison with nitriles lacking a fluorine atom in the *ortho* position (**53a-d**).

The HRMS (m/z) results for these compounds are as expected, thus confirming successful coupling reactions (Table 12).

Table 12: HRMS (m/z) for the synthesized biaryl compounds (**53f-h**).

	53f	53g	53h
Expected mass (M + H)⁺	234.0525	232.0324	258.0925
Found mass (M + H)⁺	234.0525	232.0321	258.0922

IR spectroscopy also confirmed the presence of a nitrile group in these compounds by the presence of a strong peak between 2219 cm⁻¹ and 2230 cm⁻¹ for the synthesized biaryl compounds (**53a-h**) (**Table 13**).

Table 13: IR spectroscopic data for the CN functional group.

	53a	53b	53c	53d	53e	53f	53g	53h
CN(cm⁻¹)	2221 (s)	2222 (s)	2219 (s)	2222 (s)	2226 (s)	2230 (s)	2229 (s)	2223 (s)

***S-strong**

3-Bromobenzonitrile (**51c**) was used as the starting material with the boronic acid (**52**) being varied in order to obtain *meta*-substituted biaryl compounds. The synthesized *meta*-substituted biaryl compounds (**53i-l**) were prepared in moderate to high yields ranging from 50-98%. Compounds substituted *ortho* to the nitrile group (**53m** and **53n**) were synthesized from 2-bromo-5-fluorobenzonitrile (**51d**) in 70% and 50% yields (**Figure 11**). Compounds **53j-n** are reported for the first time here while **53i** has been reported before in literature.⁹⁹

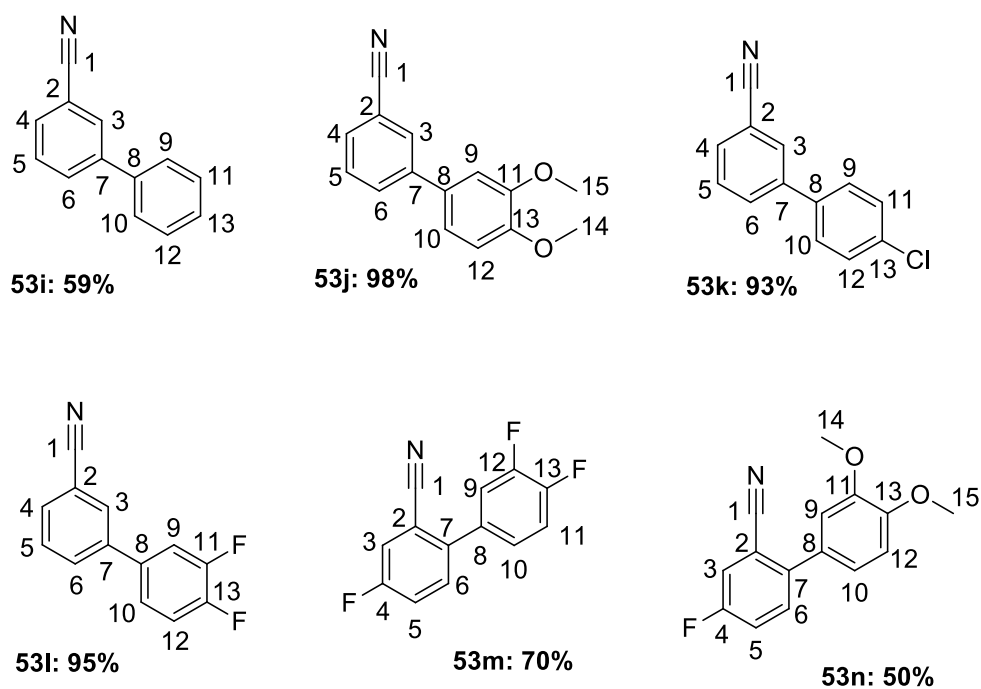


Figure 11: Synthesized biaryl nitrile compounds **53i-n**.

Synthesis of biaryl compounds with the secondary ring *meta* (**53i-l**) and *ortho* (**53m-n**) to the nitrile group was confirmed by the presence of a C-7 and C-8 signal in the ^{13}C NMR spectra. C-7 signals appear between δ 139.7 and δ 142.4 for compounds **53i-n**. The C-7 signal for compound **53i** has a coupling constant (J_{CF}) of 1.7 Hz since it is 4 bonds away from the fluorine atom at C-11. The C-7 signal for **53m** appears as a doublet of doublets with coupling constants (J_{CF}) of 3.9 and 1.7 Hz which are $^4J_{\text{CF}}$ couplings, since it is 4 bonds away from fluorine atoms at C-4 and C-12. The C-7 signal for **53n** has a coupling constant (J_{CF}) of 3.6 Hz therefore it is a $^4J_{\text{CF}}$ coupling since it is 4 bonds away from the fluorine atom at C-4. The signal for C-8 appears between δ 129.7 and δ 138.8 for both the *meta*- and *ortho*-substituted biaryl compounds (**Table 14**). The C-8 signals for **53i** and **53m** appear as doublets of doublets with coupling constants (J_{CF}) of 5.9, 3.9 Hz and $J_{\text{CF}} = 6.2, 4.0$ Hz, respectively, due to coupling with fluorine atoms attached at C-11 and C-13 for **53i** and for **53m** it is the coupling of C-8 with fluorine atoms at C-12 and C-13.

For ^1H NMR spectroscopy the signal for H-3 appears as a triplet for **53i** and **53l** at δ 7.85, and δ 7.80, respectively, in which the coupling constant ranges between $J = 1.8$ -1.7 Hz which corresponds to that of a *meta* coupling between H-3 and H-4 and H-3 and H-6. The signals for H-3 for **53j**, **53k** and **53m** appear as multiplets at δ 7.82 – 7.80, δ 7.82 – 7.78 and δ 7.49-

7.44, respectively. The H-3 signal for **53n** appears as a doublet of doublets with coupling constants (J) of 8.1, 2.6 Hz because of coupling to a fluorine atom (C-4) in the *ortho* position and H-5 in the *meta* position. The H-3 signal for **53m** overlaps with the H-6 signal and integrates for 2 protons at δ 7.49-7.44. The signal for H-4 appears as a doublet of triplets for **53i-l** with two coupling constants (J) ranging between 7.8-6.4 Hz and 1.4-1.3 Hz corresponding to an *ortho* coupling to H-5 and a *meta* coupling to H-6 and H-3.

Table 14: Selected ^1H and ^{13}C NMR chemical shifts for biaryl nitrile compounds (**53i-n**) substituted *ortho* and *meta* to the nitrile group.

	H-3	H-4	C-7	C-8	CN
53i	δ 7.85 (t, J = 1.7 Hz, 1H)	δ 7.61 (dt, J = 7.7, 1.4 Hz, 1H)	δ 142.4	δ 138.8	δ 118.8
53j	δ δ 7.82-7.80 (m, 1H)	δ 7.57 (dt, J = 6.4, 1.3 Hz, 1H)	δ 142.2	δ 131.6	δ 118.9
53k	δ 7.82 – 7.78 (m, 1H)	δ 7.63 (dt, J = 7.8, 1.4 Hz, 1H)	δ 141.1	δ 137.2	δ 118.6
53l	δ 7.80 (t, J = 1.8 Hz, 1H)	δ 7.66 (dt, J = 7.7, 1.4 Hz, 1H)	δ 140.4 (d, J_{CF} = 1.7 Hz)	δ 135.9 (dd, J_{CF} = 5.9, 3.9 Hz)	δ 118.5
53m	δ 7.49-7.44 (m, 2H)		δ 139.7 (dd, J_{CF} = 3.9, 1.7 Hz)	δ 134.0 (dd, J_{CF} = 6.2, 4.0 Hz)	δ 117.0 (d, J_{CF} = 2.7 Hz)
53n	δ 7.43 (dd, J = 8.1, 2.6 Hz, 1H)		δ 141.8 (d, J_{CF} = 3.6 Hz)	δ 129.7	δ 117.8 (d, J_{CF} = 2.8 Hz)

In the ^{13}C NMR spectra, the nitrile signal appears between δ 117.0 and δ 118.9 (**Table 14**) for *meta* and *ortho*- substituted biaryl compounds (**53i-n**) which is as expected for a nitrile functional group. The nitrile signal for **53m** and **53n** showed a coupling constant (J_{CF}) of 2.7 Hz and 2.8 Hz, respectively which corresponds to a $^4J_{\text{CF}}$ coupling since the fluorine atoms at C-4 are four bonds away from the nitrile carbon. The nitrile signals for **53m** and **53n** appear

to be slightly shielded in comparison with compounds **53i-l** in which the *meta*-substituted fluorine atom relative to the nitrile group is absent.

HRMS results were as expected, further confirming formation of these compounds. The peaks ranging between 2230-2224 cm^{-1} for these compounds in the IR spectra confirmed the presence of a nitrile group in these compounds (**Table 15**).

Table 15: IR spectroscopy for the nitrile functional group in **53i-n**.

	53i	53j	53k	53l	53m	53n
CN (cm^{-1})	2228	2224	2226	2228	2230	2229

Compound **53o** and **53p** were synthesized in high yields of 98% and 92%, respectively, where 2-cyano-6-bromopyridine (**51e**) was coupled with 4-chlorophenyl boronic acid (**52b**) and 3,4-dimethoxyphenyl boronic acid (**52c**) respectively, to afford the synthesized compounds (**Figure 12**). Compound **53o** and **53p** are reported for the first time here.

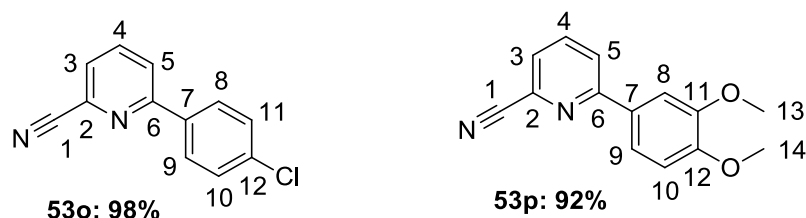


Figure 12: Synthesized nitrile compounds from 2-cyano-6-bromopyridine.

Synthesis of these biaryl compounds was confirmed by the presence of C-6 and C-7 signals in the ^{13}C NMR spectra. The signal for C-6 appears downfield as compared to the signal for C-7 because the C-6 signal is deshielded by being attached to a nitrogen atom (**Table 16**). In the ^1H NMR spectrum the H-3 signal for **53o** appears as a doublet of doublets with coupling constants (J) of 6.9, 1.7 Hz due to *ortho* coupling with H-4 and a *meta* coupling to H-5. The H-3 signal for **53p** overlaps with protons from H-9 and appears as a multiplet. The H-4 signal for **53p** appears as a triplet and has a coupling constant (J) of 7.8 Hz due to *ortho* couplings with H-3 and H-5. The signals for H-4 and H-5 for **53o** overlap and appear as a multiplet. The H-5 signal for **53p** appears as a doublet of doublets and has coupling constants (J) of 8.2, 1.0

Hz due to an *ortho* coupling to H-4 and a *meta* coupling to H-3. The nitrile groups appeared at δ 117.3 and δ 117.6 in the ^{13}C NMR spectrum which is the expected chemical shift range for a nitrile functional group.

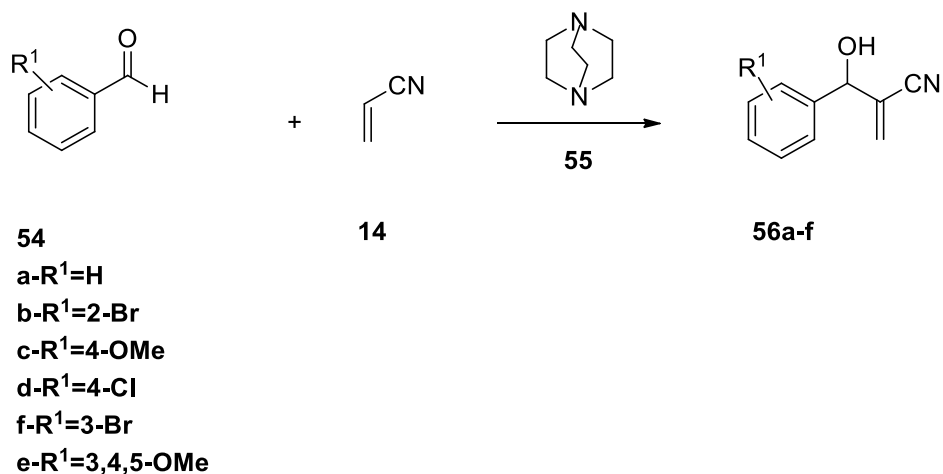
Table 16: Selected ^1H and ^{13}C NMR chemical shifts for the bi-aryl compounds (**53o** and **53p**) bearing a nitrile functional group.

	H-3	H-4	H-5	C-6	C-7	CN
53o	δ 7.63 (dd, $J = 6.9, 1.7$ Hz, 1H)	δ 7.93-7.89 (m, 2H)		δ 157.7	δ 136.5	δ 117.3
53p	δ 7.60-7.50 (m, 2H)	δ 7.83 (t, $J = 7.8$ Hz, 1H)	δ 7.90 (dd, $J = 8.2, 1.0$ Hz, 1H)	δ 158.5	δ 130.0	δ 117.6

The IR spectra for **53o** and **53p** further confirmed the presence of a nitrile group in the compounds by the appearance of weak peaks at 2234 cm^{-1} for **53o** and 2227 cm^{-1} for **53p**, which are the expected positions for a nitrile group. The HRMS results were as expected, further confirming formation of the compounds.

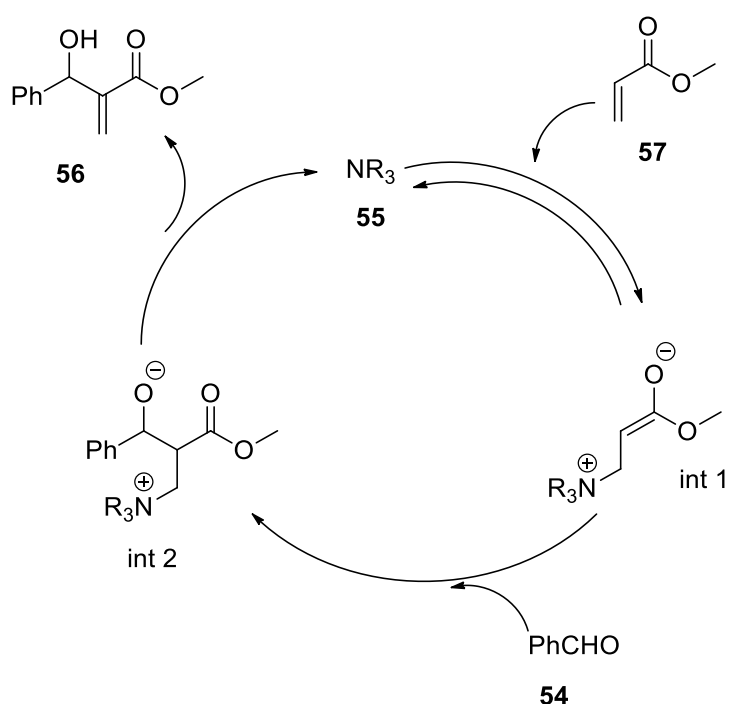
2.3 Synthesis of Morita-Baylis-Hillman (MBH) derivatives

The MBH reaction was applied for the synthesis of vinyl nitriles (**56**) (**Scheme 20**). These nitriles were chosen to see if NHase and nitrilase would be able to hydrolyze them and also to compare the activity of NHase and nitrilase between the vinyl and the aromatic nitriles. The reaction was performed in the presence of acrylonitrile (**14**), benzaldehyde (**54**) and DABCO (**55**) which functions as a nucleophilic amine base.



Scheme 20: MBH reaction.

This mechanism is initiated by the reversible Michael addition of the nucleophilic amine catalyst (**55**) to an acrylate (**57**) giving an enolate (int1). Nucleophilic addition of the enolate to the aldehyde (**54**) gives a second zwitterionic intermediate (int2). This is followed by a proton transfer and elimination yielding the product and also liberating the amine catalyst (**Scheme 21**).



Scheme 21: Proposed MBH reaction mechanism.

The MBH compounds (**56a-f**) were prepared by using acrylonitrile (**14**) and a variety of benzaldehydes (**54a-e**). The MBH compounds were successfully synthesized in moderate to

excellent yields of 60-95% (**Figure 13**). Compounds **56a-d** and **56f** have previously been reported in literature.^{36,100-102}

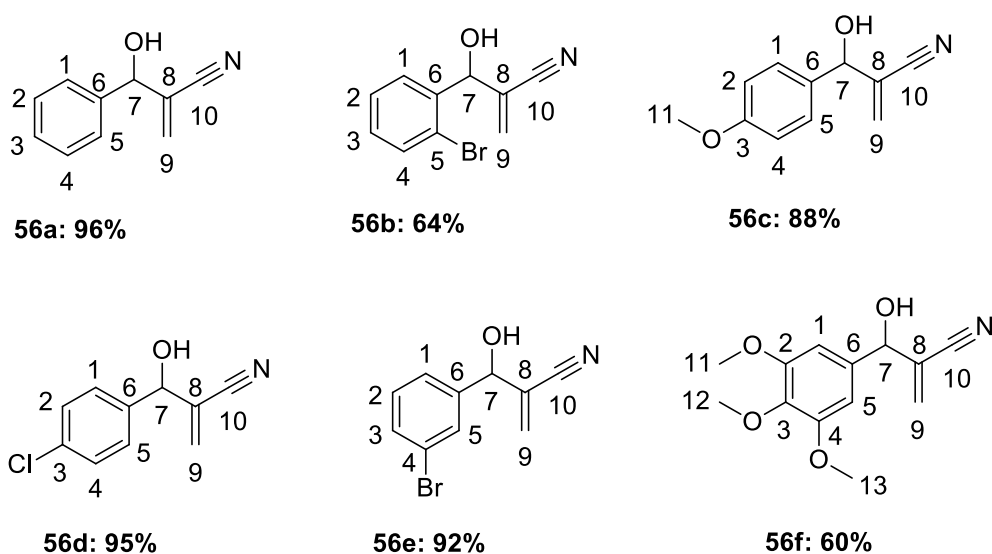


Figure 13: Synthesized MBH compounds **56a-f** and their isolated yields.

Synthesis of the compounds was confirmed by the presence of a broad signal for an OH group in the ¹H NMR spectrum appearing at δ 3.23 for **56a**, δ 3.27 for **56b**, δ 3.30 for **56c** and δ 3.38 for **56d**, while the OH group from **56e** appears as a multiplet. The OH signal for **56f** overlaps with the signal from the trimethoxy protons at δ 3.84-3.76 and appears as a multiplet that integrates for 10 protons, as expected. The H-7 signal appears between δ 5.14 and δ 5.67 for the prepared MBH compounds (**Table 17**). The two H-9 protons appear at two different chemical shifts as doublets with a coupling constant ranging between $J = 1.0$ - 1.6 Hz which is due to the germinal coupling of the alkene protons (H-9). However, the H-9 protons from **56b** appear at the same chemical shift as a multiplet integrating for 2 protons (**Table 17**).

¹³C NMR spectroscopy further confirmed formation of the compounds by the presence of a C-7 signal ranging between δ 72.5 and δ 74.0. The C-7 signal is the most shielded, excluding the signal from the methoxy groups (**56c** and **56f**). The nitrile signals range between δ 116.7 and δ 117.1 which is the expected chemical shift range for a nitrile functional group. The signal for C-9 was seen between δ 131.7 and δ 129.6 in the ¹³C NMR spectra. The signal for C-9 appears as the only negative signal in the DEPT 135 spectra for the prepared MBH compounds since it is the only secondary carbon (CH₂) in the molecules.

Table 17: Selected ^1H and ^{13}C NMR chemical shifts for MBH compounds **56a-f**.

	H-7	H-9	OH	C-7	C-9	CN
56a	δ 5.19 (s, 1H)	δ 6.02 (d, $J = 1.5$ Hz, 1H), 5.95 (d, $J = 1.2$ Hz, 1H)	δ 3.23 (br s, 1H)	δ 74.0	δ 130.1	δ 117.0
56b	δ 5.67 (s, 1H)	δ 6.06-6.01 (m, 2H)	δ 3.27 (br s, 1H)	δ 72.5	δ 131.7	δ 116.7
56c	δ 5.14 (s, 1H)	δ 6.02 (d, $J = 1.6$ Hz, 1H), 5.94 (d, $J = 1.4$ Hz, 1H)	δ 3.30 (br s, 1H)	δ 73.5	δ 129.6	δ 117.1
56d	δ 5.17 (s, 1H)	δ 6.01 (d, $J = 1.4$ Hz, 1H), 5.95 (d, $J = 1.0$ Hz, 1H)	δ 3.81 (br s, 1H)	δ 73.2	δ 130.6	δ 116.8
56e	δ 5.17 (s, 1H)	δ 6.05 (d, $J = 1.5$ Hz, 1H), 5.99 (d, $J = 1.1$ Hz, 1H)	δ 3.58-3.57 (m, 1H)	δ 73.1	δ 130.8	δ 116.7
56f	δ 5.17 (d, $J = 3.5$ Hz, 1H)	δ 6.08 (d, $J = 1.5$ Hz, 1H), 5.98 (d, $J = 1.2$ Hz, 1H)	δ 3.84-3.76 (m, 10H)	δ 74.0	δ 129.8	δ 117.1

IR spectroscopy further confirmed the presence of a nitrile and an OH group. The nitrile signals appeared between 2223 cm^{-1} and 2231 cm^{-1} (**Table 18**). The OH signal appeared as broad peaks ranging between 3427 cm^{-1} and 3473 cm^{-1} which is as expected.

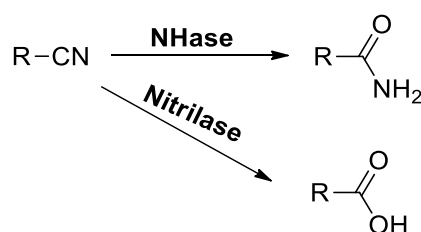
Table 18: Selected IR peaks for the synthesized MBH compounds.

	56a	56b	56c	56d	56e	56f
CN (cm^{-1})	2230 (w)	2230 (w)	2229 (w)	2228(s)	2231 (w)	2223 (w)
OH (cm^{-1})	3427 (br)	3443 (br)	3439 (br)	3434 (br)	3428 (br)	3473 (br)

*S-strong, W-weak, br- broad

2.4 NHase and nitrilase activity

NHase isolated from *R. rhodochrous* ATCC BAA 870 and the whole cell nitrilase from *R. rhodochrous* A29 and A99 were applied on a range of nitrile compounds for hydrolysis (Scheme 22). A selection of commercially available nitriles as well as the synthesized compounds were subjected to NHase and whole cell nitrilases. The enzyme or whole cell catalyst together with the nitriles were incubated in a buffer on a shaker at 30 °C and the reaction was continually monitored by TLC analysis.



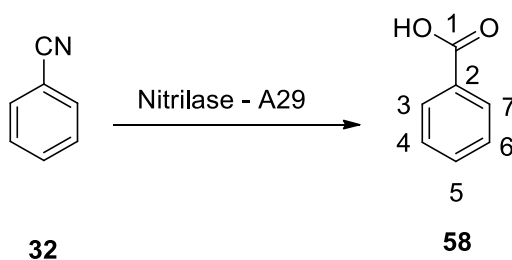
Scheme 22: Hydrolysis of the nitrile functional group by NHase and whole cell nitrilase.

The majority of the nitrile substrates were solids and acetone and methanol were used as co-solvents to solubilise the compounds in buffer. Both the synthesized and commercial nitrile compounds were dissolved in methanol, except for the biaryl compounds which were insoluble in methanol due to being non-polar, and therefore for these compounds acetone was used as the co-solvent. In the presence of an amine group on the nitrile substrates the pH of the buffer was changed from pH 7 to pH 9 to avoid protonation of the amine group.¹⁰³

2.4.1 Standard Reaction

NHase (*R. rhodochrous* ATCC BAA 870) and whole cell nitrilases (*R. rhodochrous* A29 and A99) were tested for activity on benzonitrile which is the standard substrate for both enzymes.

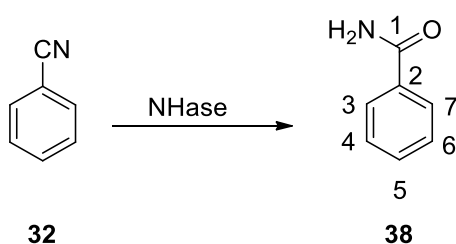
Both whole cell nitrilases (A29 and A99) were active towards benzonitrile as benzoic acid (Scheme 23) was obtained and formation was confirmed by ¹H and ¹³C NMR spectroscopy.



Scheme 23: Whole cell nitrilase (A29 and A99) activity towards benzonitrile.

Formation of the benzoic acid (**58**) was confirmed by the presence of a broad signal in the ^1H NMR spectra at δ 12.73 corresponding to an OH group and the appearance of a carbonyl signal at δ 167.4 in the ^{13}C NMR spectrum further confirmed formation of the benzoic acid. The signals obtained correspond with literature values for this compound.¹⁰⁴

The isolated NHase was also found to be active towards benzonitrile (**Scheme 24**).



Scheme 24: NHase activity towards benzonitrile.

Formation of the benzamide (**38**) was confirmed by ^1H and ^{13}C NMR spectroscopy. The presence of two broad signal at δ 7.99 and at δ 7.38 each corresponding to an NH signal in the ^1H NMR spectrum confirmed formation of the benzamide. Formation of the benzamide was further confirmed by the presence of a carbonyl signal at δ 168.0 in the ^{13}C NMR spectrum. Data agreed with that previously reported in the literature for benzamide.¹⁰⁵

Since the three biocatalysts (NHase, A29 and A99) were able to hydrolyse benzonitrile their standard activity is confirmed and they can therefore be tested in the hydrolysis of a range of the synthesized and commercially available nitriles.

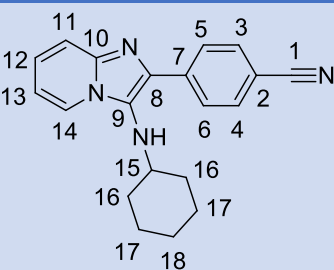
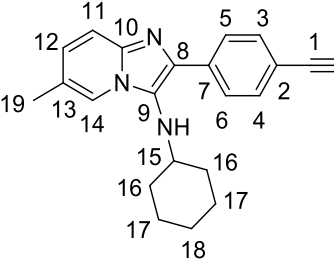
2.4.2 NHase and nitrilase activity towards imidazo[1,2-*a*]pyridine compounds bearing a nitrile functional group

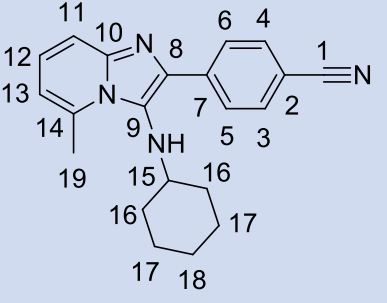
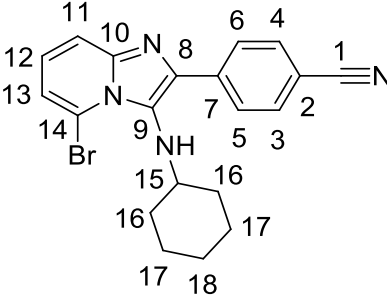
The nitrile functional group is electron withdrawing while the carbon atom of the nitrile group is electron deficient. It has been suggested that NHase requires an electron deficient nitrile carbon atom (electrophile) for best activity since the first step in the proposed mechanisms is a nucleophilic attack on the nitrile carbon atom. Electron-withdrawing substituents on the aromatic ring would withdraw electron density from the nitrile group making the nitrile carbon atom more electrophilic while electron-donating groups on the aromatic ring would make the nitrile carbon atom less electrophilic.

The prepared compounds **50a-d** were subjected to NHase and whole cell nitrilase (A99 and A29) enzymes (**Table 19**), however no hydrolytic activity was observed as there was no new

spot being observed on the TLC plate. Leaving the reaction for longer in the incubator did not lead to any significant changes. The synthesized imidazo[1,2-*a*]pyridine compounds have nitrogen atoms fused within the ring which withdraws electron density that is being donated into the ring thus making the nitrile carbon atom electron deficient. However, the nitrile group in these compounds is on the phenyl ring and so any electronic effect is likely to be small. Therefore, the inability of NHase and whole cell nitrilase to hydrolyze these compounds might not be due to electronic effects, however, it might be due to steric effects introduced by the flexible and bulky cyclohexyl group. The inability of the enzymes to hydrolyse these nitriles was surprising considering that the nitrile group is relatively far away from the bulky cyclohexyl group.

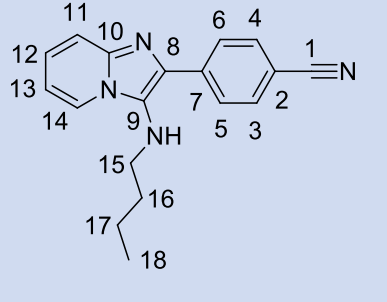
Table 19: Hydrolytic activity of NHase and whole cell nitrilase towards the synthesized nitrile-bearing imidazo[1,2-*a*]pyridine compounds.

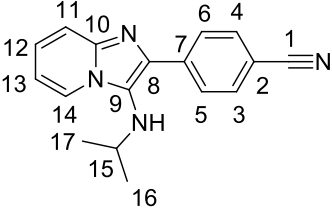
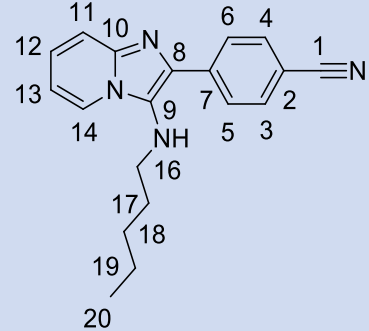
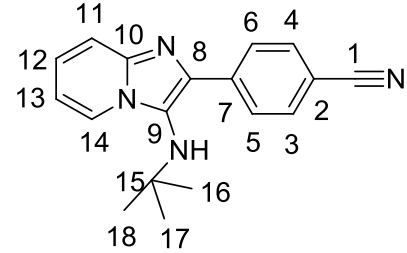
	NHase activity	Nitrilase activity (A29 and A99)
 <p>50a</p>	No activity	No activity
 <p>50b</p>	No activity	No activity

 <p style="text-align: center;">50c</p>	No activity	No activity
 <p style="text-align: center;">50d</p>	No activity	No activity

Imidazo[1,2-*a*]pyridine compounds bearing a less bulky acyclic aliphatic group (**50e-f**) in place of the cyclohexyl group were subjected to NHase and whole cell nitrilases (A29 and A99) (**Table 20**). The acyclic aliphatic group was assumed to reduce the steric hindrance as they are not as bulky as the cyclohexyl group. The exception to this was compound **50h** bearing a bulky *t*-butyl group.

Table 20: Hydrolytic activity of NHase and nitrilase towards the synthesized nitrile-bearing imidazo[1,2-*a*]pyridine compounds with an aliphatic chain.

	NHase	Whole cell Nitrilase (A29 and A99)
 <p style="text-align: center;">50e</p>	No activity	No activity

 <p>50f</p>	No activity	No activity
 <p>50g</p>	No activity	No activity
 <p>50h</p>	No activity	No activity

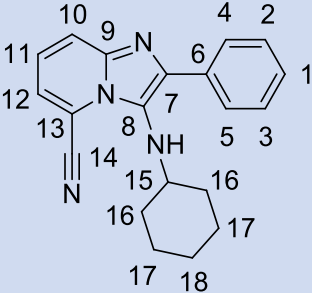
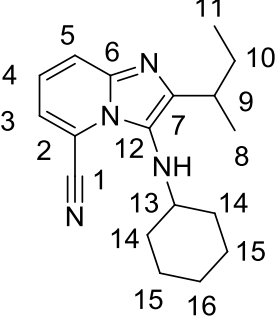
NHase and whole cell nitrilase were unable to hydrolyze **50e** and **50g** which have longer acyclic aliphatic groups, however, even in the presence of shorter acyclic aliphatic groups in **50f** and **50h** there was still no hydrolytic activity (**Table 20**). This seems to indicate that the way in which these enzymes interact with the nitrile group requires the whole molecule to access the active site, making it prone to steric hindrance and resulting in no hydrolytic activity even for compounds bearing short acyclic aliphatic groups.

Since no hydrolytic activity was observed for any of the synthesized compounds **50e-h** the reaction mixtures were allowed more time (days) in the incubator, however, there was still no significant difference observed.

The imidazo[1,2-*a*]pyridines were modified by changing the position of the nitrile group to be on the pyridine ring (**50i** and **50j**) to see how this would affect the activity of NHase and whole cell nitrilases.

This resulted in no activity, as indicated by TLC analysis where no new spot was observed (**Table 21**).

Table 21: NHase and whole cell nitrilase hydrolytic activity towards the modified nitrile-bearing imidazo[1,2-*a*]pyridine compounds **50i-j**.

Nitrile compounds	NHase activity	Whole cell Nitrilase (A29 and A99) activity
 <p style="text-align: center;">50i</p>	No activity	No activity
 <p style="text-align: center;">50j</p>	No activity	No activity

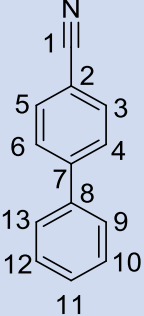
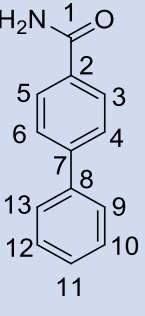
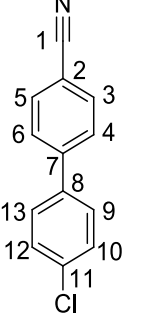
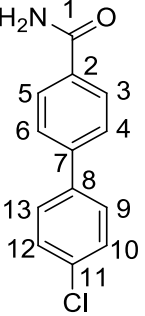
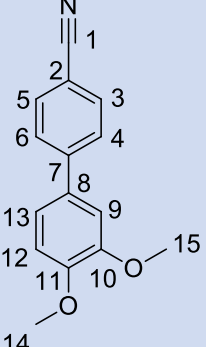
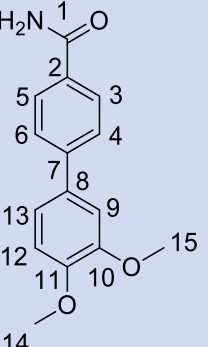
The same reason why compounds **50a-h** were not hydrolyzed by NHase and whole cell nitrilases could also apply to compounds **50i** and **50j**. The nitrile group in compound **50i** and **50j** is closer to the cyclohexyl group than in compounds **50a-h** and steric bulk of this group might prevent the interaction between the nitrile group and both the NHase and whole cell nitrilases.

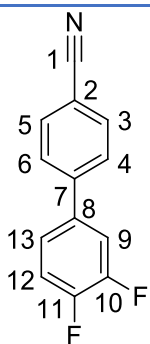
2.4.3 NHase activity towards biaryl compounds bearing a nitrile functional group

The synthesized biaryl compounds were subjected to NHase to observe how the varying substituents on the compounds might influence the activity of NHase (**Table 22**). The

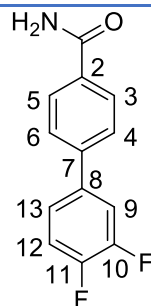
compounds were subjected to NHase for two days. These compounds were not subjected to whole cell nitrilases (A29 and A99) due to time constraints.

Table 22: NHase activity towards biaryl compounds bearing a nitrile functional group.

Nitrile compound	NHase activity stated as percentage isolated product yield
 <p>53a</p>	 <p>59a</p> <p>22%</p>
 <p>53b</p>	 <p>59b</p> <p>42%</p>
 <p>53c</p>	 <p>59c</p> <p>0%</p>

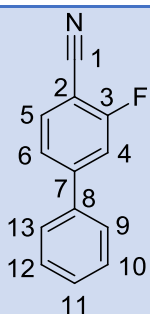


53d

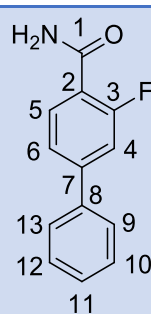


59d

31%

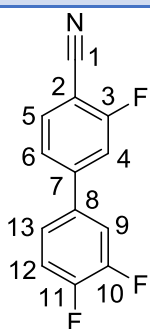


53e

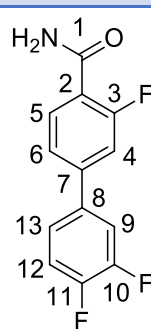


59e

13%

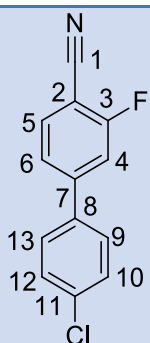


53f

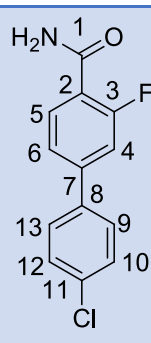


59f

23%

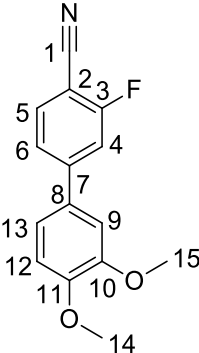
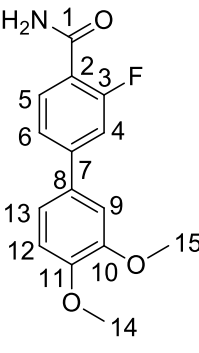
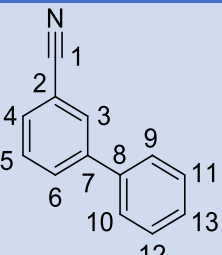
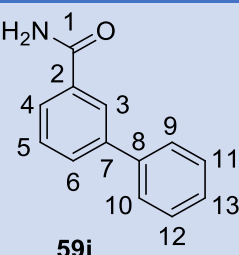
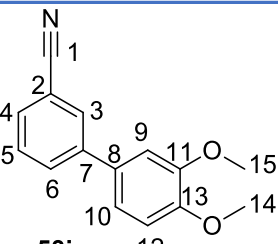
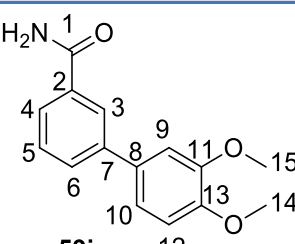
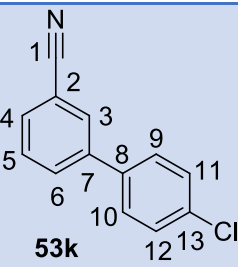
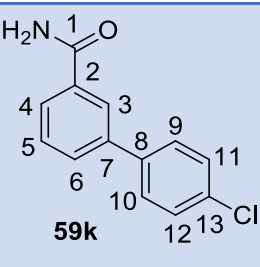
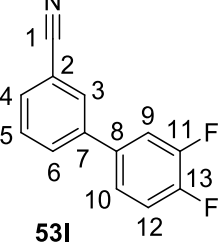
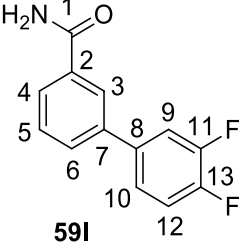


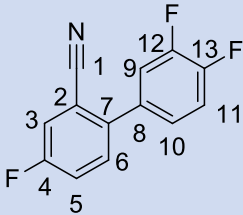
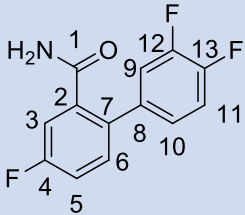
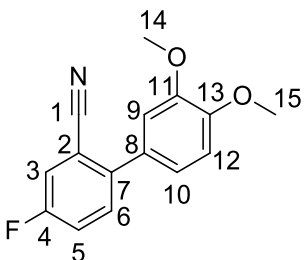
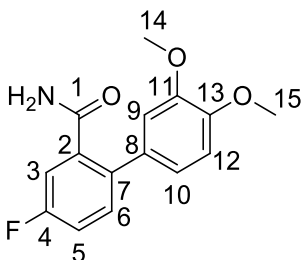
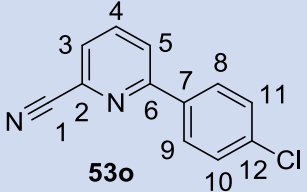
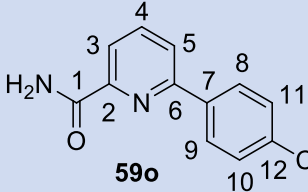
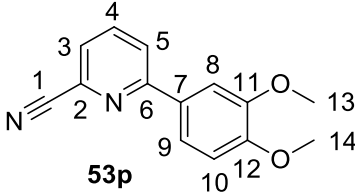
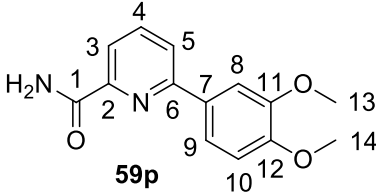
53g



59g

15%

 <p>53h</p>	 <p>59h</p> <p>0%</p>
 <p>53i</p>	 <p>59i</p> <p>20%</p>
 <p>53j</p>	 <p>59j</p> <p>0%</p>
 <p>53k</p>	 <p>59k</p> <p>11%</p>
 <p>53l</p>	 <p>59l</p>

	42%
 <p>53m</p>	 <p>59m</p> <p>0%</p>
 <p>53n</p>	 <p>59n</p> <p>0%</p>
 <p>53o</p>	 <p>59o</p> <p>5%</p>
 <p>53p</p>	 <p>59p</p> <p>0%</p>

Formation of the amide products from **53a**, **53b**, **53d**, **53e**, **53f**, **53g**, **53i**, **53k**, **53l** and **53o** was confirmed through ^{13}C NMR spectroscopy by the disappearance of the signal corresponding to a nitrile functional group and the appearance of a carbonyl signal for the amide ranging between δ 167.8-167.3 for **59a**, **59b**, **59d**, **59i**, **59k** and **59l** (Table 23). The carbonyl signal for compounds with a fluorine atom in the *ortho* position appeared upfield with the signal ranging between δ 165.2-164.8 for **59e**, **59f** and **59g** due to the fluorine atom

donating electron density to the amide carbon atom by resonance. The carbonyl signal for **59o** appears at δ 166.2. The carbonyl signal for the amide compounds with fluorine in the *ortho* position (**59e**, **59f** and **59g**) appear as doublets with a coupling constant (J_{CF}) range between 1.4-1.26 Hz.

The presence of NH₂ signals in the ¹H NMR spectra confirmed formation of the amide group where the two protons appear at two different chemical shifts for **59a**, **59b**, **59d**, **59e** and **59i** between δ 7.38-7.65 and δ 7.70-8.10. The NH₂ protons for **59f**, **59g**, **59i**, **59k** and **59o** also appear at different chemical shifts but one of the protons overlaps with the signal of one of the aromatic protons (**Table 23**).

Table 23: Selected ¹H and ¹³C NMR chemical shifts for the amide derivatives of the biaryl compounds.

	N-H	Carbonyl signal
59a	δ 7.38 (br s, 1H); 8.02 (br s, 1H)	δ 167.5
59b	δ 8.03 (br s, 1H), 7.40 (br s, 1H)	δ 167.4
59d	δ 8.04 (br s, 1H), 7.41 (br s, 1H)	δ 167.3
59e	δ 7.70 (br s, 1H), 7.65 (br s, 1H)	δ 164.9 (d, J_{CF} = 1.4 Hz)
59f	δ 7.74 (t, J = 7.9 Hz, 2H), 7.68 (dd, J = 12.1, 1.7 Hz, 1H)	δ 164.8 (d, J_{CF} = 1.26 Hz)
59g	δ 7.72 (br s, 1H), 7.68-7.59 (m, 3H)	δ 165.2 (d, J_{CF} = 1.4 Hz)
59i	δ 8.09 (br s, 1H), 7.41 (dt, J = 8.1, 5.2 Hz, 2H)	δ 167.8
59k	δ 8.11 (br s, 1H), 7.47-7.39 (m, 2H)	δ 167.6
59l	δ 8.10 (br s, 1H), 7.46 (br s, 1H)	δ 167.6

59o	δ 8.39-8.31 (m, 3H, H8, H9 overlapping with NH), 7.70 (br s, 1H)	δ 166.2
------------	---	----------------

IR spectroscopy further confirmed the presence of an amide by the disappearance of the nitrile signal ranging at 2219-2230 cm^{-1} and the appearance of strong NH signals ranging between 3408-3383 cm^{-1} and 3180-3163 cm^{-1} and a strong carbonyl signal ranging between 1651-1645 cm^{-1} . These amide compounds are reported for the first time here, except for compound **59a** which has been reported in literature before.

The HRMS (m/z) results for these compounds were as expected, confirming formation of an amide (**Table 24**).

Table 24: HRMS (m/z) for the amide products.

	59b	59d	59e	59f	59g	59i	59o
Expected mass (M + H)⁺	232.0524	234.0725	216.0819	252.0631	250.0429	234.0725	233.0476
Found mass (M + H)⁺	232.0524	234.0726	216.0874	252.0631	250.0427	234.0728	233.0475

Compounds which did not demonstrate any amide formation such as compounds **53c**, **53h**, **53j**, **53m**, **53n** and **53p** were allowed more time to react, however, still there were no significant changes.

As indicated from **Table 22** the presence of an electron donating group (3,4-dimethoxyphenyl group) irrespective of its position (*ortho*, *para* or *meta*) relative to a nitrile group resulted in no NHase activity and hence no amide was obtained from **53c**, **53h**, **53j**, **53n** and **53p**. The 3,4-dimethoxyphenyl group decreases the electrophilicity of the nitrile carbon atom therefore making it less reactive for hydrolysis. NHase was also not able to hydrolyse **53m** which has the 3,4-difluorophenyl group *ortho* to the nitrile group and a fluorine atom in the *meta* position, however, **53f** with the 3,4-difluorophenyl group in the

para-position and the fluorine atom in the *ortho*-position was hydrolysed to give 23% of the amide product (**59e**). It is therefore assumed that **53m** was not hydrolysed due to steric hindrance introduced by the 3,4-difluorophenyl group in the *ortho*-position, rather than any electronic effects. Compound **53o**, even in the presence of an electron withdrawing group, still gave low amide yields (5%) and this might be due to steric hindrance introduced by the 4-chlorophenyl group.

NHase hydrolysis of **53a** and **53i** gave a similar amide yield, therefore NHase was not affected by the phenyl group being in the *para* or *meta* position, however, for **53d** and **53l** a small decrease in activity is observed when the 3,4-difluorophenyl group is in the *para* position, while for **53b** and **53k** a large decrease in NHase activity was observed when the 4-chlorophenyl group is in the *meta*-position. *Meta*-substitution on an aromatic nitrile has been previously found to negatively affect the activity of the NHase, as discussed in the introduction.¹⁰⁶

The nitrile signal for compounds with a fluorine atom *ortho* to the nitrile group such as **53e**, **53f**, **53g** and **53h** appeared to be upfield in comparison with signals for compounds lacking an *ortho*-substituted fluorine atom. It is assumed that this decrease in chemical shift is because the fluorine atom donates electron density to the nitrile carbon atom, thus making it less electron poor and hence is less easily hydrolysed by the NHase, resulting in low amide yields (**59e**, **59f** and **59g**) being obtained. Therefore, the presence of a fluorine atom *ortho* to the nitrile group decreases the hydrolytic activity of NHase and hence a decrease in the amide yields, as observed in **59e**, **59f** and **59g** in comparison to **59a**, **59d** and **59b**, respectively. However, results from *Black et al.* demonstrate that the fluorine atom in the *ortho*-position does not affect the activity of NHase from *Rhododopseudomonas palustris* CGA009.⁴⁷

It was anticipated that the simple *para*-substituted biaryl compounds such as **53a**, **53b**, **53d**, **53e**, **53f** and **53g** would be easily hydrolysed by NHase since they appear to be flat molecules and lack a sterically demanding substituent. However, the biaryl compounds are not entirely flat molecules as one benzene ring can twist relative to the other ring along the C-C bond in varying degrees (45° and 90°) in order to avoid steric crowding. This is made possible by the lack of sterically demanding substituents close to the central C-C bond which if present would be capable of hindering the twist along the C-C bond (**Figure 14**).

Therefore, this twist of the benzene ring might introduce steric hindrance and slightly hinder the interaction between the nitrile group and the NHase active site.

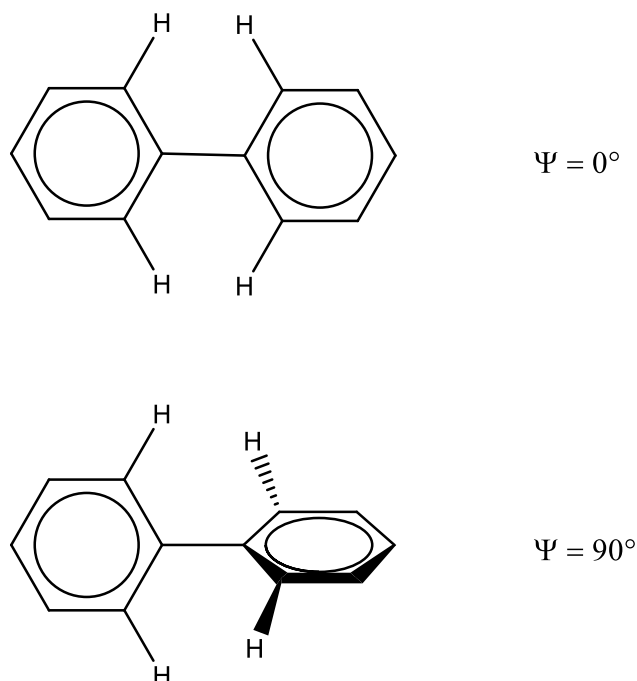


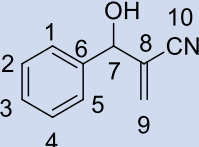
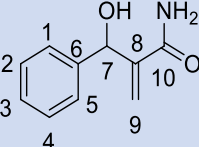
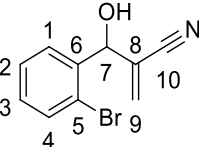
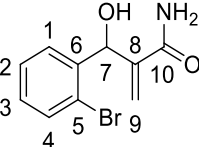
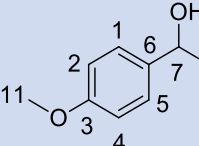
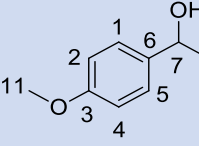
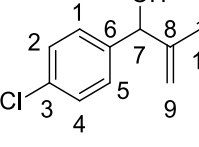
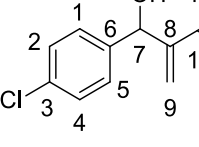
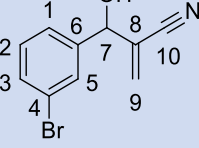
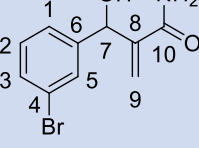
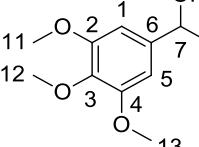
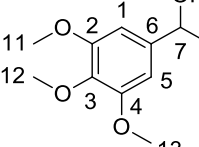
Figure 14: Bi-phenyl configuration.¹⁰⁷

2.4.4 NHase and nitrilase activity towards MBH compounds (56a-f) bearing a nitrile functional group

The synthesized MBH compounds (**56a-f**) were subjected to NHase and whole cell nitrilase (A29 and A99) activity for hydrolysis. The hydrolytic reaction towards the MBH compounds by NHase was slow, therefore the reaction mixtures were incubated on a shaker for 5 days. NHase and whole cell nitrilase activity towards these compounds is shown in **Table 25**. Compounds **60a**, **60c** and **60d** have been reported in literature before.¹⁰⁸⁻¹¹⁰

Table 25: NHase and nitrilase activity on a variety of MBH compounds.

MBH compounds	NHase activity expressed as isolated yields of amide	Whole cell nitrilase (A29 and A99) activity

 <p>56a</p>	 <p>60a</p> <p>84%</p>	No activity
 <p>56b</p>	 <p>60b</p> <p>93%</p>	No activity
 <p>56c</p>	 <p>60c</p> <p>57%</p>	No activity
 <p>56d</p>	 <p>60d</p> <p>61%</p>	No activity
 <p>56e</p>	 <p>60e</p> <p>0%</p>	No activity
 <p>56f</p>	 <p>60f</p> <p>0%</p>	No activity

Formation of the amide was confirmed by ^1H and ^{13}C NMR spectroscopy (**Table 26**). The NH_2 protons appear at two different chemical shifts in the ^1H NMR spectra ranging between δ 6.95-7.02 and δ 7.40-7.58 for **60a**, **60c** and **60d**. The NH_2 protons for **60b** also appear at two different chemical shifts with one of the protons overlapping with an aromatic proton (H-4). Formation of the amide was further confirmed by the presence of a carbonyl signal in the ^{13}C NMR spectra ranging between δ 168.5-169.1 for the amide compounds (**60a-d**).

Table 26: Selected ^1H and ^{13}C NMR chemical shifts for the MBH compounds **60a-d**.

	NH signals (ppm)	Carbonyl signals (ppm)
60a	δ 7.45 (br s, 1H), δ 6.95(br s, 1H)	δ 169.1
60b	δ 7.58-7.53 (m, 2H), δ 7.02 (br s, 1H)	δ 168.7
60c	δ 7.40 (br s, 1H), δ 6.95 (br s, 1H)	δ 168.7
60d	δ 7.45 (br s, 1H), δ 6.99 (br s, 1H)	δ 168.5

The rate of hydrolysis for **56a** and **56b** was faster than that for other MBH compounds, hence they were fully hydrolysed to the amide (**Table 25**). NHase was able to fully convert **56b** (*ortho*-bromine) but was unable to hydrolyse **56e** which has bromine is in the *meta*-position. Hydrolysis of **56e** was monitored by TLC where formation of the amide was observed under a UV lamp, however, conversion was too low for product to be isolated and allowing the reaction to proceed longer in the incubator resulted in no significant changes.

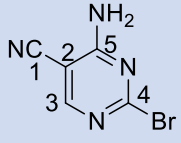
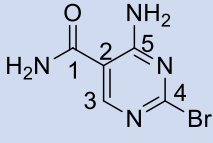
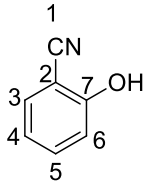
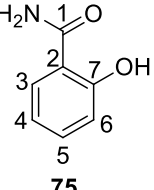
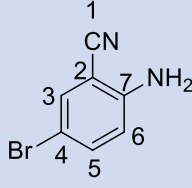
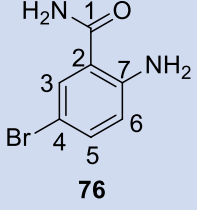
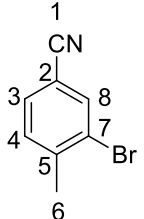
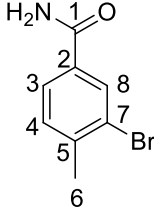
The presence of an electron withdrawing substituent (chlorine) in **56d** and an electron donating substituent (methoxy) in **56c** did not seem to influence the hydrolytic activity of NHase to a large extent as the amide yields were similar, however, when a trimethoxy group was present as in **56f** there was no hydrolytic activity.

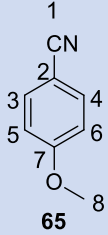
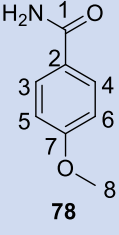
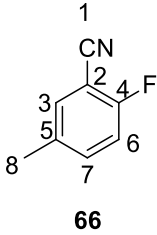
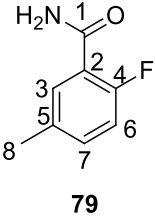
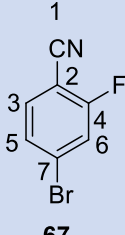
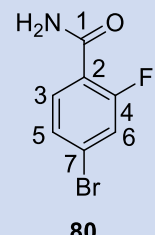
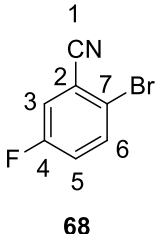
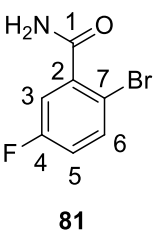
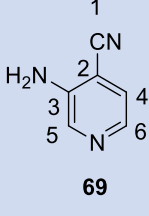
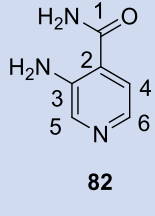
The synthesized MBH compounds were also subjected to whole cell nitrilase activity in which no hydrolytic activity was observed, giving the reaction more time resulted in no significant changes. The reason whole cell nitrilases (A29 and A99) were unable to hydrolyse any of the MBH compounds could be due to hydrogen bonding between the OH groups with the amine group from the tetrahedral intermediate as illustrated in **Scheme 9**.

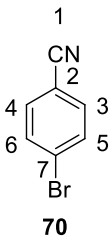
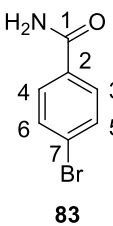
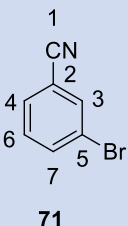
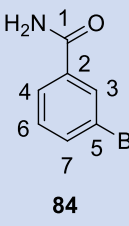
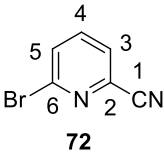
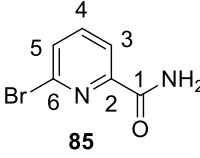
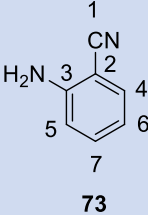
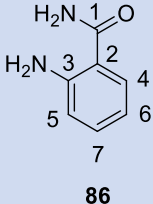
2.4.5 NHase activity towards a range of commercially available nitriles

Commercially available simple aromatic nitrile compounds with varying substituents were purchased from Sigma Aldrich and subjected to NHase activity (**Table 27**) to observe the effect the varying substituents might have on the activity of NHase. Whole cell nitrilases (A29 and A99) were not subjected to these compounds due to time constraints.

Table 27: NHase activity towards a range of commercially available simple nitrile compounds.

Nitrile compounds	NHase activity
 <p>61</p>	 <p>74</p> <p>80%</p>
 <p>62</p>	 <p>75</p> <p>32%</p>
 <p>63</p>	 <p>76</p> <p>98%</p>
 <p>64</p>	 <p>77</p> <p>95%</p>

 <p>65</p>	 <p>78</p> <p>48%</p>
 <p>66</p>	 <p>79</p> <p>96%</p>
 <p>67</p>	 <p>80</p> <p>97%</p>
 <p>68</p>	 <p>81</p> <p>93%</p>
 <p>69</p>	 <p>82</p> <p>75%</p>

 <p>70</p>	 <p>83</p> <p>95%</p>
 <p>71</p>	 <p>84</p> <p>81%</p>
 <p>72</p>	 <p>85</p> <p>90%</p>
 <p>73</p>	 <p>86</p> <p>40%</p>

To confirm that hydrolysis had occurred, ^1H and ^{13}C NMR spectroscopy were used where the NH signal and the carbonyl signal were indications of the presence of an amide functional group in the compounds (**Table 28**).

Table 28: Selected ^1H and ^{13}C NMR chemical shift of simple amide products.

Compound	NH signals	Carbonyl signal
74	δ 8.39, δ 8.23, δ 8.12 & δ 7.60 (4 \times br s, 4H, NH ₂ & NH ₂)	δ 167.5

75	δ 8.39 (br s), δ 7.89 (br s, 1H)	δ 172.1
76	δ 7.84 (br s, 1H, NH), δ 7.17 (br s, 1H, NH), δ 6.70 (br s, 2H, NH ₂)	δ 170.0
77	δ 8.02 (br s, 1H, NH), δ 7.42 (br s, 1H, NH)	δ 166.2
78	δ 7.86-7.82 (m, $J = 8.9$ Hz, 3H), δ 7.17 (br s, 1H, NH)	δ 167.9
79	δ 7.63 (br s, 1H, NH), δ 7.58 (br s, 1H, NH)	δ 165.3 (d, $J_{CF} = 1.0$ Hz)
80	δ 7.76 (br s, 1H, NH), δ 7.70 (br s, 1H, NH),	δ 164.4 (d, $J_{CF} = 1.2$ Hz)
81	δ 7.94 (br s, 1H), δ 7.65-7.70 (m, 2H, H6 overlapping with NH)	δ 167.8 (d, $J_{CF} = 1.6$ Hz)
82	δ 8.05 (br s, 2H, H7 overlapping with NH) & δ 6.31 (br s, 2H, NH ₂),	δ 171.1
83	δ 8.05 (br s, 1H), δ 7.47 (br s, 1H)	δ 166.9
84	δ 8.1 (br s, 1H), δ 7.53 (br s, 1H)	δ 166.3
85	δ 8.05-8.01 (m, 2H, H3 overlapping with NH), δ 7.78 (br s, 1H, NH);	δ 164.6
86	δ 7.70 (br s, 1H), δ 7.04 (br s, 1H), δ 6.54 (br s, 2H)	δ 171.3

In the ¹H NMR spectra the NH₂ protons appear at different chemical shifts ranging between δ 6.31-8.39. In some cases NH₂ protons overlapped with aromatic protons within the compound as observed for **78**, **81**, **82** and **85** (**Table 28**). The presence of the carbonyl signal in the ¹³C NMR spectra further confirmed the presence of an amide functional group at chemical shifts between δ 164.4-172.1. The carbonyl signal for **79** and **80** in which the compounds have a fluorine atom in the *ortho*-position appear as doublets at δ 165.3 and δ 164.4, respectively, with a coupling constant (J_{CF}) of 1.0 Hz and 1.2 Hz, respectively. The carbonyl signal for **81** also appears as a doublet at δ 167.8 due to the presence of a fluorine atom in the *meta* position and has a coupling constant (J_{CF}) of 1.6 Hz.

Peaks from the IR spectra further confirmed the presence of an amide by the appearance of carbonyl peaks ranging between 1634-1678 cm⁻¹ with the NH peaks appearing in a range of 3393-3156 cm⁻¹ (**Table 29**).

Table 29: Selected peaks from IR spectroscopy of **75-85**.

	75	76	77	78	79	80	81	83	84	85
C=O (cm⁻¹)	1672	1676	1653	1645	1645	1658	1634	1656	1656	1661
N-H (cm⁻¹)	3181, 3391	3156, 3393	3159, 3355	3159, 3389	3179, 3387	3175, 3350	3173, 3353	3169, 3353	3161, 3346	3182, 3381

NHase was able to fully hydrolyse commercially available nitrile compounds **61**, **63**, **64**, **66**, **67**, **68**, **69**, **70**, **71** and **72** within a day. Compound **63**, **64** and **66** contain both an electron donating and withdrawing substituents which are *para* (**63** and **66**) or *ortho* (**64**) to each other, therefore, the electron withdrawing group is able to withdraw the electron density being donated to the ring. Compounds **69** and **72** are pyridines while **61** is a pyrimidine derivative and therefore they are electron poor compared to the benzene ring. The nitrogen atom in the ring (pyridine and pyrimidine) withdraws the electron density being donated to the ring. Therefore, the nitrile carbon atom is electron poor and hence these compounds were easily hydrolysed even in the presence of an electron donating substituent (**61** and **69**). Compounds containing electron donating substituents such as **62**, **65** and **73** were not fully hydrolysed by NHase within a day, however, after two days they were also fully hydrolysed. The rate of hydrolysis by NHase varies as it was able to fully hydrolyse compounds with electron withdrawing substituents within a day, and unable to fully hydrolyse those with electron donating substituents, however after two day they were also fully converted.

The ease of NHase to fully hydrolyse nitriles with electron withdrawing substituents could be due to the electrophilicity of the nitrile carbon atom being increased. The presence of a fluorine atom in the *ortho*-position didn't hinder the activity of NHase as observed for **66** and **67** in contrast to the 2,6-difluorobenzonitrile derivative which was reported to have decreased the activity of NHase from *Rhodococcus erythropolis*, as discussed previously in

the introduction. Compounds with *ortho*-substituents (**61**, **62**, **63**, **66**, **67**, **68**, **69** and **73**) can hinder the activity of NHase by steric hindrance, however, this was not the case for these compounds as electronic effects seem to predominantly influence the activity of NHase towards these simple compounds.

2.4.6 Substrate preference of NHase

NHase was generally more active towards the simple commercial nitrile compounds compared to the synthesized biaryl and MBH compounds, while it was completely inactive towards the imidazo[1,2-*a*]pyridine compounds. This could be due to the smaller size of the commercial nitriles in comparison with the more complicated synthesized nitrile substrates. Better amide conversions were obtained for the synthesized MBH compounds in comparison with the biaryl compounds, however, the rate of hydrolysis for the MBH compounds was slow in comparison with the biaryl compounds. MBH compounds were subjected to NHase for 5 days while the biaryl compounds required 2 days reaction time.

Chapter 3

3.0 Conclusions and future work

We were successful in synthesizing nitrile-bearing compounds using the GBB, MBH and the Suzuki-Miyaura coupling reactions. The prepared nitrile compounds, together with the commercial nitrile compounds, were subjected to NHase. The amide yields obtained and the duration of the reaction were used to postulate some of the factors which affect the activity of NHase. Steric hindrance and electronic effects were the two factors which we focused on in order to understand and be able to predict the activity of NHase.

Electronic effects as initially hypothesized affect the activity of NHase as observed for biaryl compounds with electron donating substituents (3,4-dimethoxy group) such as **53c** and **53j** in which there was complete loss of NHase activity. NHase was still not active towards biaryl compounds containing a 3,4-dimethoxyphenyl group and an electron withdrawing substituent (**53h** and **53p**). Compound **53o** contains an electron withdrawing group (4-chlorophenyl), however only 5% of the amide was obtained. This low amide yield is likely due to steric hindrance which is introduced by the 4-chlorophenyl group. This could indicate that both **53o** and **53p** are sterically demanding. Therefore the activity of NHase towards these compounds (**53o** and **53p**) is highly influenced by steric effects and not electronic effects as the nitrile carbon atom for **53o** is highly electrophilic due to the presence of the chlorine atom and the nitrogen atom within the ring.

NHase was able to convert **53a** which has an electron donating group (phenyl group), however better amide yields were obtained for **53b** which has an electron withdrawing group (4-chlorophenyl group). High amide yields for the biaryl compounds were not obtained even for compounds with electron withdrawing substituents possibly due to conformations (twist along the C-C bond) adopted by the biaryl compounds.

NHase was not able to hydrolyze imidazo[1,2-*a*]pyridine compounds. We propose that the inability of NHase to hydrolyze the compounds could be due to steric effects. This indicates that even if the nitrile carbon atom is highly electrophilic if the NHase is unable to access the nitrile group due to steric hindrance, hydrolysis will not occur.

Commercially available simple nitriles with electron donating substituents (**62**, **65** and **73**) were fully converted, however, the hydrolysis was slower in comparison with the other simple nitriles. Commercially available nitriles containing both electron-withdrawing and donating group were fully hydrolyzed within a day (**Table 28**). This indicates that NHase prefers the smaller simple nitrile compounds as it was able to fully convert the compounds with electron donating groups, however, was unable to hydrolyze biaryl compounds and MBH compounds (**56f**) with electron donating substituents.

The work described here has been published in part in *Molecules* **2020**, *25*(1), 238; <https://doi.org/10.3390/molecules25010238>

In future the activity of NHase against the varying nitrile compounds should be subjected to computational protein modeling and docking studies in order to explain the yields obtained and extrapolate other potential nitrile substrates. Computational chemistry should also be used to identify other amino acids that the nitrile compounds interact with other than the amino acids in the active site so as to understand the role these amino acids play in NHase activity, such as those in the channel to the active site. As observed from the results, NHase prefers smaller and simple nitrile compounds in comparison with bulky nitrile compounds, therefore an amino acid that hinders the interaction between the substrate and NHase could be identified through computational studies. This amino acid could be modified through directed evolution (genetic engineering) to introduce an amino acid that will allow NHase to interact with nitriles from more sterically demanding compounds. This will also broaden its commercial application as it can be applied to a number of larger compounds. Whole cell Nitrilases (A29 and A99) should also be extensively studied through substrate profiling in order to clearly understand some of the factors which affect their catalytic activity.

Chapter 4

4. Experimental procedures

4.1 General laboratory procedures

Hexane and ethyl acetate were used for chromatographic purifications after distillation. Solvents such as THF, MeCN, toluene, DCM and DMF were distilled under nitrogen before use.

TLC (Thin layer chromatography) was applied to monitor progress of the reactions using aluminium-backed Merck silica gel 60 F₂₅₄ plates. The plates were visualized under UV light (254 nm and 366 nm).

Compounds were purified under gravity using either normal (particle size 0.063-0.200 mm) or flash (0.040-0.063 mm) silica gel purchased from Merck.

Nuclear magnetic resonance (NMR) spectroscopy was used for compound characterization. NMR spectra were recorded using a Bruker AVANCE 300, 400 or 500 MHz spectrometer. Deuterated chloroform and dimethyl sulfoxide-*d*₆ were used to dissolve the compounds for NMR spectroscopic analysis. ¹H and ¹³C NMR were referenced to trimethylsilane at 0.00 ppm for CDCl₃ solutions. For DMSO solutions, DMSO-*d*₆ signals at 2.50 ppm for ¹H NMR, and at 39.52 ppm for ¹³C NMR were used for referencing purposes.

High resolution mass spectra were recorded on a Bruker Compact Q-TOF high resolution Compact mass spectrometer.

Infrared spectra were recorded on a Bruker Tensor 27 standard system spectrophotometer. The measurements were reported on the wavenumber scale (cm⁻¹).

Melting points were recorded on a Stuart SMP10-4 melting point instrument and are uncorrected.

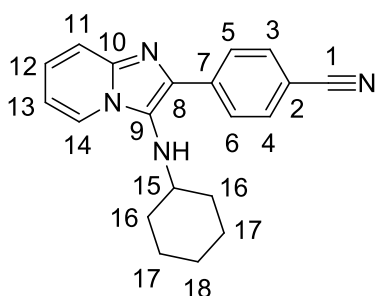
4.2 Experimental procedures

4.2.1 Groebke-Blackburn-Bienaymé multicomponent reaction general procedure.

2-Aminopyridine (1.33 mmol), aldehyde (1.33 mmol), isocyanide (1.36 mmol) and montmorillonite K-10 clay (250 mg) were reacted in dioxane (2.5 ml) in a closed system overnight at 100 °C. After reaction completion the reaction mixture was cooled and filtered to remove the K-10 clay from the mixture. The reaction mixture was extracted with ethyl acetate (30 ml) and washed with water (2 × 30 ml). The organic layer was dried over anhydrous Na₂SO₄ and the solvent was removed *in vacuo*. The mixture was purified by flash silica gel column chromatography using 5-15% ethyl acetate / hexane as eluent.

4.2.1.1 Synthesis of 4-(3-(cyclohexylamino)imidazo[1,2-*a*]pyridin-2-yl)benzotrile¹¹¹ (50a)

2-Aminopyridine (125 mg), 4-formylbenzotrile (174 mg), cyclohexyl isocyanide (148 mg) in the presence of K-10 clay and dioxane were reacted overnight as described in 4.2.3 to afford compound **50a** (105.9 mg, 25%) as a yellow powder.

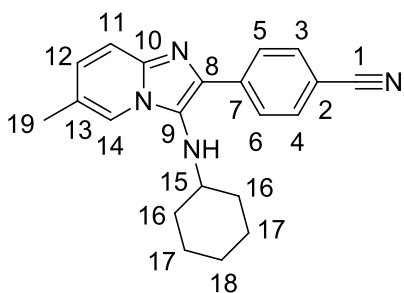


R_f (50% EtOAc/ hexane) 0.44; **mp** 189-193 °C; **IR** ($\nu_{\max}/\text{cm}^{-1}$) 3306 (N-H), 2926 (C-H), 2220 (C=N); **¹H NMR** (400 MHz, CDCl₃): δ 8.32-8.18 (m, 2H, H5 & H6), 8.05 (dt, J = 6.9, 1.2 Hz, 1H, H14), 7.75-7.65 (m, 2H, H3 & H4), 7.53 (dt, J = 9.1, 1.1 Hz, 1H, H11), 7.17 (ddd, J = 9.1, 6.6, 1.3 Hz, 1H, H12), 6.81 (td, J = 6.8, 1.1 Hz, 1H, H13), 3.08 (br s, 1H, NH), 2.97-2.92 (m, 1H,

H15), 1.89-1.54 (m, 5H_{eq}, H16, H17 & H18), 1.33-1.09 (m, 5H_{ax}, H16, H17 & H18); **¹³C NMR** (101 MHz, CDCl₃): δ 141.9 (C10), 139.1 (C7), 134.5 (C8), 132.2 (C3 & C4), 127.2 (C5 & C6), 126.2 (C9), 124.8 (C12), 122.7 (C14), 119.2 (C1), 117.7 (C11), 112.2 (C13), 110.3 (C2), 57.0 (C15), 34.3 (C16), 25.6 (C18), 24.8 (C17).

4.2.1.2 Synthesis of 3-(cyclohexylamino)-6-methylimidazo[1,2-*a*]pyridin-2-yl)benzotrile (50b)

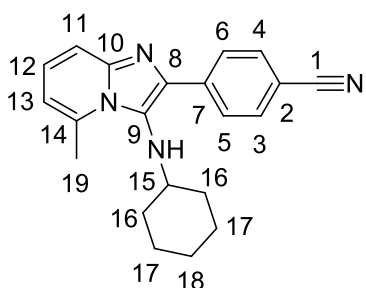
2-Amino-5-methylpyridine (144 mg), 4-formylbenzotrile (174 mg) and cyclohexyl isocyanide (148 mg) dissolved in dioxane were reacted in the presence of K-10 clay to give compound **50b** as a yellow powder (90 mg, 21%).



R_f (50% EtOAc/ hexane) 0.5; **mp** 230-240 °C; **IR** ($\nu_{\max}/\text{cm}^{-1}$) 3236 (N-H), 2929 (C-H), 2219 (C=N); **¹H NMR** (400 MHz, CDCl₃): δ 8.40-8.15 (m, 2H, H5 & H6), 7.92-7.78 (m, 1H, H14), 7.77-7.63 (m, 2H, H3 & H4), 7.50-7.43 (m, 1H, H11), 7.14-6.96 (m, 1H, H12), 3.10-2.90 (m, 2H, NH & H15), 2.48-2.33 (m, 3H, H19), 1.91-1.56 (m, 5H_{eq}, H16, H17 & H18), 1.39-1.13 (m, 5H_{ax}, H16, H17 & H18); **¹³C NMR** (101 MHz, CDCl₃): δ 141.1 (C10), 139.3 (C7), 134.6 (C8), 132.2 (C3 & C4), 128.0 (C12), 127.1 (C5 & C6), 125.8 (C9), 121.9 (C13), 120.2 (C14), 119.3 (C1), 117.1 (C11), 110.1 (C2), 57.0 (C15), 34.3 (C16), 25.7 (C18), 24.9 (C17), 18.5 (C19); **HRMS** (m/z), calculated for C₂₁H₂₃N₄: 331.1917, found (M + H)⁺: 331.1920.

4.2.1.3 Synthesis of 4-(3-(cyclohexylamino)-5-methylimidazo[1,2-a]pyridin-2-yl)benzotrile (50c)

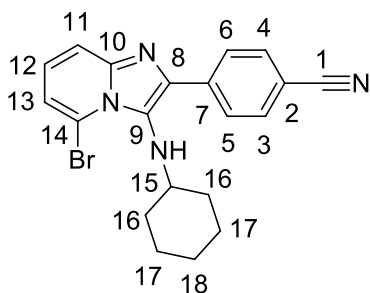
2-Amino-6-methylpyridine (144 mg), 4-formylbenzotrile (174 mg) and cyclohexyl isocyanide (148 mg) in dioxane were reacted in the presence of K-10 clay to afford compound **50c** as a yellow oil (90 mg, 25%).



R_f (50% EtOAc/ hexane) 0.56; **IR** ($\nu_{\max}/\text{cm}^{-1}$) 3343 (N-H), 2928 (C-H), 2224 (C=N); **¹H NMR** (400 MHz, CDCl₃): δ 8.18 (d, J = 8.4 Hz, 2H, H5 & 6), 7.69 (d, J = 8.4 Hz, 2H, H3 & H4), 7.41 (d, J = 9.0 Hz, 1H, H11), 7.04 (dd, J = 9.0, 6.8 Hz, 1H, H12), 6.46 (d, J = 6.8 Hz, 1H, H13), 3.07 (s, 1H, NH), 2.92 (s, 3H, H19), 2.82-2.72 (m, 1H, H15), 1.76-1.47 (m, 5H_{eq}, H16, H17 & H18), 1.10-1.06 (m, 5H_{ax}, H16, H17 & H18); **¹³C NMR** (101 MHz, CDCl₃): δ 143.7 (C10), 139.8 (C7), 137.1 (C8), 136.2 (C14), 132.1 (C3 & C4), 128.0 (C5 & C6), 127.5 (C9), 124.9 (C12), 119.3 (C1), 116.2 (C11), 114.0 (C13), 110.4 (C2), 59.2 (C15), 33.3 (C16), 25.7 (C18), 24.9 (C17), 20.0 (C19); **HRMS** (m/z), calculated for C₂₁H₂₃N₄: 331.1917, found (M + H)⁺: 331.1922.

4.2.1.4 Synthesis of 4-(5-bromo-3-(cyclohexylamino)imidazo[1,2-*a*]pyridin-2-yl)benzotrile (50d)

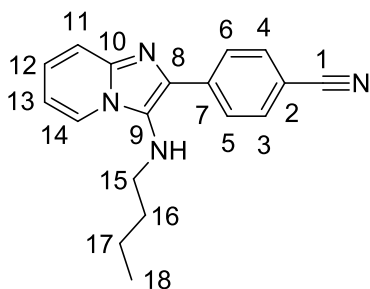
2-Amino-6-bromopyridine (230 mg), 4-formylbenzotrile (174 mg) and cyclohexyl isocyanide (148 mg) in dioxane were reacted in the presence of K-10 clay to give compound **91** as a yellow powder (221.3 mg, 42%).



R_f (50% EtOAc/ hexane) 0.68; **mp** 165-168°C; **IR** ($\nu_{\max}/\text{cm}^{-1}$) 3368 (N-H), 2927 (C-H), 2218 (C=N); **¹H NMR** (400 MHz, CDCl₃): δ 8.50-8.41 (m, H5 & H6), 7.73-7.66 (m, H3 & H4), 7.53 (dd, $J = 8.4$ Hz, 1.7 Hz, 1H, H13), 7.07-6.90 (m, 2H, H11 & 12), 3.72 (d, $J = 4.0$ Hz, 1H, NH), 2.96-2.86 (m, 1H, H15), 1.73-1.50 (m, 5H_{eq}, H16, H17 & H18), 1.26-1.05 (m, 5H_{ax}, H16, H17 & H18); **¹³C NMR** (101 MHz, CDCl₃): δ 144.4 (C10), 139.1 (C7), 137.2 (C8), 132.0 (C3 & C4), 128.4 (C9), 128.1 (C5 & C6), 124.9 (C11), 119.3 (C1), 118.9 (C12), 117.7 (C13), 111.8 (C14), 110.6 (C2), 59.4 (C15), 33.0 (C16), 25.8 (C18), 24.9 (C17). **HRMS** (m/z), calculated for C₂₀H₂₀BrN₄: 395.0866, found (M + H)⁺: 395.0868.

4.2.1.5 Synthesis of 4-(3-(Butylamino)imidazo[1,2-*a*]pyridin-2-yl)benzotrile (50e)

2-Aminopyridine (125 mg), 4-formylbenzotrile (174 mg) and butyl isocyanide (113 mg) in dioxane were reacted in the presence of K-10 clay to give compound **50e** as a yellow powder (64.4 mg, 17%).

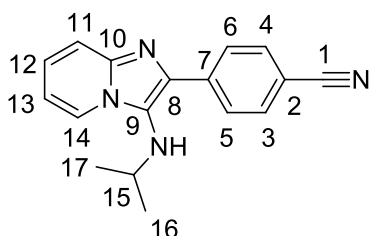


R_f (50% EtOAc/ hexane) 0.56; **mp** 124-126 °C; **IR** ($\nu_{\max}/\text{cm}^{-1}$) 3310 (N-H), 2955 (C-H), 2217 (C=N); **¹H NMR** (400 MHz, CDCl₃): δ 8.18 (d, $J = 8.2$ Hz, 2H, H5 & H6), 8.02 (d, $J = 6.9$ Hz, 1H, H11), 7.69 (d, $J = 8.2$ Hz, 2H, H3 & H4), 7.54 (d, $J = 9.1$ Hz, 1H, H14), 7.17 (ddd, $J = 9.1, 6.6, 1.3$ Hz, 1H, H13), 6.83 (t, $J = 6.7$ Hz, 1H, H12), 3.11-3.02 (m, 3H, NH & H15), 1.70-1.50 (m, 2H, H16), 1.48-1.38 (m, 2H, H17), 0.93 (t, $J = 7.3$ Hz, 3H, H18); **¹³C NMR** (101 MHz, CDCl₃): δ

141.9 (C10), 139.1 (C7), 133.8 (C8), 132.3 (C3 & C4), 127.5 (C9), 127.1 (C5 & C6), 124.7 (C13), 122.4 (C11), 119.2 (C1), 117.9 (C14), 112.2 (C12), 110.3 (C2), 48.1 (C15), 32.9 (C16), 20.2 (C17), 13.9 (C18). **HRMS** (m/z), calculated for C₁₈H₁₉N₄: 291.1604, found (M + H)⁺: 291.1609.

4.2.1.6 Synthesis of 4-(3-(isopropylamino)imidazo[1,2-a]pyridin-2-yl)benzonitrile (**50f**)

2-Aminopyridine (125 mg), 4-formylbenzonitrile (174 mg) and isopropyl isocyanide (92 mg) in dioxane were reacted in the presence of K-10 clay to afford **50f** as a yellow powder (81 mg, 22%).



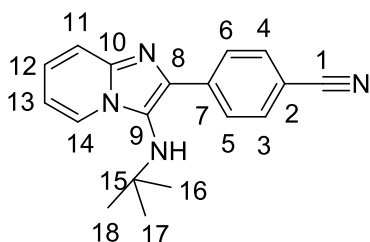
R_f (50% EtOAc/ hexane) 0.47; **mp** 122-124 °C; **IR** (ν_{max}/cm⁻¹)

3245 (N-H), 2955 (C-H), 2220 (C=N); **¹H NMR** (300 MHz, CDCl₃): δ 8.32-8.18 (m, 2H, H5 & H6), 8.07 (dt, *J* = 6.9, 1.2 Hz, 1H, H14), 7.77-7.63 (m, 2H, H3 & H4), 7.54 (dt, *J* = 9.2, 1.1 Hz, 1H, H11), 7.18 (ddd, *J* = 9.1, 6.6, 1.3 Hz, 1H, H12), 6.82 (td, *J* =

6.8, 1.2 Hz, 1H, H13), 3.51-3.32 (m, 1H, H15), 3.07 (d, *J* = 4.5 Hz, 1H, NH), 1.12 (d, *J* = 6.2 Hz, 6H, H16 & H17); **¹³C NMR** (75 MHz, CDCl₃): δ 142.0 (C10), 139.1 (C7), 134.9 (C8), 132.2 (C3 & C4), 127.2 (C5 & C6), 126.3 (C9), 124.8 (C12), 122.7 (C14), 119.2 (C1), 117.7 (C11), 112.2 (C13), 110.2 (C2), 49.2 (C15), 23.4 (C16 & 17); **HRMS** (m/z), calculated for C₁₇H₁₇N₄: 277.1448, found (M + H)⁺: 277.1454.

4.2.1.7 Synthesis of 4-(3-(*tert*-butylamino)imidazo[1,2-*a*]pyridin-2-yl)benzonitrile⁹¹ (**50h**)

2-Aminopyridine (125 mg), 4-formylbenzonitrile (174 mg) and *tert*-butyl isocyanide (0.15 ml) in dioxane were reacted in the presence of K-10 clay to give compound **50h** as a yellow powder (67.4 mg, 17%).



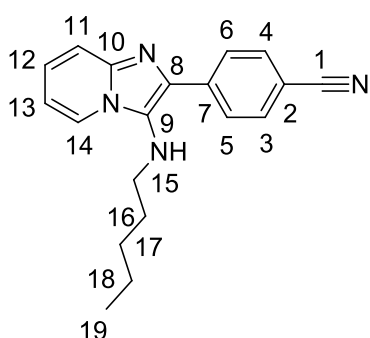
R_f (50% EtOAc/ hexane) 0.47; **mp** 170-173°C; [lit 155-160 °C];

IR (ν_{max}/cm⁻¹); 3280 (N-H), 2964 (C-H), 2224 (C=N); **¹H NMR** (400 MHz, CDCl₃): δ 8.28-8.03 (m, 3H, H5, H6 & H11), 7.82-7.63 (m, 2H, H3 & H4), 7.54 (d, *J* = 9.0, 1H, H14), 7.18 (ddd, *J* = 9.2, 6.5, 1.3 Hz, 1H, H12), 6.81 (td, *J* = 6.8, 1.2 Hz, 1H, H13),

3.02 (s, 1H, NH), 1.07 (s, 9H, H16, H17 & H18); ^{13}C NMR (101 MHz, CDCl_3): δ 142.5 (C10), 140.0 (C7), 137.5 (C8), 132.0 (C3 & C4), 128.4 (C5 & C6), 124.8 (C12), 124.5 (C9), 123.4 (C11), 119.2 (C1), 117.7 (C14), 111.9 (C13), 110.5 (C2), 56.7 (C15), 30.5 (C16, 17 & 18).

4.2.1.8 Synthesis of 4-(3-(pentylamino)imidazo[1,2-a]pyridin-2-yl)benzotrile (50g)

2-Aminopyridine (125 mg), 4-formylbenzotrile (174 mg) and 1-pentyl isocyanide (129 mg) in dioxane were reacted in the presence of K-10 clay to give compound **50g** as a yellow powder (142.2 mg, 35%).

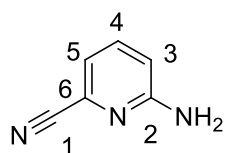


R_f (50% EtOAc/ hexane) 0.5; mp 120-122 °C; IR (ν_{max}/cm^{-1}) 3232 (N-H), 2953 (C-H), 2221 (C=N); ^1H NMR (300 MHz, CDCl_3): δ 8.29-8.13 (m, 2H, H5 & H6), 8.02 (dt, $J = 6.9, 1.2$ Hz, 1H, H14), 7.73-7.65 (m, 2H, H3 & H4), 7.54 (dt, $J = 9.1, 1.1$ Hz, 1H, H11), 7.18 (ddd, $J = 9.1, 6.7, 1.3$ Hz, 1H, H12), 6.83 (td, $J = 6.8, 1.1$ Hz, 1H, H13), 3.12-3.10 (m, 1H, NH), 3.09-2.97 (m, 2H, H15), 1.67-1.55 (m, 2H, H16), 1.46-1.26 (m, 4H, H17 & H18), 1.03-0.80 (m, 3H, H19); ^{13}C NMR (75 MHz, CDCl_3): δ 141.9 (C10), 139.1 (C7), 133.8 (C8), 132.3 (C3 & C4), 127.5 (C9), 127.1 (C5 & C6), 124.7 (C12), 122.4 (C14), 119.2 (C1), 117.8 (C11), 112.2 (C13), 110.3 (C2), 48.3 (C15), 30.5 (C16), 29.2 (C17), 22.5 (C18), 14.0 (C19).

4.2.2 Groebke-Blackburn-Bienaymé multicomponent reaction with 2-cyano-6-aminopyridine as a starting material

4.2.2.1 Synthesis of 2-amino-6-cyanopyridine⁹² (48e)

2-Amino-6-bromopyridine (2.05 g) was reacted with $\text{CuCN}\cdot\text{H}_2\text{O}$ (7 g, 3 eq) in the presence of DMF overnight at 100 °C in a closed system. After reaction completion the mixture was extracted with ethyl acetate (40 ml) and washed with saturated ammonium chloride (4 × 20 ml) and water (4 × 10 ml). The saturated ammonium chloride was added to form copper hydroxide which precipitates and gives of a light blue colour. After extraction the organic layer was dried over anhydrous Na_2SO_4 and the solvent was removed *in vacuo*. The mixture was purified by flash silica gel column chromatography using 5-15% ethyl acetate / hexane as eluent to afford **48e** as a white powder (70 mg, 5%).

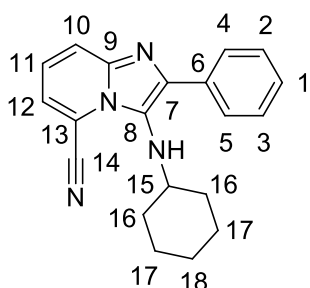


R_f (50% EtOAc/ hexane) 0.59; **IR** ($\nu_{\max}/\text{cm}^{-1}$) 3425 (N-H), 3191 (N-H), 2236 (CN); **¹H NMR** (400 MHz, DMSO-*d*₆): δ 7.51 (dd, *J* = 8.6, 7.1 Hz, 1H, H4), 7.02 (dd, *J* = 7.1, 0.8 Hz, 1H, H5), 6.71 (dd, *J* = 8.6, 0.9 Hz, 1H, H3), 6.55 (br s, 2H, NH₂); **¹³C NMR**: δ 160.2 (C2), 137.9 (C4), 130.3 (C6), 118.0 (C1), 117.1 (C5), 113.1 (C3); **HRMS** (*m/z*), calculated for C₆H₆N₃: 120.0556, found (M + H)⁺: 120.0558.

4.2.2.2 Synthesis of 3-(cyclohexylamino)-2-phenylimidazo[1,2-*a*]pyridine-5-carbonitrile

(50i)

2-Cyano-6-aminopyridine (30 mg, 0.25 mmol), benzaldehyde (0.026 ml), cyclohexyl isocyanide (0.031 ml) were reacted in the presence of K-10 clay and dioxane as described in 4.2.3 to afford compound **50i** as a yellow powder (11.6 mg, 15%).

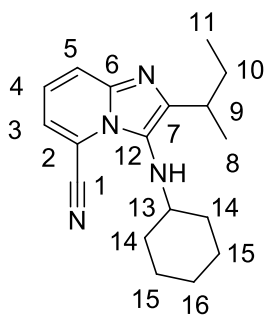


R_f (50% EtOAc/ hexane) 0.68; **mp** 143-145°C; **IR** ($\nu_{\max}/\text{cm}^{-1}$) 3376 (N-H), 2922 (C-H), 2216 (C=N) **¹H NMR** (400 MHz, CDCl₃): δ 8.07 (d, *J* = 7.5 Hz, 2H, H4 & H5), 7.81 (d, *J* = 8.6 Hz, 1H, H10), 7.47 (t, *J* = 7.6 Hz, 2H, H2 & H3), 7.35-7.38 (m, 2H, H1 & H12), 7.14 (t, *J* = 7.9 Hz, 1H, H11), 3.37 (d, *J* = 4.9 Hz, 1H, NH), 3.01 (s, 1H, H15), 1.87-1.48 (m, 5H_{eq}, H16, H17 & H18), 1.30-1.09 (m, 5H_{ax}, H16, H17 & H18); **¹³C NMR** (101 MHz, CDCl₃): δ 141.0 (C9), 139.7 (C6), 133.4 (C7), 128.6 (C2 & C3), 128.2 (C1), 127.6 (C4 & C5), 126.7 (C8), 124.1 (C12), 122.8 (C10), 121.9 (C11), 114.2 (C14), 107.7 (C13), 57.4 (C15), 33.0 (C16), 25.7 (C18), 24.9 (C17); **HRMS** (*m/z*), calculated for C₂₀H₂₁N₄: 317.1761, found (M + H)⁺: 317.1764.

4.2.2.3 Synthesis of 2-(*sec*-butyl)-3-(cyclohexylamino)imidazo[1,2-*a*]pyridine-5-carbonitrile

(50j)

2-Cyano-6-aminopyridine (45 mg), 2-methylbutyraldehyde (32.56 mg), cyclohexyl isocyanide (41.26 mg) were reacted in the presence of K-10 clay and dioxane to afford **50j** as a yellow oil (25.6 mg, 23%).



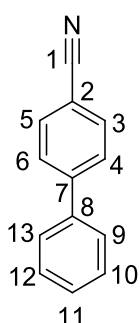
R_f (50% EtOAc/ hexane) 0.68; **IR** ($\nu_{\max}/\text{cm}^{-1}$) 3333 (N-H), 2926 (C-H), 2219 (C=N); **¹H NMR** (300 MHz, CDCl₃): δ 7.74 (dd, $J = 8.9, 1.2$ Hz, 1H, H5), 7.32 (dd, $J = 7.0, 1.2$ Hz, 1H, H3), 7.07 (dd, $J = 8.9, 7.1$ Hz, 1H, H4), 3.15-2.98 (m, 1H, H13), 2.93-2.88 (m, 1H, NH), 2.00-1.60 (m, 8H, H9, H10, H14, H15 & H16), 1.41-1.16 (m, 8H, H8, H14, H15 & H16), 0.85 (t, $J = 7.4$ Hz, 3H, H11); **¹³C NMR** (75 MHz, CDCl₃): δ 147.7 (C6), 141.3 (C7), 126.0 (C12), 123.5 (C3), 122.3 (C5), 121.0 (C4), 114.3 (C1), 107.4 (C2), 58.1 (C13), 33.22 (C9), 33.18 (C14), 33.0 (C14), 29.8 (C10), 25.8 (C16), 25.1 (C15), 25.0 (C15), 20.6 (C8), 12.5 (C11). **HRMS** (m/z), calculated for C₁₈H₂₄N₄: 297.2074, found (M + H)⁺: 297.2077.

4.2.3 Suzuki coupling reaction- general procedure

A benzonitrile derivative was reacted with boronic acid in the presence of Pd(PPh₃)₄ (5 mol%) which was freshly prepared, and 2M Na₂CO₃ (4 mol) in DME (15 ml) and the reaction mixture was refluxed overnight under nitrogen. After reaction completion the reaction mixture was cooled and was extracted with ethyl acetate (30 ml) and washed with water (2×10 ml). The organic layer was dried over anhydrous Na₂SO₄ and the solvent was removed *in vacuo*. The mixture was purified by flash silica gel column chromatography using 0-5 % ethyl acetate / hexane as eluent.

4.2.3.1 Synthesis of [1,1'-biphenyl]-4-carbonitrile⁹⁴ (53a)

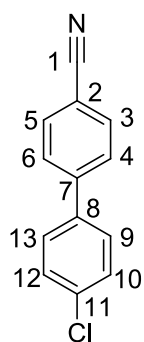
4-Bromobenzonitrile (100 mg, 0.55 mol), phenylboronic acid (80 mg, 0.66 mol), Pd(PPh₃)₄ (32.46 mg) and Na₂CO₃ (238 mg, 1.12 ml) were reacted in the presence of DME as described in 4.2.1 to give compound **53a** (79 mg, 98%), as a white powder.



R_f (50% EtOAc/ hexane) 0.83; **mp** 85-86 °C; [lit 80-81 °C] **IR** ($\nu_{\max}/\text{cm}^{-1}$) 2923 (C-H), 2221 (C=N); **¹H NMR** (400 MHz, CDCl₃) δ 7.71 (2×d, $J = 8.4, 8.3$ Hz, 4H, H3, H4, H5 & H6), 7.58 (d, $J = 7.1$ Hz, 2H, H9 & H13), 7.48 (t, $J = 7.3$ Hz, 2H, 10 & H12), 7.42 (t, $J = 7.2$ Hz, 1H, H11); **¹³C NMR** (101 MHz, CDCl₃): δ 145.6 (C7), 139.1 (C8), 132.6 (C3 & C5), 129.1 (C9 & C13), 128.7 (C11), 127.7 (C4 & C6), 127.2 (C10 & C12), 118.9 (C1), 110.9 (C2). **HRMS** (m/z), calculated for C₁₃H₁₀N: 180.0808, found (M + H)⁺: 180.0805

4.2.3.2 Synthesis of 4'-chloro-[1,1'-biphenyl]-4-carbonitrile⁹⁸ (53b)

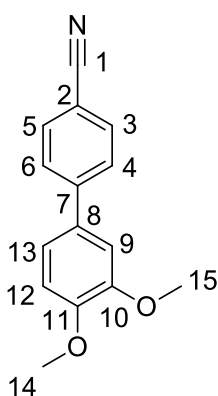
4-Bromobenzonitrile (100 mg, 0.55 mol), 4-chlorophenyl boronic acid (103 mg, 0.66 mol), Pd(PPh₃)₄ (32.46 mg) and Na₂CO₃ (238 mg, 1.12 ml) were reacted in the presence of DME to give compound **53b** as a white powder (90.3 mg, 77%).



R_f (50% EtOAc/ hexane) 0.83; **mp** 129-132°C; [**lit.** 130-132 °C]; **IR** (ν_{max}/cm⁻¹); 2957 (C-H), 2222 (C=N); **¹H NMR** (300 MHz, CDCl₃): δ 7.76-7.70 (m, 2H, H4 & H6), 7.68-7.62 (m, 2H, H 3 & H5), 7.55-7.49 (m, 2H, H10 & H12), 7.48-7.43 (m, 2H, H9 & H13); **¹³C NMR** (75 MHz, CDCl₃): δ 144.7 (C7), 137.9 (C8), 135.3 (C11), 133.1 (C4 & C6), 129.7 (C9 & C13) , 128.8 (C10 & C12), 127.9 (C3 & C5), 119.1 (C1), 111.6 (C2); **HRMS** (m/z), calculated for C₁₃H₁₀ClN: 214.0418, found (M + H)⁺ :214.0419.

4.2.3.3 Synthesis of 3', 4'-dimethoxy-[1,1'-biphenyl]-4-carbonitrile⁹⁷ (53c)

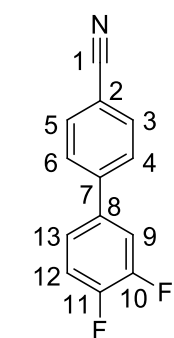
4-Bromobenzonitrile (44 mg, 0.24 mol), 3, 4-dimethoxyphenyl boronic acid (52 mg, 0.29 mol), Pd(PPh₃)₄ (14.0 mg) and Na₂CO₃ (104.8 mg, 0.49 ml) were reacted in the presence of DME (10 ml) to afford compound **53c** as a yellow powder (32.6 mg, 55%).



R_f (50% EtOAc/ hexane) 0.67; **mp** 139-140°C; **IR** (ν_{max}/cm⁻¹) 2926 (C-H), 2219 (C=N); **¹H NMR** (300 MHz, CDCl₃): δ 7.73-7.62 (m, 4H, H3, H4, H5 & H6), 7.17 (dd, *J* = 8.3, 2.1 Hz, 1H, H 13), 7.09 (d, *J* = 2.0 Hz, 1H, H 9), 6.97 (d, *J* = 8.3 Hz, 1H, H 12), 3.96 & 3.94(2xs, 6H, H14 & H15) **¹³C NMR** (75 MHz, CDCl₃): δ 149.8 & 149.5 (C10 & C11), 145.4 (C7), 132.7 (C3 & 5), 131.9 (C8), 127.3 (C4 & 6), 119.9 (C13), 119.0 (C1), 111.6 (C12), 110.3 (C9), 56.1 & 56.0 (C14 & C15).

4.2.3.4 Synthesis of 3',4'-difluoro-[1,1'-biphenyl]-4-carbonitrile⁹⁵ (53d)

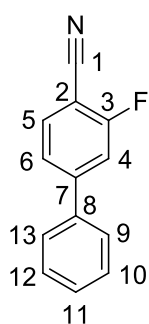
4-Bromobenzonitrile (100 mg, 0.55 mol), 3,4-difluorophenyl boronic acid (173.54 mg, 1.01 mol), Pd(PPh₃)₄ (32.46 mg) and Na₂CO₃ (238 mg, 1.12 ml) were reacted in the presence of DME to afford compound **53d** as a white powder (125.2 mg, 98%).



R_f (50% EtOAc/ hexane) 0.83; **mp** 105-106 °C; **IR** ($\nu_{\max}/\text{cm}^{-1}$) 3061 (C-H), 2222 (C=N); **¹H NMR** (400 MHz, CDCl₃): δ 7.76-7.71 (m, 2H, H3 & H5), 7.65-7.60 (m, 2H, H6 & H4), 7.40 (ddd, $J = 11.2, 7.4, 2.2$ Hz, 1H, H9), 7.36-7.29 (m, 1H, H13), 7.26-7.29 (m, 1H, H12); **¹³C NMR** (101 MHz, CDCl₃): δ 150.8 & 150.7 (d, $J_{\text{CF}} = 250.5, 12.6$ Hz & d, $J_{\text{CF}} = 251.5, 12.5$ Hz, C10 & C11), 143.5 (d, $J_{\text{CF}} = 1.7$ Hz, C7), 136.3 (dd, $J_{\text{CF}} = 5.9, 3.9$ Hz, C8), 132.8 (C5 & C3), 127.6 (C6 & C4), 123.4 (dd, $J_{\text{CF}} = 6.4, 3.6$ Hz, C13), 118.6 (C1), 118.1 (d, $J_{\text{CF}} = 17.5$ Hz, C12), 116.3 (d, $J_{\text{CF}} = 18.1$ Hz, C9), 111.6 (C2).

4.2.3.5 Synthesis of 3-fluoro-[1,1'-biphenyl]-4-carbonitrile⁹⁶ (53e)

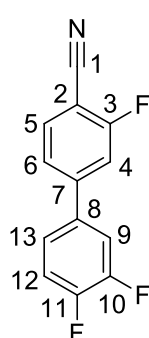
4-Bromo-2-fluorobenzonitrile (100 mg, 0.50 mol), phenylboronic acid (73.16 mg, 0.60 mol), Pd(PPh₃)₄ (30.0 mg) and Na₂CO₃ (212 mg, 1.0 ml) were reacted in the presence of DME to give compound **53e** (89 mg, 82%) as a yellow powder.



R_f (50% EtOAc/ hexane) 0.83; **mp** 102-104°C; **IR** ($\nu_{\max}/\text{cm}^{-1}$) 3050 (C-H), 2226 (C=N); **¹H NMR** (400 MHz, CDCl₃): δ 7.67 (dd, $J = 8.1, 6.7$ Hz, 1H, H5), 7.59-7.55 (m, 2H, H9 & H13), 7.52-7.44 (m, 4H, H6, H10, H11 & H12), 7.42 (dd, $J = 10.2, 1.7$ Hz, 1H, H4); **¹³C NMR** (101 MHz, CDCl₃): δ 163.4 (d, $J = 258.5$ Hz, C3), 148.6 (d, $J = 8.1$ Hz, C7), 137.9 (d, $J = 2.0$ Hz, C8), 133.7 (C5), 129.31 (C11), 129.25 (C10 & C12), 127.2 (C9 & 13), 123.4 (d, $J = 3.2$ Hz, C6), 114.8 (d, $J = 20.2$ Hz, C4), 114.1 (C1), 99.7 (d, $J = 15.7$ Hz, C2).

4.2.3.6 Synthesis of 3,3',4'-trifluoro-[1,1'-biphenyl]-4-carbonitrile (53f)

2-Fluoro-4-bromobenzonitrile (100 mg, 0.50 mol), 3, 4-difluorophenyl boronic acid (93 mg, 0.59 mol), Pd(PPh₃)₄ (30.0 mg) and Na₂CO₃ (212 mg, 1.0 ml) were reacted in the presence of DME to give compound **53f** as a white powder (117 mg, 98%).

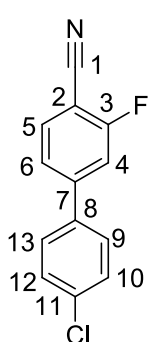


R_f (50% EtOAc/ hexane) 0.83; **mp** 154-156 °C; **IR** ($\nu_{\max}/\text{cm}^{-1}$) 2968 (C-H), 2230 (C=N); **¹H NMR** (400 MHz, CDCl₃): δ 7.71 (dd, $J = 8.1, 6.6$ Hz, 1H, H5), 7.43 (dd, $J = 8.1, 1.7$ Hz, 1H, H6), 7.42-7.39 (m, 1H, H12), 7.38-7.36 (m, 1H, H4), 7.34-7.30 (m, 2H, H9 & H13); **¹³C NMR** (101 MHz, CDCl₃): δ 163.5 (d, $J_{\text{CF}} = 259.4$ Hz, C3),

151.1 & 150.8 (dd, $J_{CF} = 250.7, 41.1$ Hz & dd, $J_{CF} = 244.8, 35.5$ Hz, C10 & C11), 146.3 (d, $J_{CF} = 7.6$ Hz, C7), 135.1 (ddd, $J_{CF} = 6.1, 4.0, 2.1$ Hz, C8), 134.0 (C5), 123.5 (dd, $J_{CF} = 6.6, 3.6$ Hz, C13), 123.3 (d, $J_{CF} = 3.3$ Hz, C6), 118.3 (d, $J_{CF} = 17.4$ Hz, C9), 116.4 (d, $J_{CF} = 18.3$ Hz, C12), 114.8 (d, $J_{CF} = 20.6$ Hz, C4), 113.8 (C1), 100.6 (d, $J_{CF} = 15.6$ Hz, C2); **HRMS** (m/z), calculated for $C_{13}H_7F_3N$: 234.0525, found (M + H)⁺: 234.0525.

4.2.3.7 Synthesis of 4'-chloro-3-fluoro-[1,1'-biphenyl]-4-carbonitrile (**53g**)

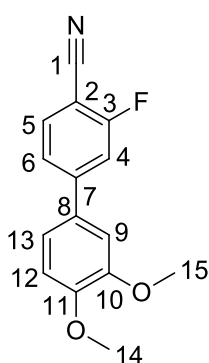
4-Bromo-2-fluorobenzonitrile (100 mg, 0.50 mol), 4-chlorophenyl boronic acid (94.0 mg, 0.60 mol), $Pd(PPh_3)_4$ (29.0 mg) and Na_2CO_3 (212 mg, 1.0 ml) were reacted in the presence of DME to give compound **53g** as a white powder (96.5 mg, 83%).



R_f (50% EtOAc/ hexane) 0.83; **mp** 175-177 °C; **IR** (ν_{max}/cm^{-1}) 2925 (C-H), 2229 (C=N); **¹H NMR** (500 MHz, $CDCl_3$): δ 7.69 (dd, $J = 8.1, 6.6$ Hz, 1H, H5), 7.53-7.49 (m, 2H, H9 & H13), 7.49-7.44 (m, 3H, H6, H10 & H12), 7.40 (dd, $J = 10.1, 1.7$ Hz, 1H, H4); **¹³C NMR**: δ 163.5 (d, $J_{CF} = 259.2$ Hz, C3), 147.2 (d, $J_{CF} = 8.2$ Hz, C7), 136.4 (d, $J_{CF} = 1.8$ Hz, C8), 135.7 (C11), 133.9 (C5), 129.5 (C10 & C12), 128.4 (C9 & C13), 123.2 (d, $J_{CF} = 3.5$ Hz, C6), 114.7 (d, $J_{CF} = 20.4$ Hz, C4), 113.9 (C1), 100.2 (d, $J_{CF} = 15.8$ Hz, C2); **HRMS** (m/z), calculated for $C_{13}H_8ClFN$: 232.0324, found (M + H)⁺: 232.0321.

4.2.3.8 Synthesis of 3-fluoro-3',4'-dimethoxy-[1,1'-biphenyl]-4-carbonitrile (**53h**)

4-Bromo-2-fluorobenzonitrile (100 mg, 0.50 mol), 3, 4-dimethoxyphenyl boronic acid (110 mg, 0.60 mol), $Pd(PPh_3)_4$ (29.0 mg) and Na_2CO_3 (212 mg, 1.0 ml) were reacted in the presence of DME to give compound **53h** as a yellow powder (68.3 mg, 53%).

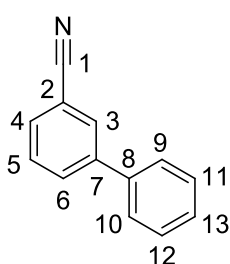


R_f (50% EtOAc/ hexane) 0.71; **mp** 127-128 °C; **IR** (ν_{max}/cm^{-1}) 2922 (C-H), 2223 (C=N); **¹H NMR** (300 MHz, $CDCl_3$): δ 7.64 (t, $J = 7.1$ Hz, 1H, H5), 7.45 (d, $J = 8.0$ Hz, 1H, H6), 7.39 (d, $J = 10.4$ Hz, 1H, H4), 7.17 (d, $J = 7.8$ Hz, 1H, H13), 7.08 (s, 1H, H9), 6.97 (d, $J = 8.2$ Hz, 1H, H12), 3.96 & 3.94 (2xs, 6H, H14 & H15); **¹³C NMR** (75 MHz, $CDCl_3$): δ 163.5 (d, $J_{CF} = 258.0$ Hz, C3), 150.3 & 149.5 (C10 & C11), 148.3 (d, $J_{CF} = 8.2$ Hz, C7), 133.6 (C5), 130.7 (d,

$J_{CF} = 2.1$ Hz, C8), 122.9 (d, $J_{CF} = 3.1$ Hz, C6), 119.9 (C13), 114.22 (C1), 114.20 (d, $J_{CF} = 20.2$ Hz, C4), 111.6 (C12), 110.1 (C9), 99.0 (d, $J_{CF} = 15.7$ Hz, C2), 56.1 & 56.0 (C14 & C15); **HRMS** (m/z), calculated for $C_{15}H_{13}NFO_2$: 258.0925, found (M + H)⁺: 258.0922.

4.2.3.9 Synthesis of [1,1'-biphenyl]-3-carbonitrile⁹⁹ (53i)

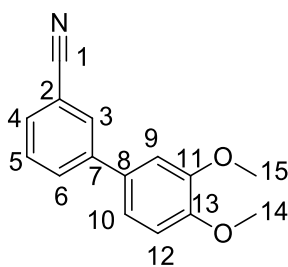
3-Bromobenzonitrile (100 mg, 0.55 mol), phenyl boronic acid (80 mg, 0.66 mol), Pd(PPh₃)₄ (32.0 mg) and Na₂CO₃ (238 mg, 1.12 ml) were reacted in the presence of DME to give compound **53i** (58 mg, 59%) as a colourless oil.



R_f (50% EtOAc/ hexane) 0.79; **IR** (ν_{max}/cm^{-1}) 2967 (C-H), 2228 (C=N); **¹H NMR** (400 MHz, CDCl₃): δ 7.85 (t, $J = 1.7$ Hz, 1H, H3), 7.80 (dt, $J = 7.8$, 1.5 Hz, 1H, H6), 7.61 (dt, $J = 7.7$, 1.4 Hz, 1H, H4), 7.57-7.55 (m, 1H, H5), 7.54-7.53 (m, 2H, H9 & H10), 7.50-7.44 (m, 2H, H11 & H12), 7.43-7.40 (m, 1H, H13); **¹³C NMR** (101 MHz, CDCl₃): δ 142.4 (C7), 138.8 (C8), 131.5 (C6), 130.7 (C4), 129.6 (C3), 129.1 (C11 & C12), 128.4 (C13), 127.1 (C9 & C10), 118.8 (C1), 112.9 (C2).

4.2.3.10 Synthesis of 3',4'-dimethoxy-[1,1'-biphenyl]-3-carbonitrile (53j)

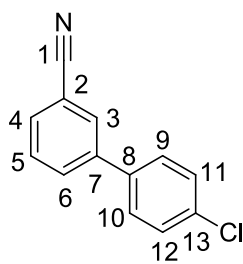
3-Bromobenzonitrile (100 mg, 0.55 mol), 3, 4-dimethoxyphenyl boronic acid (204.52 mg, 1.12 mol), Pd(PPh₃)₄ (32.46 mg) and Na₂CO₃ (238.23 mg, 1.12 ml) were reacted in the presence of DME to give compound **53j** (129.2 mg, 98%) as a white powder.



R_f (50% EtOAc/ hexane) 0.71; **mp** 120-123 °C; **IR** (ν_{max}/cm^{-1}); 2910 (C-H), 2224 (C=N); **¹H NMR** (300 MHz, CDCl₃): δ 7.82-7.80 (m, 1H, H3), 7.77 (dt, $J = 7.7$, 1.4 Hz, 1H, H6), 7.57 (dt, $J = 6.4$, 1.3 Hz, 1H, H4), 7.50 (t, $J = 7.6$ Hz, 1H, H5), 7.11 (dd, $J = 8.3$, 2.1 Hz, 1H, H10), 7.06 (d, $J = 2.0$ Hz, 1H, H9), 6.96 (d, $J = 8.3$ Hz, 1H, H12), 3.95 & 3.93(2*s, 6H, H14 & H15); **¹³C NMR** (75 MHz, CDCl₃): δ 149.5 & 149.4(C11 & C13), 142.2 (C7), 131.6 (C8), 131.1 (C6), 130.3 (C3), 130.1 (C4), 129.5 (C5), 119.5 (C10), 118.9 (C1), 112.8 (C2), 111.6 (C9), 110.1 (C12), 56.02 & 55.99 (C14 & 15). **HRMS** (m/z), calculated for $C_{15}H_{14}NO_2$: 240.1019, found (M + H)⁺: 240.1078.

4.2.3.11 Synthesis of 4'-chloro-[1,1'-biphenyl]-3-carbonitrile (**53k**)

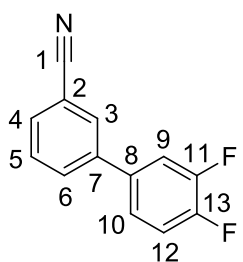
3-Bromobenzonitrile (100 mg, 0.55 mol), 4-chlorophenyl boronic acid (105 mg, 0.67 mol), Pd(PPh₃)₄ (32.46 mg) and Na₂CO₃ (238.23 mg, 1.12 ml) were reacted in the presence of DME to afford compound **53k** (112 mg, 93%) as a white powder.



R_f (50% EtOAc/ hexane) 0.88; **mp** 96-99 °C; **IR** ($\nu_{\max}/\text{cm}^{-1}$) 2928 (C-H), 2226 (C=N); **¹H NMR** (400 MHz, CDCl₃): δ 7.82 – 7.78 (m, 1H, H3), 7.76 (dt, J = 7.9, 1.6 Hz, 1H, H6), 7.63 (dt, J = 7.8, 1.4 Hz, 1H, H4), 7.54 (t, J = 7.8 Hz, 1H, H5), 7.50-7.42 (m, 4H, H9, H10, H11 & H12); **¹³C NMR** (101 MHz, CDCl₃): δ 141.2 (C7), 137.3 (C8), 134.7 (C13), 131.3 (C6), 131.0 (C4), 130.5 (C3), 129.7 (C5), 129.3 (C11 & C12), 128.3 (C9 & C10), 118.6 (C1), 113.1 (C2); **HRMS** (m/z), calculated for C₁₃H₉ClN: 214.0418, found (M + H)⁺: 214.0418.

4.2.3.12 Synthesis of 3',4'-difluoro-[1,1'-biphenyl]-3-carbonitrile (**53l**)

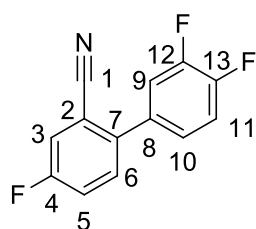
3-Bromobenzonitrile (100 mg, 0.55 mol), 3, 4-difluorophenyl boronic acid (173.54 mg, 1.01 mol), Pd(PPh₃)₄ (32.4 mg) and Na₂CO₃ (238.23 mg, 1.12 ml) were reacted in the presence of DME to give compound **53l** (112.2 mg, 95%) as a white powder.



R_f (50% EtOAc/ hexane) 0.85; **mp** 114-117 °C; **IR** ($\nu_{\max}/\text{cm}^{-1}$); 2923 (C-H), 2228 (C=N); **¹H NMR** (400 MHz, CDCl₃): δ 7.80 (t, J = 1.8 Hz, 1H, H3), 7.75 (dt, J = 7.9, 1.6 Hz, 1H, H6), 7.66 (dt, J = 7.7, 1.4 Hz, 1H, H4), 7.56 (t, J = 7.8 Hz, 1H, H5), 7.41-7.34 (m, 1H, H12), 7.31-7.24 (m, 2H, H9 & H10); **¹³C NMR** (101 MHz, CDCl₃): δ 150.7 & 150.6 (dd, J_{CF} = 251.5, 12.8 Hz & dd, J_{CF} = 250.5, 12.8 Hz, C11 & C13), 140.4 (d, J_{CF} = 1.7 Hz, C7), 135.9 (dd, J_{CF} = 5.9, 3.9 Hz, C8), 131.28 (C4), 131.25 (C6), 130.5 (C3), 129.9 (C5), 123.2 (dd, J_{CF} = 6.4, 3.6 Hz, C10), 118.5 (C1), 118.1 (d, J_{CF} = 17.5 Hz, C9), 116.2 (d, J_{CF} = 18.1 Hz, C12), 113.3 (C2); **HRMS** (m/z), calculated for C₁₃H₈F₂N: 216.0619, found (M + H)⁺: 216.0618.

4.2.3.13 Synthesis of 3',4,4'-trifluoro-[1,1'-biphenyl]-2-carbonitrile (53m)

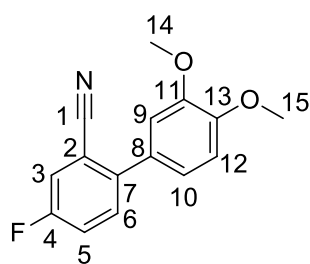
2-Bromo-5-fluorobenzonitrile (100 mg, 0.50 mol), 3, 4-difluorophenyl boronic acid (95 mg, 0.60 mol), Pd(PPh₃)₄ (30.0 mg) and Na₂CO₃ (212.0 mg, 1.0 ml) were reacted in the presence of DME to give compound **53m** (81.4 mg, 70%) as a white powder.



R_f (50% EtOAc/ hexane) 0.91; **mp** 119-121 °C; **IR** (ν_{max}/cm⁻¹); 2932 (C-H), 2230 (C=N); **¹H NMR** (400 MHz, CDCl₃): δ 7.49-7.44 (m, 2H, H3 & H6), 7.41-7.30 (m, 2H, H5 & H11), 7.29-7.25 (m, 2H, H9 & H10); **¹³C NMR** (101 MHz, CDCl₃): δ 161.6 (d, J_{CF} = 251.5 Hz, C4), 150.6 & 150.5 (dd, J_{CF} = 251.5 , 55.4 Hz & dd, J_{CF} = 251.5 , 55.5 Hz, C12 & C13), 139.7 (dd, J_{CF} = 3.9, 1.7 Hz, C7), 134.0 (dd, J_{CF} = 6.2, 4.0 Hz, C8), 132.0 (d, J_{CF} = 8.2 Hz, C6), 125.2 (dd, J_{CF} = 6.6, 3.8 Hz, C10), 120.8 (d, J_{CF} = 21.1 Hz, C5), 120.4 (d, J_{CF} = 24.8 Hz, C3), 118.1 (d, J_{CF} = 18.05, C11), 117.9 (d, J_{CF} = 17.7 Hz, C9), 117.0 (d, J_{CF} = 2.7 Hz, C1), 112.7 (d, J_{CF} = 9.4 Hz, C2). **HRMS** (m/z), calculated for C₁₃H₇F₃N: 234.0525, found (M + H)⁺: 234.0527.

4.2.3.14 Synthesis of 4-fluoro-3',4'-dimethoxy-[1,1'-biphenyl]-2-carbonitrile (53n)

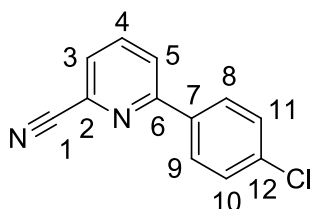
2-Bromo-5-fluorobenzonitrile (100 mg, 0.51 mol), 3, 4-dimethoxyphenyl boronic acid (111 mg, 0.61 mol), Pd(PPh₃)₄ (30.0 mg) and Na₂CO₃ (215.0 mg, 1.01 ml) were reacted in the presence of DME to give compound **53n** (63.1 mg, 50%) as a yellow powder.



R_f (50% EtOAc/ hexane) 0.76; **mp** 127-129 °C; **IR** (ν_{max}/cm⁻¹); 2940 (C-H), 2229 (C=N); **¹H NMR** (300 MHz, CDCl₃): δ 7.49 (dd, J = 8.7, 5.3 Hz, 1H, H6), 7.43 (dd, J = 8.1, 2.6 Hz, 1H, H3), 7.34 (td, J = 8.3, 2.7 Hz, 1H, H5), 7.12-7.04 (m, 2H, H9 & H10), 6.97 (d, J = 8.1 Hz, 1H, H12), 3.94 & 3.93 (2×s, 6H, H14 & H15); **¹³C NMR** (75 MHz, CDCl₃): δ 160.9 (d, J_{CF} = 249.6 Hz, C4), 149.7 & 149.0 (C11 & C13), 141.8 (d, J_{CF} = 3.6 Hz, C7), 131.8 (d, J_{CF} = 8.1 Hz, C6), 129.7 (C8), 121.4 (C9), 120.5 (d, J_{CF} = 21.2 Hz, C5), 120.2 (d, J_{CF} = 24.6 Hz, C3). 117.8 (d, J_{CF} = 2.8 Hz, C1), 112.3 (d, J_{CF} = 9.2 Hz, C2), 111.9 (C10), 111.3 (C12), 56.1 & 56.0 (C14 & C15). **HRMS** (m/z), calculated for C₁₅H₁₃NO₂: 258.0925, found (M + H)⁺: 258.0926.

4.2.3.15 Synthesis of 6-(4-chlorophenyl)picolinonitrile (53o)

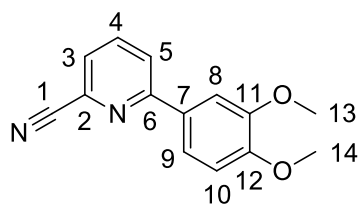
6-Bromo-2-pyridine carbonitrile (200 mg, 1.09 mol), 4-chlorophenyl boronic acid (205 mg, 1.31 mol), Pd(PPh₃)₄ (63.0 mg) and Na₂CO₃ (463.37 mg, 2.19 ml) were reacted in the presence of DME (20 ml) to give compound **53o** as a white powder (237.1 mg, 98%).



R_f (50% EtOAc/ hexane) 0.76; **mp** 97-99 °C; **IR** ($\nu_{\max}/\text{cm}^{-1}$) 2967 (C-H), 2234 (C=N); **¹H NMR** (400 MHz, CDCl₃): δ 8.01-7.96 (m, 2H, H8 & H9), 7.93-7.89 (m, 2H, H4 & H5), 7.63 (dd, J = 6.9, 1.7 Hz, 1H, H3), 7.51-7.44 (m, 2H, H10 & H11); **¹³C NMR** (101 MHz, CDCl₃): δ 157.7 (C6), 137.9 (C4), 136.5 (C7), 135.6 (C12), 133.9 (C2), 129.2 (C10 & C11), 128.3 (C8 & C9), 126.8 (C3), 123.2 (C5), 117.3 (C1). **HRMS** (m/z), calculated for C₁₂H₈ClN₂: 215.0371, found (M + H)⁺:215.0424.

4.2.3.16 Synthesis of 6-(3,4-dimethoxyphenyl)picolinonitrile (53p)

6-Bromo-2-pyridine carbonitrile (200 mg, 1.09 mol), 3, 4-dimethoxyphenyl boronic acid (239 mg, 1.31 mol), Pd(PPh₃)₄ (63.0 mg) and Na₂CO₃ (463.37 mg, 2.19 ml) were reacted in the presence of DME (20 ml) to give compound **53p** as a yellow powder (242 mg, 92%).



R_f (50% EtOAc/ hexane) 0.65; **mp** 125-128 °C; **IR** ($\nu_{\max}/\text{cm}^{-1}$); 2938 (C-H), 2227 (C=N); **¹H NMR** (400 MHz, CDCl₃): δ 7.90 (dd, J = 8.2, 1.0 Hz, 1H, H5), 7.83 (t, J = 7.8 Hz, 1H, H4), 7.70 (d, J = 2.1 Hz, 1H, H8), 7.60-7.50 (m, 2H, H3 & H9), 6.96 (d, J = 8.4 Hz, 1H, H10), 4.01 & 3.95 (2xs, 6H, H13 & H14); **¹³C NMR** (101 MHz, CDCl₃): δ 158.5 (C6), 151.0 & 149.5 (C11 & C12), 137.5 (C4), 133.6 (C2), 130.0 (C7), 126.0 (C3), 122.8 (C5), 119.7 (C9), 117.6 (C1), 111.1 (C10), 109.9 (C8), 56.1 & 56.0 (C13 & C14); **HRMS** (m/z), calculated for C₁₄H₁₃N₂O₂: 241.0972, found (M + H)⁺:241.0973.

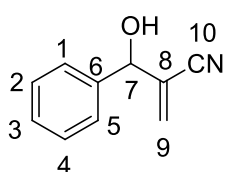
4.2.4 The Morita Baylis-Hillman reaction: general procedure

A mixture of aldehyde (1 eq), acrylonitrile (6.20 eq) and DABCO (1 eq) were stirred at room temperature overnight. After reaction completion the reaction mixture was extracted with

ethyl acetate (20 ml) and washed with water (2 × 10 ml). The organic layer was dried over anhydrous Na₂SO₄ and the solvent was removed *in vacuo*. The mixture was purified by flash silica gel column chromatography using 15-20% ethyl acetate / hexane as eluent.

4.2.4.1 Synthesis of 2-(hydroxy(phenyl)methyl)acrylonitrile¹⁰⁰ (56a)

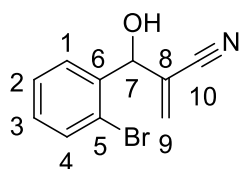
Benzaldehyde (2.09 g, 0.020 mol) and acrylonitrile (8 ml) were reacted in the presence of DABCO (2.24 g, 0.020 mol) as described in 4.2.2 to give compound **56a** as a colourless oil (2.89 g, 96%).



R_f (50% EtOAc/ hexane) 0.74; **IR** ($\nu_{\max}/\text{cm}^{-1}$) 3427 (O-H), 2230 (C=N); **¹H NMR** (300 MHz, CDCl₃): δ 7.39-7.31 (m, 5H, H1, H2, H3, H4 & H5), 6.02 (d, $J = 1.5$ Hz, 1H, H9a), 5.95 (d, $J = 1.2$ Hz, 1H, H9b), 5.19 (s, 1H, H7), 3.23 (br s, 1H, OH); **¹³C NMR** (75 MHz, CDCl₃) : δ 139.2 (C6), 130.1 (C9), 128.86 (C2 & C4), 128.85 (C3), 126.5 (C1 & C5), 126.2 (C8), 117.0 (C10), 74.0 (C7).

4.2.2.2 Synthesis of 2-((2-bromophenyl)(hydroxy)methyl)acrylonitrile¹⁰¹ (56b)

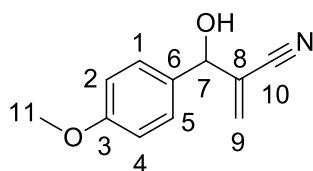
2-Bromobenzaldehyde (1.84 g, 0.01 mol) and DABCO (1.12 g, 0.01 mol) were reacted in the presence of acrylonitrile (4 ml) to give compound **56b** as a colourless oil (1.70 g, 64%).



R_f (50% EtOAc/ hexane) 0.82; **IR** ($\nu_{\max}/\text{cm}^{-1}$); 3443 (O-H), 2230 (C=N); **¹H NMR** (300 MHz, CDCl₃): δ 7.60-7.52 (m, 2H, H1 & H4), 7.38 (td, $J = 7.6, 1.3$ Hz, 1H, H2), 7.20 (td, $J = 7.7, 1.8$ Hz, 1H, H3), 6.06-6.01 (m, 2H, H9), 5.67 (s, 1H, H7), 3.27 (br s, 1H, OH); **¹³C NMR** (75 MHz, CDCl₃): δ 138.0 (C6), 133.0 (C4), 131.7 (C9), 130.3 (C3), 128.3 (C1), 128.1 (C2), 124.5 (C8), 122.7 (C5), 116.7 (C10), 72.5 (C7).

4.2.4.3 Synthesis of 2-(hydroxy(4-methoxyphenyl)methyl)acrylonitrile³⁶ (56c)

4-Methoxybenzaldehyde (1.36 g, 0.01 mol) and acrylonitrile (4 ml) were reacted in the presence of DABCO (1.12 g, 0.01 mol) to give compound **56c** as a colourless oil (1.23 g, 88%).

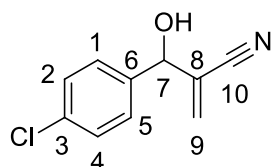


R_f (50% EtOAc/ hexane) 0.59; **IR** ($\nu_{\max}/\text{cm}^{-1}$); 3439 (O-H), 2229 (C=N); **¹H NMR** (300 MHz, CDCl₃): δ 7.27-7.10 (m, 2H, H1& H5),

6.90-6.84 (m, 2H, H2 & H4), 6.02 (d, $J = 1.6$ Hz, 1H, H9a), 5.94 (d, $J = 1.4$ Hz, 1H, H9b), 5.14 (s, 1H, H7), 3.76 (s, 3H, H11), 3.30 (br s, 1H, OH); $^{13}\text{C NMR}$ (75 MHz, CDCl_3): δ 159.8 (C3), 131.4 (C6), 129.6 (C9), 127.9 (C1 & C5), 126.4 (C8), 117.1 (C10), 114.2 (C2 & C4), 73.5 (C7), 55.3 (C11).

4.2.4.4 Synthesis of 2-((4-chlorophenyl)(hydroxy)methyl)acrylonitrile¹⁰² (56d)

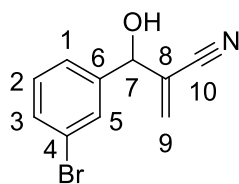
4-Chlorobenzaldehyde (1.42 g, 0.01 mol) and acrylonitrile (4 ml) were reacted in the presence of DABCO (1.12 g, 0.01 mol) to give compound **56d** as a colourless oil (1.45 g, 95%).



R_f (50% EtOAc/ hexane) 0.63; IR ($\nu_{\text{max}}/\text{cm}^{-1}$) 3434 (O-H), 2228 (C=N); $^1\text{H NMR}$ (300 MHz, CDCl_3): δ 7.33-7.29 (m, 2H, H2 & H4), 7.27-7.22 (m, 2H, H1 & H5) 6.01 (d, $J = 1.4$ Hz, 1H, H9a), 5.95 (d, $J = 1.0$ Hz, 1H, H9b), 5.17 (s, 1H, H7), 3.38 (br s, 1H, OH); $^{13}\text{C NMR}$ (70 MHz, CDCl_3): δ 137.7 (C6), 134.4 (C3), 130.6 (C9), 128.9 (C2 & C4), 127.9 (C1 & C5), 125.8 (C8), 116.8 (C10), 73.2 (C7).

4.2.4.5 Synthesis of 2-((3-bromophenyl)(hydroxy)methyl)acrylonitrile (56e)

3-Bromobenzonitrile (1.84 g, 0.01 mol), acrylonitrile (4 ml) were reacted in the presence of DABCO (1.12 g, 0.01 mol) to give compound **56e** as a colourless oil (1.18 g, 92%).



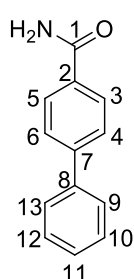
R_f (50% EtOAc/ hexane) 0.76; IR ($\nu_{\text{max}}/\text{cm}^{-1}$) 3438 (O-H), 2231 (C=N); $^1\text{H NMR}$ (300 MHz, CDCl_3): δ 7.54-7.38 (m, 2H, ArH), 7.34-7.19 (m, 2H, ArH), 6.05 (d, $J = 1.5$ Hz, 1H, H9a), 5.99 (d, $J = 1.1$ Hz, 1H, H9b), 5.17 (s, 1H, H7), 3.58-3.57 (m, 1H, OH); $^{13}\text{C NMR}$: δ 141.4 (C6), 131.8 (C5), 130.8 (C9), 130.4 (C3), 129.4 (C2), 125.5 (C8), 125.2 (C1), 122.8 (C4), 116.7 (C10), 73.1 (C7).

4.2.4.6 Synthesis of 2-(hydroxy(3,4,5-trimethoxyphenyl)methyl)acrylonitrile¹⁰² (56f)

3, 4, 5-Trimethoxybenzaldehyde (1.96 g, 0.01 mol), DABCO (1.12 g, 0.01 mol) were reacted in the presence of acrylonitrile (4 ml) to give compound **56f** was isolated as a white powder (2.18 g, 60%).

4.2.5.2 Synthesis of [1,1'-biphenyl]-4-carboxamide¹¹² (59a)

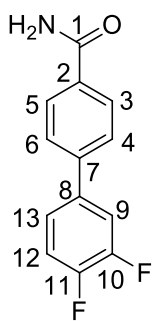
[1,1'-Biphenyl]-4-carbonitrile (20 mg, 0.11 mmol) was dissolved in acetone (400 μ l) and subjected to NHase (20 mg) in the presence of a Tris buffer (50 mM, pH 7.6) as described in 4.2.5 to afford compound **59a** (4.4 mg, 22%) as a white powder.



R_f (50% EtOAc/ hexane) 0.24; **mp** 232-234 °C; lit [229-231 °C]; **IR** ($\nu_{\max}/\text{cm}^{-1}$) 3404 (N-H), 3175 (N-H), 1645 (C=O); **¹H NMR** (400 MHz, DMSO): δ 8.02 (br s, 1H, NH), 7.97 (d, $J = 8.4$ Hz, 2H, H3 & H5), 7.77-7.70 (m, 4H, H4, H6, H9 & H13), 7.49 (t, $J = 7.5$ Hz, 2H, H10 & H12), 7.40 (t, $J = 7.3$ Hz, 1H, H11), 7.38 (br s, 1H, NH); **¹³C NMR** (101 MHz, CDCl₃): δ 167.5 (C1), 142.7 (C7), 139.2 (C8), 133.1 (C2), 129.0 (C10 & C12), 128.2 (C3 & C5), 128.0 (C11), 126.9 (C9 & C13), 126.4 (C4 & C6).

4.2.5.3 Synthesis of 3',4'-difluoro-[1,1'-biphenyl]-4-carboxamide (59d)

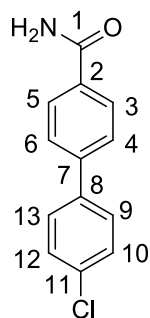
3',4'-Difluoro-[1,1'-biphenyl]-4-carbonitrile (30 mg, 0.14 mmol) was dissolved in acetone and subjected to NHase (30 mg) in the presence of a Tris buffer (50 mM, pH 7.6) to afford **59d** (9.3 mg, 31%) as a white powder.



R_f (50% EtOAc/ hexane) 0.18; **mp** 190-192 °C; **IR** ($\nu_{\max}/\text{cm}^{-1}$) 3393 (N-H), 3179 (N-H), 1645 (C=O); **¹H NMR** (500 MHz, DMSO-*d*₆): δ 8.04 (br s, 1H, NH), 7.97 (d, $J = 8.5$ Hz, 2H, H3 & H5), 7.86 (ddd, $J = 12.2, 7.7, 2.2$ Hz, 1H, H12), 7.78 (d, $J = 8.5$ Hz, 2H, H4 & H6), 7.61 (dddd, $J = 7.9, 4.5, 2.3, 1.1$ Hz, 1H, H13), 7.57-7.50 (m, 1H, H9), 7.41 (br s, 1H, NH); **¹³C NMR** (125 MHz, DMSO-*d*₆): δ 167.3 (C1), 150.6 & 148.6 (dd, $J_{\text{CF}} = 259.56, 48.3$ Hz, dd, $J_{\text{CF}} = 246.96, 49.8$ Hz, C10 & C11), 140.4 (C7), 136.8 (dd, $J_{\text{CF}} = 6.2, 3.7$ Hz, C8), 133.5 (C2), 128.2 (C3 & 5), 126.6 (C4 & C6), 123.7 (dd, $J_{\text{CF}} = 6.5, 3.2$ Hz, C13), 117.9 (d, $J_{\text{CF}} = 17.2$ Hz, C9), 115.9 (d, $J_{\text{CF}} = 17.9$ Hz, C12). **HRMS** (m/z), calculated for C₁₃H₁₀F₂NO: 234.0725, found (M + H)⁺ :234.0726.

4.2.5.4 Synthesis of 4'-chloro-[1,1'-biphenyl]-4-carboxamide (59b)

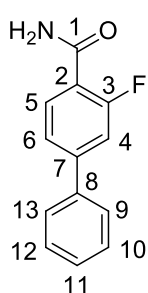
4'-Chloro-[1,1'-biphenyl]-4-carbonitrile (30 mg, 0.14 mmol) was dissolved in acetone and subjected to NHase (30 mg) in the presence of a Tris buffer (50 mM, pH 7.6) to afford **59b** (12.5 mg, 42%) as a white powder.



R_f (50% EtOAc/ hexane) 0.28; **mp** 263-269 °C; **IR** ($\nu_{\max}/\text{cm}^{-1}$) 3344 (N-H), 3164 (N-H), 1657 (C=O); **¹H NMR** (500 MHz, DMSO-*d*₆): δ 8.03 (br s, 1H, NH), 7.99-7.93 (m, 2H, H3 & H5), 7.79-7.71 (m, 4H, H4, H6, H9 & H13), 7.57-7.51 (m, 2H, H10 & H12), 7.40 (br s, 1H, NH); **¹³C NMR** (125 MHz, DMSO-*d*₆) : δ 167.4 (C1), 141.4 (C7), 138.0 (C8), 133.4 (C2), 132.9 (C11), 129.0 (C10 & C12), 128.7 (C9 & C13), 128.2 (C3 & C5), 126.4 (C4 & C6); **HRMS** (m/z), calculated for C₁₃H₁₁ClNO: 232.0524, found (M + H)⁺: 232.0524.

4.2.5.5 Synthesis of 4'-chloro-[1,1'-biphenyl]-4-carboxamide (59e)

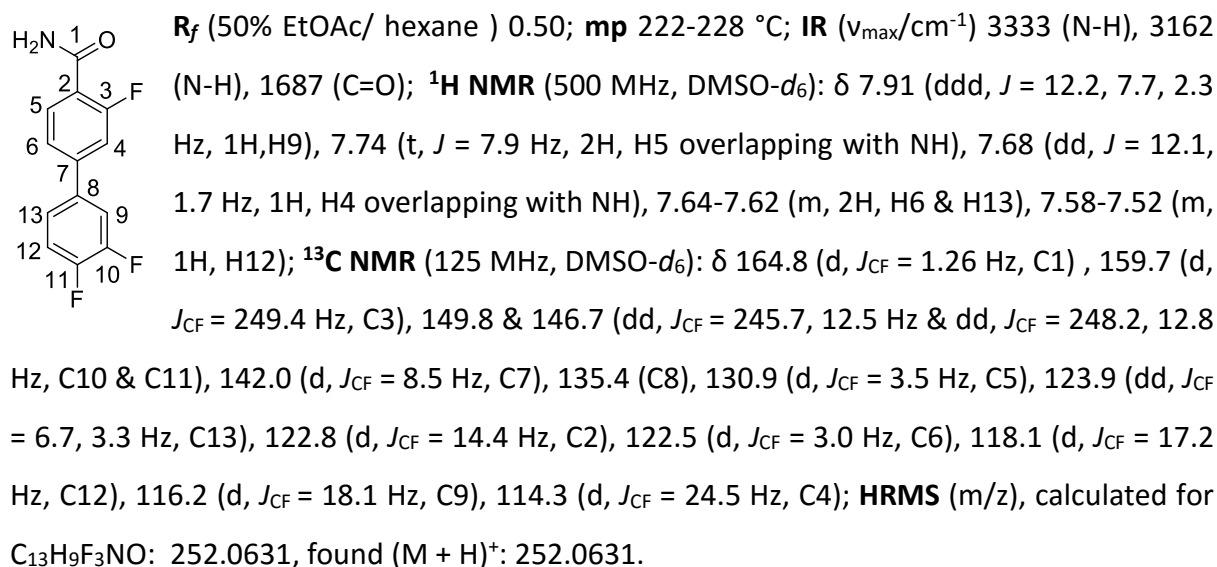
3-Fluoro-[1,1'-biphenyl]-4-carbonitrile (27 mg, 0.14 mmol) was dissolved in acetone and subjected to NHase (27 mg) in the presence of a Tris buffer (50 mM, pH 7.6) to afford **59e** (3.4 mg, 13%) as a white powder.



R_f (50% EtOAc/ hexane) 0.55; **mp** 194-196 °C; **IR** ($\nu_{\max}/\text{cm}^{-1}$) 3408 (N-H), 3163 (N-H), 1650 (C=O); **¹H NMR** (400 MHz, DMSO-*d*₆): δ 7.76-7.73 (m, 3H, H5, H9 & H13), 7.70 (br s, 1H, NH), 7.65 (br s, 1H, NH), 7.63-7.57 (m, 2H, H4 & H6), 7.52-7.48 (m, 2H, H10 & H12), 7.45-7.40 (m, 1H, H11); **¹³C NMR** (101 MHz, DMSO-*d*₆): δ 164.9 (d, $J_{\text{CF}} = 1.4$ Hz, C1), 159.8 (d, $J_{\text{CF}} = 249.2$ Hz, C3), 144.4 (d, $J_{\text{CF}} = 8.4$ Hz, C7), 137.9 (d, $J_{\text{CF}} = 1.8$ Hz, C8), 130.9 (d, $J_{\text{CF}} = 3.5$ Hz, C5), 129.1 (C10 & C12), 128.6 (C11), 126.9 (C9 & C13), 122.4 (d, $J_{\text{CF}} = 3.0$ Hz, C6), 122.3 (d, $J_{\text{CF}} = 14.4$ Hz, C2), 114.0 (d, $J_{\text{CF}} = 23.9$ Hz, C4). **HRMS** (m/z), calculated for C₁₃H₁₁FNO: 216.0819, found (M + H)⁺: 216.0874.

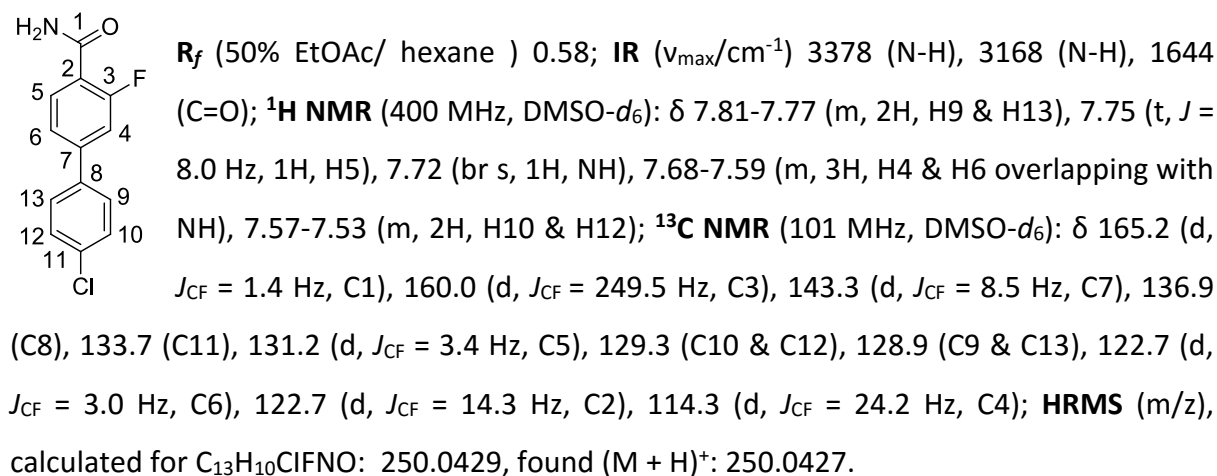
4.2.5.6 Synthesis of 3,3',4'-Trifluoro-[1,1'-biphenyl]-4-carboxamide (59f)

3,3',4'-Trifluoro-[1,1'-biphenyl]-4-carbonitrile (30 mg, 0.13 mmol) was dissolved in acetone and subjected to NHase (30 mg) in the presence of a Tris buffer (50 mM, pH 7.6) to afford **59f** (6.8 mg, 23%) as a white powder.



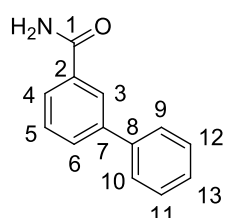
4.2.5.7 Synthesis of 4'-Chloro-3-fluoro-[1,1'-biphenyl]-4-carboxamide (59g)

4'-Chloro-3-fluoro-[1,1'-biphenyl]-4-carbonitrile (35 mg, 0.15 mmol) was dissolved in acetone and subjected to NHase (35 mg) in the presence of a Tris buffer (50 mM, pH 7.6) to afford **59g** (5.3 mg, 15%) as a yellow powder.



4.2.5.8 Synthesis of [1,1'-biphenyl]-3-carboxamide (59i)

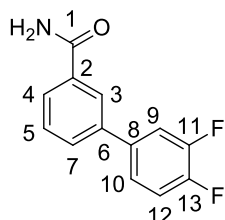
[1,1'-Biphenyl]-3-carboxamide (30 mg, 0.17 mmol) was dissolved in acetone and subjected to NHase (30 mg) in the presence of a Tris buffer (50 mM, pH 7.6) to afford **59i** (4.6 mg, 20%) as a white powder.



¹H NMR (400 MHz, DMSO-*d*₆): δ 8.16-8.15 (m, 1H, H3), 8.09 (br s, 1H, NH), 7.90-7.84 (m, 1H, H4), 7.82 (d, *J* = 7.7 Hz, 1H, H6), 7.77-7.69 (m, 2H, H9 & H10), 7.55 (t, *J* = 7.7 Hz, 1H, H13), 7.50 (t, *J* = 7.7 Hz, 2H, H11 & H12), 7.41 (dt, *J* = 8.1, 5.2 Hz, 2H, H5 overlapping with NH); **¹³C NMR** (101 MHz, DMSO-*d*₆): δ 167.8 (C1), 140.1 (C7), 139.6 (C8), 134.9 (C2), 129.4 (C6), 129.0 (C11 & C12), 128.9 (C13), 127.7 (C3), 126.8 (C9 & C10), 126.6 (C4), 125.7 (C5).

4.2.5.9 Synthesis of 3',4'-difluoro-[1,1'-biphenyl]-3-carboxamide (59l)

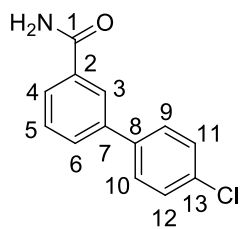
3',4'-Difluoro-[1,1'-biphenyl]-3-carbonitrile (30 mg, 0.14 mmol) was dissolved in acetone and subjected to NHase (30 mg) in the presence of a Tris buffer (50 mM, pH 7.6) to afford **59l** (12.5 mg, 42%) as a white powder.



R_f (50% EtOAc/ hexane) 0.24; **mp** 182-184 °C; **IR** (*v*_{max}/cm⁻¹) 3383 (N-H), 3180 (N-H), 1651 (C=O); **¹H NMR** (500 MHz, DMSO-*d*₆): δ 8.16 (t, *J* = 1.7 Hz, 1H, H3), 8.10 (br s, 1H, NH), 7.90-7.83 (m, 3H, H4, H5 & H12), 7.61-7.60 (m, 1H, H10), 7.59-7.52 (m, 2H, H7 & H9), 7.46 (br s, 1H, NH); **¹³C NMR** (126 MHz, CDCl₃): δ 167.6 (C1), 149.6 & 149.5 (dd, *J*_{CF} = 247.0, 67.9 Hz & dd, *J*_{CF} = 247.0, 69.2 Hz, C11 & C13), 137.9 (C6), 137.2 (dd, *J*_{CF} = 6.3, 3.6 Hz, C8), 135.0 (C2), 129.4 (C4), 129.1 (C7), 127.2 (C5), 125.6 (C3), 123.6 (dd, *J*_{CF} = 6.5, 3.3 Hz, C10), 118.0 (d, *J*_{CF} = 17.2 Hz, C9), 115.9 (d, *J*_{CF} = 17.8 Hz, C12). **HRMS** (*m/z*), calculated for C₁₃H₁₀F₂NO: 234.0725, found (M + H)⁺: 234.0728.

4.2.5.10 Synthesis of 4'-Chloro-[1,1'-biphenyl]-3-carboxamide (59k)

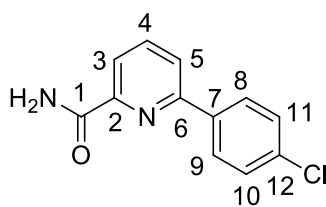
4'-Chloro-[1,1'-biphenyl]-3-carbonitrile (20 mg, 0.10 mmol) was dissolved in acetone and subjected to NHase (20 mg) in the presence of a Tris buffer (50 mM, pH 7.6) to afford **59k** (2.2 mg, 11%) as a white powder.



¹H NMR (500 MHz, DMSO-*d*₆): δ 8.16 (t, *J* = 1.9 Hz, 1H, H3), 8.11 (br s, 1H, NH), 7.79-7.76 (m, 2H, ArH), 7.58-7.53 (m, 3H, ArH), 7.47-7.39 (m, 2H, ArH overlapping with NH); **¹³C NMR** (126 MHz, DMSO-*d*₆) δ 167.6 (C1), 138.7 (ArH), 138.4 (ArH), 135.0 (ArH), 133.9 (ArH), 132.6 (ArH), 130.5 (ArH), 128.9 (ArH), 128.6 (ArH), 126.5 (ArH), 125.6 (ArH).

4.2.5.11 Synthesis of 6-(4-Chlorophenyl)picolinamide (59o)

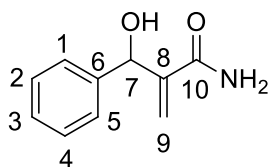
6-(4-Chlorophenyl)picolinonitrile (20 mg, 0.16 mmol) was dissolved in acetone and subjected to NHase (20 mg) in the presence of a Tris buffer (50 mM, pH 7.6) to afford **59o** (1.7 mg, 5%) as a white powder.



R_f (50% EtOAc/ hexane) 0.47; **¹H NMR** (400 MHz, DMSO-*d*₆): δ 8.39-8.31 (m, 3H, H8, H9 overlapping with NH), 8.18 (dd, *J* = 7.9, 1.1 Hz, 1H, H5), 8.06 (t, *J* = 7.8 Hz, 1H, H4), 7.99 (dd, *J* = 7.6, 1.0 Hz, 1H, H3), 7.70 (br s, 1H, NH), 7.58-7.51 (m, 2H, H10 & H11); **¹³C NMR**: δ 166.2 (C1), 153.8 (C6), 150.3 (C2), 139.0 (C4), 136.5 (C7), 134.5 (C12), 128.94 (C8 & C9), 128.88 (C10 & C11), 122.7 (C5), 120.9 (C3). **HRMS** (*m/z*), calculated for C₁₂H₁₀ClN₂O: 233.0476, found (*M* + *H*)⁺: 233.0475.

4.2.5.12 Synthesis of 2-(Hydroxy(phenyl)methyl)acrylamide¹¹⁰ (60a)

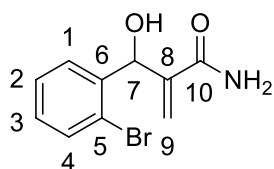
2-(Hydroxy(phenyl)methyl)acrylonitrile (23 mg, 0.14 mmol) was dissolved in methanol and subjected to NHase (23 mg) in the presence of a Tris buffer (50 mM, pH 7.6) to afford **60a** (19.8 mg, 84%) as a colourless oil.



ARM 130- 2-(Hydroxy(phenyl)methyl)acrylamide. Yield: (19.8 mg) 84% (colourless oil); **R_f** (50 % EtOAc/ hexane) 0.66; **¹H NMR** (300 MHz, DMSO-*d*₆): δ 7.45 (br s, 1H, NH), 7.30-7.26 (m, 4H, H1, H2, H4 & H5), 7.24-7.19 (m, 1H, H3), 6.95 (br s, 1H, NH), 5.79 (t, *J* = 1.2 Hz, 1H, H9a), 5.76 (d, *J* = 4.9 Hz, 1H, OH), 5.59 (t, *J* = 1.4 Hz, 1H, H9b), 5.48 (dt, *J* = 4.9, 1.2 Hz, 1H, H7); **¹³C NMR** (75 MHz, DMSO-*d*₆) δ 169.1 (C10), 147.4 (C8), 143.3 (C6), 128.2 (C2 & C4), 127.3 (C3), 127.0 (C1 & C5), 118.0 (C9), 71.5 (C7).

4.2.5.13 Synthesis of 2-((2-Bromophenyl)(hydroxy)methyl)acrylamide (60b)

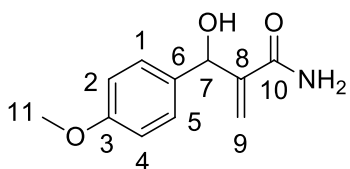
2-((2-Bromophenyl)(hydroxy)methyl)acrylonitrile (11 mg, 0.05 mmol) was dissolved in methanol and subjected to NHase (11 mg) in the presence of a Tris buffer (50 mM, pH 7.6) to afford **60b** (10.3 mg, 93%) as a white powder.



R_f (50% EtOAc/ hexane) 0.31; **mp** 83-92 °C; $^1\text{H NMR}$ (300 MHz, DMSO- d_6): δ 7.58-7.53 (m, 2H, H4 overlapping with NH), 7.43 (dd, J = 7.7, 2.0 Hz, 1H, H1) 7.37 (td, J = 7.1, 1.2 Hz, 1H, H3), 7.20 (ddd, J = 7.9, 7.1, 2.0 Hz, 1H, H2), 7.02 (br s, 1H, NH), 5.83 (t, J = 0.9 Hz, 1H, H9a), 5.80-5.74 (m, 1H, H7), 5.71-5.69 (m, 1H, OH), 5.26 (t, J = 1.2 Hz, 1H, H9b); $^{13}\text{C NMR}$ (75 MHz, DMSO- d_6): δ 168.7 (C10), 146.4 (C8), 141.9 (C6), 132.4 (C4), 129.1 (C3), 128.7 (C1), 127.5 (C2), 123.2 (C5), 118.6 (C9), 70.0 (C7); **HRMS** (m/z), calculated for $\text{C}_{10}\text{H}_{11}\text{BrNO}_2$: 255.9968, found ($M + \text{H}$) $^+$: 255.9969.

4.2.5.14 Synthesis of 2-(Hydroxy(4-methoxyphenyl)methyl)acrylamide¹⁰⁹ (60c)

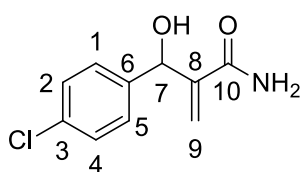
2-(Hydroxy(4-methoxyphenyl)methyl)acrylonitrile (16.5 mg, 0.1 mmol) was dissolved in methanol and subjected to NHase (16.5 mg) in the presence of a Tris buffer (50 mM, pH 7.6) to afford **60c** (9.4 mg, 57%) as a white powder.



$^1\text{H NMR}$ (300 MHz, DMSO- d_6): δ 7.40 (br s, 1H, NH), 7.23-7.17 (m, 2H, H1 & H5), 6.95 (br s, 1H, NH), 6.88-6.82 (m, 2H, H2 & H4), 5.76 (t, J = 1.3 Hz, 1H, OH), 5.58-5.54 (m, 2H, H9), 5.43 (d, J = 4.7 Hz, 1H, H7), 3.72 (s, 3H, H11); $^{13}\text{C NMR}$ (75 MHz, DMSO- d_6): δ 168.7 (C10), 158.3 (C3), 147.7 (C8), 135.2 (C6), 127.9 (C1 & C5), 116.9 (C9), 113.3 (C2 & C4), 70.7 (C7), 55.0 (C11).

4.2.5.15 Synthesis of 2-((4-Chlorophenyl)(hydroxy)methyl)acrylamide¹⁰⁸ (60d)

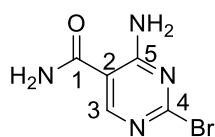
2-((4-Chlorophenyl)(hydroxy)methyl)acrylonitrile (22 mg, 0.11 mmol) was dissolved in methanol and subjected to NHase (22 mg) in the presence of a Tris buffer (50 mM, pH 7.6) to afford **60d** (13.5 mg, 61%) as a white powder.



mp 132-134; $^1\text{H NMR}$ (500 MHz, $\text{DMSO-}d_6$): δ 7.45 (br s, 1H, NH), 7.37 – 7.34 (m, 2H, H2 & H4), 7.32 – 7.29 (m, 2H, H1 & H5), 6.99 (br s, 1H, NH), 5.81 (t, $J = 1.1$ Hz, 1H, H9a), 5.77 (d, $J = 4.9$ Hz, 1H, OH), 5.62 (t, $J = 1.4$ Hz, 1H, H9b), 5.48 (d, $J = 4.8$ Hz, 1H, H7); $^{13}\text{C NMR}$ (126 MHz, $\text{DMSO-}d_6$): δ 168.5 (C10), 147.1 (C8), 142.4 (C6), 131.4 (C3), 128.5 (C2 & C4), 127.9 (C1 & C5), 117.6 (C9), 70.4 (C7).

4.2.5.16 Synthesis of 4-Amino-2-bromopyrimidinecarboxamide (74)

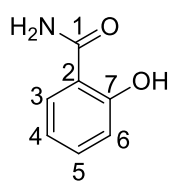
4-Amino-2-bromopyrimidinecarbonitrile (22.5 mg, 0.10 mmol) was dissolved in methanol and subjected to NHase (22.5 mg) in the presence of a Tris buffer (50 mM, pH 9) to afford **74** (18 mg, 80%) as a white powder.



$^1\text{H NMR}$ (300 MHz, $\text{DMSO-}d_6$): δ 8.47 (s, 1H, H3), 8.39, 8.23, 8.12 & 7.60 (4xbr s, 4H, NH_2 & NH_2); $^{13}\text{C NMR}$ (75 MHz, $\text{DMSO-}d_6$): δ 167.5 (C1), 163.1 (C4), 157.3 (C3), 153.3 (C5), 106.7 (C2).

4.2.5.17 Synthesis of 2-hydroxybenzamide¹¹³ (75)

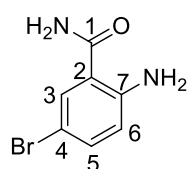
2-Hydroxybenzocarbonitrile (23.5 mg, 0.20 mmol) was dissolved in methanol and subjected to NHase (23 mg) in the presence of a Tris buffer (50 mM, pH 7.6) to afford **75** (7.5 mg, 32%) as a white powder.



R_f (50% EtOAc/ hexane) 0.59; mp 150-152 °C; IR ($\nu_{\text{max}}/\text{cm}^{-1}$): 3391 (N-H), 3181 (N-H), 1672 (C=O); $^1\text{H NMR}$ (500 MHz, $\text{DMSO-}d_6$): δ 13.02 (s, 1H, OH), 8.39 (br s, 1H, NH), 7.89 (br s, 1H, NH), 7.84 (dd, $J = 7.9, 1.5$ Hz, 1H, H3), 7.40 (ddd, $J = 8.5, 7.2, 1.6$ Hz, 1H, H5), 6.89 – 6.86 (m, 1H, H6), 6.86 – 6.83 (m, 1H, H4); $^{13}\text{C NMR}$ (125 MHz, $\text{DMSO-}d_6$): δ 172.1 (C1), 161.1 (C7), 134.01 (C5), 128.1 (C3), 118.4 (C4), 117.4 (C6), 114.4 (C2).

4.2.5.18 Synthesis of 2-amino-5-bromobenzamide¹¹⁴ (76)

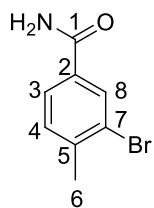
2-Amino-5-bromobenzocarbonitrile (28.5 mg, 0.15 mmol) was dissolved in methanol and subjected to NHase (28 mg) in the presence of a Tris buffer (50 mM, pH 7.6) to afford **76** (28 mg, 98%) as a brown powder.



R_f (50% EtOAc/ hexane) 0.47; **mp** 180-182 °C; **IR** ($\nu_{\max}/\text{cm}^{-1}$); 3393 (N-H), 3351 (N-H), 3286 (N-H), 3156 (N-H), 1676 (C=O); **¹H NMR** (500 MHz, DMSO-*d*₆): δ 7.84 (br s, 1H, NH), 7.70 (d, *J* = 2.4 Hz, 1H, H3), 7.25 (dd, *J* = 8.8, 2.3 Hz, 1H, H5), 7.17 (br s, 1H, NH), 6.70 (br s, 2H, NH₂), 6.66 (d, *J* = 8.8 Hz, 1H, H6); **¹³C NMR** (125 MHz, DMSO-*d*₆): δ 170.0 (C1), 149.4 (C7), 134.3 (C5), 130.8 (C3), 118.5 (C6), 115.2 (C2), 104.7 (C4).

4.2.5.19 Synthesis of 3-bromo-4-methylbenzamide¹¹⁵ (77)

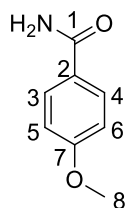
3-Bromo-4-methylbenzonitrile (26.5 mg, 0.14 mmol) was dissolved in methanol and subjected to NHase (26 mg) in the presence of a Tris buffer (50 mM, pH 7.6) to afford **77** (26 mg, 95%) as a white powder.



R_f (50% EtOAc/ hexane) 0.45; **mp** 187-189°C; **IR** ($\nu_{\max}/\text{cm}^{-1}$); 3355 (N-H), 3159 (N-H), 1653 (C=O); **¹H NMR** (500 MHz, DMSO-*d*₆): δ 8.07 (d, *J* = 1.8 Hz, 1H, H8), 8.02 (br s, 1H, NH), 7.78 (dd, *J* = 7.9, 1.9 Hz, 1H, H3), 7.43 (d, *J* = 7.8 Hz, 1H, H4) overlapping with 7.42 (br s, 1H, NH), 2.38 (s, 3H, H6); **¹³C NMR**: δ 166.2 (C1), 140.6 (C5), 133.8 (C2), 131.0 (C8), 130.9 (C4), 126.8 (C3), 123.9 (C7), 22.4 (C6).

4.2.5.20 Synthesis of 4-methoxybenzamide¹¹⁶ (78)

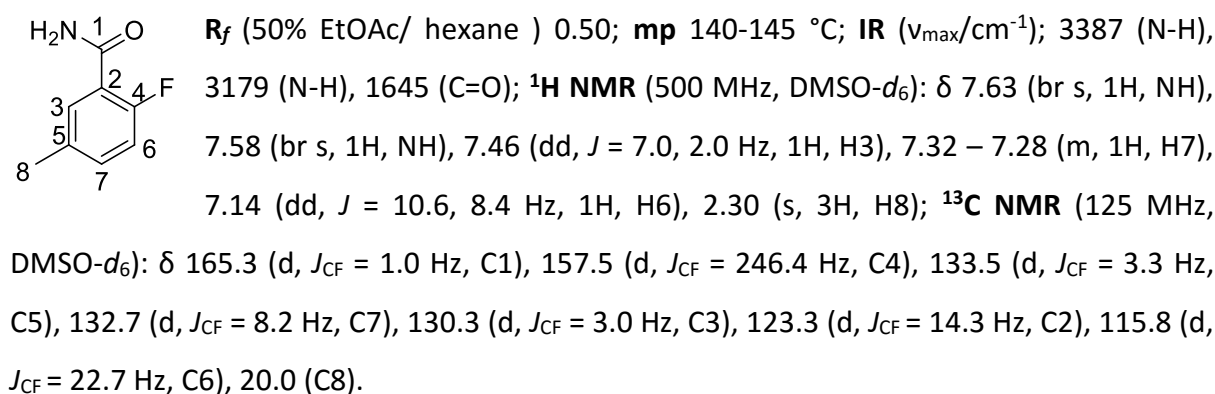
4-Methoxybenzonitrile (20 mg, 0.15 mmol) was dissolved in methanol and subjected to NHase (20 mg) in the presence of a Tris buffer (50 mM, pH 7.6) to afford **78** (9.6 mg, 48%) as a white powder.



R_f (50% EtOAc/ hexane) 0.21; **mp** 177-180 °C; [lit 166-168 °C]; **IR** ($\nu_{\max}/\text{cm}^{-1}$); 3389 (N-H), 3159 (N-H), 1643 (C=O); **¹H NMR** (500 MHz, DMSO-*d*₆): δ 7.86-7.82 (m, *J* = 8.9 Hz, 3H, H3 & H4 with overlapping NH), 7.17 (br s, 1H, NH), 6.99 – 6.94 (m, *J* = 8.9 Hz, 2H, H5 & H6), 3.80 (s, 3H, H8); **¹³C NMR** (125 MHz, DMSO-*d*₆): δ 167.9 (C1), 162.0 (C7), 129.8 (C3 & C4), 126.9 (C2), 113.8 (C5 & C6), 55.8 (C8).

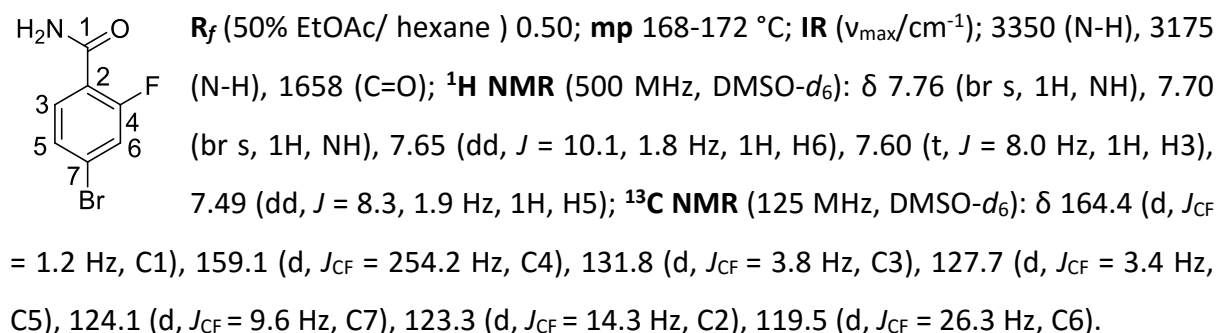
4.2.5.21 Synthesis of 2-fluoro-5-methylbenzamide (79)

2-Fluoro-5-methylbenzonitrile (28 mg, 0.21 mmol) was dissolved in methanol and subjected to NHase (28 mg) in the presence of a Tris buffer (50 mM, pH 7.6) to afford **79** (27 mg, 96%) as a white powder.



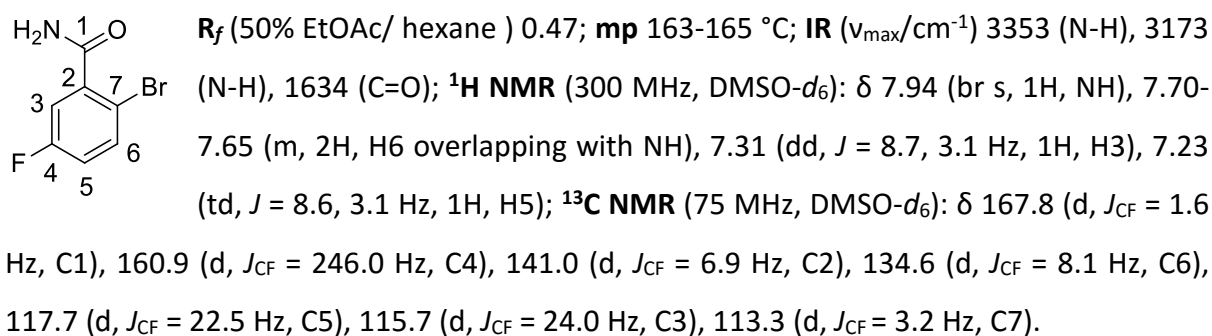
4.2.5.22 Synthesis of 4-bromo-2-fluorobenzamide¹¹⁷ (80)

4-Bromo-2-fluorobenzonitrile (28 mg, 0.14 mmol) was dissolved in methanol and subjected to NHase (28 mg) in the presence of a Tris buffer (50 mM, pH 7.6) to afford **80** (27 mg, 97%) as a white powder.



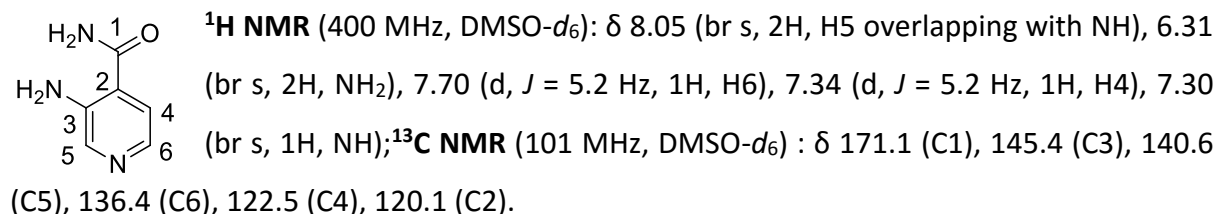
4.2.5.23 Synthesis of 2-bromo-5-fluorobenzamide (81)

2-Bromo-5-fluorobenzonitrile (21 mg, 0.11 mmol) was dissolved in methanol and subjected to NHase (20 mg) in the presence of a Tris buffer (50 mM, pH 7.6) to afford **81** (19.5 mg, 93%) as a white powder.



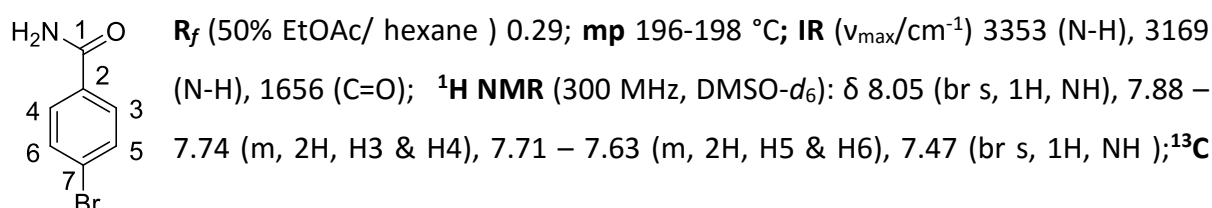
4.2.5.24 Synthesis of 3-amino-4-pyridinecarboxamide¹¹⁸ (82)

3-Amino-4-pyridinecarbonitrile (20 mg, 0.17 mmol) was dissolved in methanol and subjected to NHase (20 mg) in the presence of a Tris buffer (50 mM, pH 9) to afford **82** (15 mg, 75%) as a white powder.



4.2.5.25 Synthesis of 4-bromobenzamide¹¹⁶ (83)

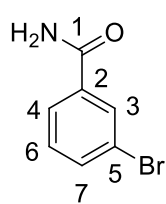
4-Bromobenzonitrile (20 mg, 0.11 mmol) was dissolved in methanol and subjected to NHase (20 mg) in the presence of a Tris buffer (50 mM, pH 7.6) to afford **83** (19.3 mg, 95%) as a white powder.



NMR (75 MHz, DMSO-*d*₆): δ 166.9 (C1), 133.4 (C2), 131.2 (C5 & C6), 129.6 (C3 & C4), 125.0 (C7).

4.2.5.26 Synthesis of 3-bromobenzamide¹¹⁶ (**84**)

3-Bromobenzonitrile (20 mg, 0.11 mmol) was dissolved in methanol and subjected to NHase (20 mg) in the presence of a Tris buffer (50 mM, pH 7.6) to afford **84** (16.1 mg, 81%) as a white powder.

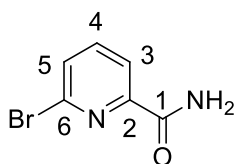


R_f (50% EtOAc/ hexane) 0.32; **mp** 166-168 °C; **IR** (v_{\max}/cm^{-1}): 3346 (N-H), 3161 (N-H), 1656 (C=O); **¹H NMR** (300 MHz, DMSO-*d*₆): δ 8.1 (br s, 1H, NH), 8.0 (t, *J* = 1.8 Hz, 1H, H 3), 7.87 (ddd, *J* = 7.8, 1.7, 1.1 Hz, 1H, H4), 7.72 (ddd, *J* = 8.0, 2.1, 1.0 Hz, 1H, H7), 7.53 (br s, 1H, NH), 7.43 (t, *J* = 7.9 Hz, 1H, H6); **¹³C**

NMR (75 MHz, DMSO-*d*₆) : δ 166.3 (C1), 136.5 (C2), 134.0 (C7), 130.5 (C6), 130.2 (C3), 126.6 (C4), 121.6 (C5).

4.2.5.27 Synthesis of 6-bromo-2-Pyridinecarboxamide (**85**)

6-Bromo-2-Pyridinecarbonitrile (21 mg, 0.12 mmol) was dissolved in methanol and subjected to NHase (20 mg) in the presence of a Tris buffer (50 mM, pH 7.6) to afford **85** (19.2 mg, 90%) as a white powder.

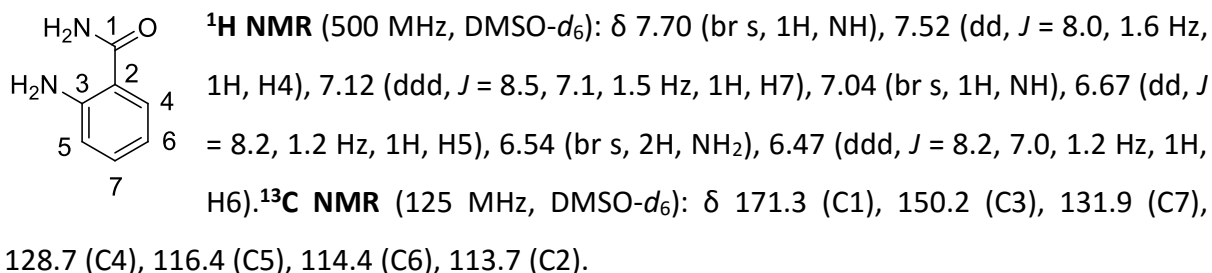


R_f (50% EtOAc/ hexane) 0.47; **mp** 148-152 °C; **IR** (v_{\max}/cm^{-1}): 3381 (N-H), 3182 (N-H), 1661 (C=O); **¹H NMR** (300 MHz, DMSO-*d*₆): δ 8.05-8.01 (m, 2H, H3 overlapping with NH), 7.93 (t, *J* = 7.7 Hz, 1H, H4), 7.84 (dd, *J* =

7.9, 1.1 Hz, 1H, H5), 7.78 (br s, 1H, NH); **¹³C NMR** (75 MHz, DMSO-*d*₆): δ 164.6 (C1) , 151.7 (C2), 140.9 (C4), 140.1 (C6) , 130.8 (C5), 121.6 (C3).

4.2.5.28 Synthesis of 2-aminobenzamide¹¹⁹ (**86**)

2-Aminobenzonitrile (20 mg, 0.17 mmol) was dissolved in methanol and subjected to NHase (20 mg) in the presence of a Tris buffer (50 mM, pH 9) to afford **86** (8 mg, 40%) as a white powder.

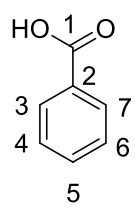


4.2.6 Nitrilase biocatalytic reaction with whole cell nitrilases (A29 and A99)

Nitrile hydrolysis by whole cell nitrilases (A29 and A99) was carried out in a 1:1 ratio of the enzyme and the substrate, with a total reaction volume of 2 ml. Composition of the reaction mixture: 1800 μL (90%) Tris buffer (50 mM, pH 7.6) and 200 μL (10%) of methanol or acetone. In a 2 ml Eppendorf whole cell nitrilase (10 mg) was added followed by Tris buffer. Nitrile substrate (10 mg dissolved in 200 μL methanol or acetone) was added to the 2 ml Eppendorf tube containing a buffer. If an amine group was present on the nitrile substrate a Tris buffer of pH 9 was used. The reaction mixture was incubated at 30 °C on an ESCO ProvoCell microplate shaker/incubator (199 rpm). After reaction completion by whole cell nitrilase, the reaction mixture was extracted with ethyl acetate (20 ml) and acidic water (4 × 10 ml). The aqueous phase was acidified to a pH of 4-4.5 by 1M of HCl. The organic layer was dried over anhydrous Na₂SO₄ and the solvent was removed *in vacuo*. The reaction mixture was further purified with silica gel column chromatography using 20-90% ethyl acetate/ hexane as eluent.

4.2.6.1 Synthesis of benzoic acid by nitrilase¹⁰⁴ (**58**)

Benzonitrile (20 mg, 0.19 mmol) was subjected to whole cell nitrilase (A29 and A99) (20 mg) in the presence of a Tris buffer (50 mM, pH 7.6) to afford **58** (17 mg, 85%) as a white powder.



Benzoic acid. ¹H NMR (500 MHz, DMSO) δ 12.73 (br s, 1H, OH), 7.98 – 7.92 (m, 2H, H3 & H7), 7.63 – 7.57 (m, 2H, H4 & H6), 7.49 (t, *J* = 7.8 Hz, 1H, H5). ¹³C NMR (126 MHz, DMSO) δ 167.38 (C1), 132.85 (C5), 130.86 (C2), 129.30 (C3 & C7), 128.57 (C4 & C6).

References

- (1) de Marco, B. A.; Rechelo, B. S.; Tótolí, E. G.; Kogawa, A. C.; Salgado, H. R. N. *Saudi Pharmaceutical Journal* **2019**, *27*, 1.
- (2) Patnaik, R. *IOP Conference Series: Earth and Environmental Science* **2018**, *120*, 012016.
- (3) Cue, B. W.; Zhang, J. *Green Chemistry Letters and Reviews* **2009**, *2*, 193.
- (4) Sheldon, R. A. *ACS Sustainable Chemistry & Engineering* **2018**, *6*, 32.
- (5) Sheldon, R. A. *Green Chemistry* **2017**, *19*, 18.
- (6) Ma, Y.; Zeng, X.; Ma, X.; Yang, R.; Zhao, W. *Journal of Cleaner Production* **2019**, *209*, 916.
- (7) Sun, H.; Zhang, H.; Ang, E. L.; Zhao, H. *Bioorganic & Medicinal Chemistry* **2018**, *26*, 1275.
- (8) Sheldon, R. A. *Journal of Molecular Catalysis A: Chemical* **1996**, *107*, 75.
- (9) Woodley, J. M. *Trends in Biotechnology* **2008**, *26*, 321.
- (10) Choi, J.-M.; Han, S.-S.; Kim, H.-S. *Biotechnology Advances* **2015**, *33*, 1443.
- (11) Pellis, A.; Cantone, S.; Ebert, C.; Gardossi, L. *New Biotechnology* **2018**, *40*, 154.
- (12) Anastas, P.; Eghbali, N. *Chemical Society Reviews* **2010**, *39*, 301.
- (13) Badami, B. V. *Resonance* **2008**, *13*, 1041.
- (14) Gong, J.-S.; Lu, Z.-M.; Li, H.; Shi, J.-S.; Zhou, Z.-M.; Xu, Z.-H. *Microbial cell factories* **2012**, *11*, 142.
- (15) Bommarius, A. S.; Riebel-Bommarius, B. R. *Biocatalysis: Fundamentals and Applications*; Wiley, 2004.
- (16) Illanes, A.; Cauerrhff, A.; Wilson, L.; Castro, G. R. *Bioresource Technology* **2012**, *115*, 48.
- (17) Pollard, D. J.; Woodley, J. M. *Trends in Biotechnology* **2007**, *25*, 66.
- (18) Brady, D.; Dube, N.; Petersen, R. *South African Journal of Science* **2006**, *102*, 339.
- (19) Sheldon, R. A.; van Pelt, S. *Chemical Society Reviews* **2013**, *42*, 6223.
- (20) Sheldon, R. A.; Brady, D. *ChemSusChem* **2019**, *12*, 2859.
- (21) Madhu, A.; Chakraborty, J. N. *Journal of Cleaner Production* **2017**, *145*, 114.
- (22) Cutlan, R.; De Rose, S.; Isupov, M. N.; Littlechild, J. A.; Harmer, N. J. *Biochimica et Biophysica Acta (BBA) - Proteins and Proteomics* **2020**, *1868*, 140322.

- (23) Al-Hawash, A. B.; Dragh, M. A.; Li, S.; Alhujaily, A.; Abbood, H. A.; Zhang, X.; Ma, F. *The Egyptian Journal of Aquatic Research* **2018**, *44*, 71.
- (24) Banerjee, A.; Dubey, S.; Kaul, P.; Barse, B.; Piotrowski, M.; Banerjee, U. C. *Molecular Biotechnology* **2009**, *41*, 35.
- (25) Sahu, R.; Meghavarnam, A. K.; Janakiraman, S. *Biotechnology Reports* **2019**, *24*, e00396.
- (26) Egelkamp, R.; Zimmermann, T.; Schneider, D.; Hertel, R.; Daniel, R. *Frontiers in Environmental Science* **2019**, *7*.
- (27) Martíňková, L. *Fungal Biology Reviews* **2019**, *33*, 149.
- (28) Mascharak, P. K. *Coordination Chemistry Reviews* **2002**, *225*, 201.
- (29) Howden, A. J. M.; Preston, G. M. *Microbial Biotechnology* **2009**, *2*, 441.
- (30) Sorokin, D. Y.; Sander Van, P.; Tourova, T. P. *FEMS Microbiology Letters* **2008**, *288*, 235.
- (31) Ramteke, P. W.; Maurice, N. G.; Joseph, B.; Wadher, B. J. *Biotechnology and Applied Biochemistry* **2013**, *60*, 459.
- (32) Nagasawa, T.; Wieser, M.; Nakamura, T.; Iwahara, H.; Yoshida, T.; Gekko, K. *European Journal of Biochemistry* **2000**, *267*, 138.
- (33) Jagadeesh, R. V.; Junge, H.; Beller, M. *Nature Communications* **2014**, *5*, 4123.
- (34) Mu, Y.; Nguyen, T. T.; Koh, M. J.; Schrock, R. R.; Hoveyda, A. H. *Nature Chemistry* **2019**, *11*, 478.
- (35) Shumei Fang, X. A., Hongyuan Liu, Yi Cheng, Ning Hou, Lu Feng, Xinning Huang, Chunyan Li *Bioresource Technology* **2015**, *185*, 28.
- (36) Coady, T. M.; Coffey, L. V.; O'Reilly, C.; Lennon, C. M. *European Journal of Organic Chemistry* **2015**, *2015*, 1108.
- (37) Turner, C. O. R. a. P. D. *Journal of Applied microbiology* **2003**, *95*, 1161.
- (38) Chen, B.-S.; Otten, L. G.; Resch, V.; Muyzer, G.; Hanefeld, U. *Standards in Genomic Sciences* **2013**, *9*, 175.
- (39) Frederick, J.; Hennessy, F.; Horn, U.; de la Torre Cortés, P.; van den Broek, M.; Strych, U.; Willson, R.; Hefer, C. A.; Daran, J.-M. G.; Sewell, T.; Otten, L. G.; Brady, D. *BMC Genomics* **2020**, *21*, 3.
- (40) Frederick, J., PhD thesis, University of Cape Town, 2013.

- (41) Ashwini L. Kamble, L. B., Vachan Singh Meena, Amit Singh, Yusuf Chisti, U. C. Banerjee *3 Biotech* **2012**, 3, 319.
- (42) Tauber, M. M.; Cavaco-Paulo, A.; Robra, K. H.; Gübitz, G. M. *Applied and Environmental Microbiology* **2000**, 66, 1634.
- (43) Prasad, S.; Bhalla, T. C. *Biotechnology Advances* **2010**, 28, 725.
- (44) Frederick, J., Msc dissertation, University of the Witwatersrand, **2006**.
- (45) Huang, W.; Jia, J.; Cummings, J.; Nelson, M.; Schneider, G.; Lindqvist, Y. *Structure* **1997**, 5, 691.
- (46) Asano, Y.; Tani, Y.; Yamada, H. *Agricultural and Biological Chemistry* **1980**, 44, 2251.
- (47) Black, G. W.; Gregson, T.; McPake, C. B.; Perry, J. J.; Zhang, M. *Tetrahedron Letters* **2010**, 51, 1639.
- (48) Martinez, S.; Yang, X.; Bennett, B.; Holz, R. C. *Biochimica et Biophysica Acta (BBA) - Proteins and Proteomics* **2017**, 1865, 107.
- (49) Nagasawa, T.; Takeuchi, K.; Yamada, H. *European Journal of Biochemistry* **1991**, 196, 581.
- (50) Pei, X.; Yang, Z.; Wang, A.; Yang, L.; Wu, J. *Journal of Biotechnology* **2017**, 251, 38.
- (51) Sari, M.-A.; Jaouen, M.; Saroja, N. R.; Artaud, I. *Journal of Inorganic Biochemistry* **2007**, 101, 614.
- (52) Weijun Huang, J. J., John Cummings, Mark Nelson, Gunter Schneider and Ylva Lindquist **1997**, 5, 691.
- (53) MacDonald, C. A.; Boyd, R. J. *Computational and Theoretical Chemistry* **2015**, 1070, 48.
- (54) Taniguchi, K.; Murata, K.; Murakami, Y.; Takahashi, S.; Nakamura, T.; Hashimoto, K.; Koshino, H.; Dohmae, N.; Yohda, M.; Hirose, T.; Maeda, M.; Odaka, M. *Journal of Bioscience and Bioengineering* **2008**, 106, 174.
- (55) Taştan Bishop, A. Ö.; Sewell, T. *Biochemical and Biophysical Research Communications* **2006**, 343, 319.
- (56) Peplowski, L.; Kubiak, K.; Nowak, W. *Chemical Physics Letters* **2008**, 467, 144.
- (57) Hopmann, K. H. *Inorganic Chemistry* **2014**, 53, 2760.
- (58) Endo, I.; Nojiri, M.; Tsujimura, M.; Nakasako, M.; Nagashima, S.; Yohda, M.; Odaka, M. *Journal of Inorganic Biochemistry* **2001**, 83, 247.

- (59) Pei, X.; Yang, L.; Xu, G.; Wang, Q.; Wu, J. *Journal of Molecular Catalysis B: Enzymatic* **2014**, *99*, 26.
- (60) Housaindokht, M. R.; Monhemi, H.; Hosseini, H. E.; Sadeghi Googheri, M. S.; Najafabadi, R. I.; Ashraf, N.; Gholizadeh, M. *Journal of Molecular Liquids* **2013**, *187*, 30.
- (61) Hastuty, A.; Mangunwardoyo, W.; Sunarko, B. *HAYATI Journal of Biosciences* **2014**, *21*, 53.
- (62) Pei, X.; Wu, Y.; Wang, J.; Chen, Z.; Liu, W.; Su, W.; Liu, F. *Nanoscale* **2020**, *12*, 967.
- (63) Mauger, J.; Nagasawa, T.; Yamada, H. *Tetrahedron* **1989**, *45*, 1347.
- (64) Kinfe, H. H.; Chhiba, V.; Frederick, J.; Bode, M. L.; Mathiba, K.; Steenkamp, P. A.; Brady, D. *Journal of Molecular Catalysis B: Enzymatic* **2009**, *59*, 231.
- (65) Shen, Y. *African Journal of Microbiology Research* **2012**, *6*.
- (66) Dennett, G. V.; Blamey, J. M. *Frontiers in Bioengineering and Biotechnology* **2016**, *4*.
- (67) Thuku, R. N.; Brady, D.; Benedik, M. J.; Sewell, B. T. *Journal of Applied Microbiology* **2009**, *106*, 703.
- (68) Jiang, W.; Tao, R.; Yang, Y.; Xu, Y.; Kang, H.; Zhou, X.; Zhou, Z. *Biochemical Engineering Journal* **2017**, *127*, 32.
- (69) Agarwal, A.; Nigam, V. *International Journal of Pharma and Bio Sciences* **2012**, *3*, 232.
- (70) Chhiba-Govindjee, V. P.; van der Westhuyzen, C. W.; Bode, M. L.; Brady, D. *Applied Microbiology and Biotechnology* **2019**, *103*, 4679.
- (71) Brenner, C. *Genome Biology* **2001**, *2*, 1.
- (72) Pace, H. C.; Brenner, C. *Genome Biology* **2001**, *2*, reviews0001.1.
- (73) Seffernick, J. L.; Samanta, S. K.; Louie, T. M.; Wackett, L. P.; Subramanian, M. *Journal of Biotechnology* **2009**, *143*, 17.
- (74) Thuku, R. N. *The Structure of the Nitrilase from Rhodococcus Rhodochrous J1: Homology Modeling and Three-dimensional Reconstruction*; University of the Western Cape, 2006.
- (75) Joni Frederick, D. B., Brandon Weber and Trevor Sewell **2008**, 1.
- (76) Lujia Zhang, B. Y., Chao Wang, Shuiqin Jiang, Hualei Wang, Y. Adam Yuan, Dongzhi Wei *Journal of Structural Biology* **2014**, *188*, 93.
- (77) Piotrowski, M.; Schönfelder, S.; Weiler, E. *The Journal of biological chemistry* **2001**, *276*, 2616.

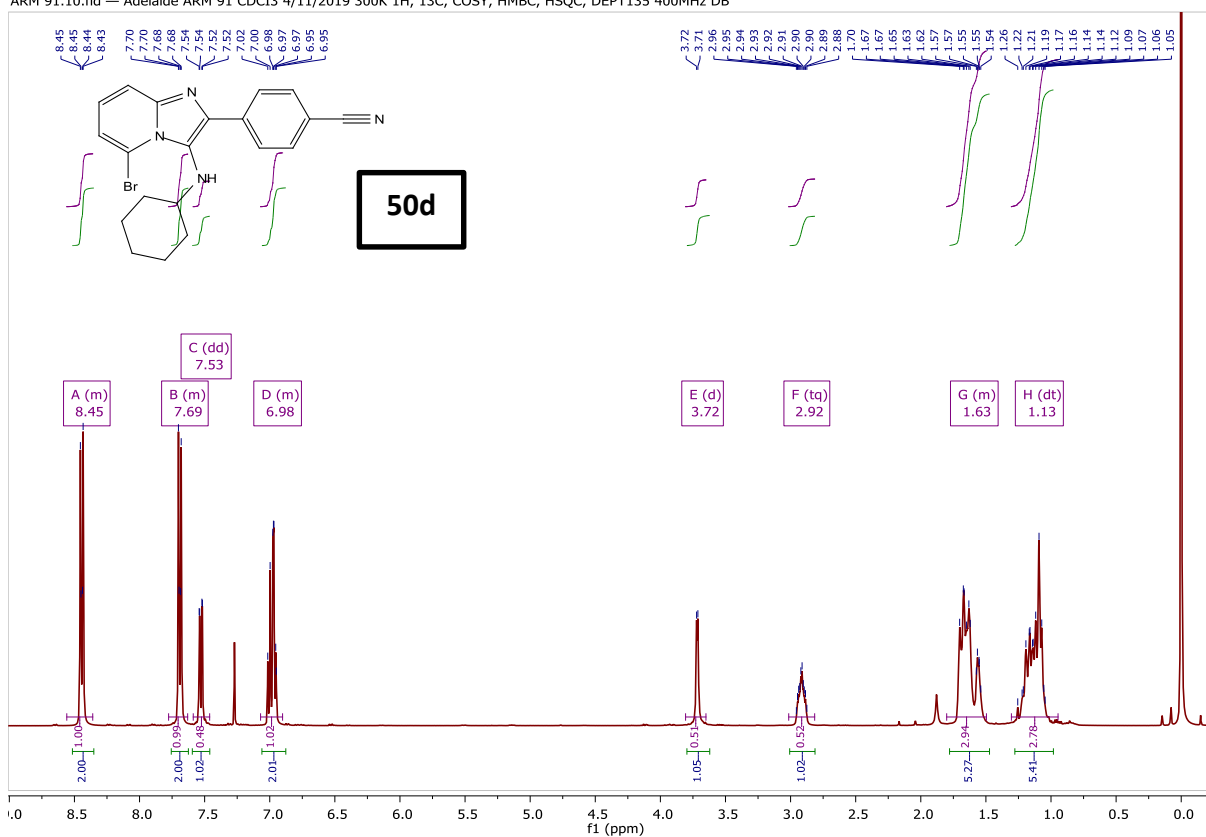
- (78) Kobayashi, M.; Nagasawa, T.; Yamada, H. *Applied Microbiology and Biotechnology* **1988**, *29*, 231.
- (79) Kumari, P.; Poddar, R. *Computational Biology and Chemistry* **2019**, *83*, 107095.
- (80) Woodward, J. D.; Trompetter, I.; Sewell, B. T.; Piotrowski, M. *Communications Biology* **2018**, *1*, 186.
- (81) Gong, J.-S.; Zhang, Q.; Gu, B.-C.; Dong, T.-T.; Li, H.; Li, H.; Lu, Z.-M.; Shi, J.-S.; Xu, Z.-H. *Bioresource Technology* **2018**, *260*, 427.
- (82) Mathew, C. D.; Nagasawa, T.; Kobayashi, M.; Yamada, H. *Applied and Environmental Microbiology* **1988**, *54*, 1030.
- (83) Badoei-Dalfard, A.; Karami, Z.; Ramezani-pour, N. *Journal of Molecular Catalysis B: Enzymatic* **2016**, *133*, S552.
- (84) Meth-Cohn, O.; Wang, M.-X. *Journal of the Chemical Society, Perkin Transactions 1* **1997**, 1099.
- (85) Nigam, V. K.; Khandelwal, A. K.; Gothwal, R. K.; Mohan, M. K.; Choudhury, B.; Vidyarthi, A. S.; Ghosh, P. *Journal of Biosciences* **2009**, *34*, 21.
- (86) Vidyacharan, S.; Shinde, A. H.; Satpathi, B.; Sharada, D. S. *Green Chemistry* **2014**, *16*, 1168.
- (87) Bienaymé, H.; Bouzid, K. *Angewandte Chemie International Edition* **1998**, *37*, 2234.
- (88) Boltjes, A.; Dömling, A. *European Journal of Organic Chemistry* **2019**, *2019*, 7007.
- (89) Bahulayan, D.; Das, S. K.; Iqbal, J. *The Journal of Organic Chemistry* **2003**, *68*, 5735.
- (90) Nagendrappa, G. *Resonance* **2002**, *7*, 64.
- (91) Shivhare, K.; Jaiswal, M.; Srivastava, A.; Tiwari, S.; Siddiqui, I. *New Journal of Chemistry* **2018**, 42.
- (92) Bode, M. L.; Gravestock, D.; Moleele, S. S.; van der Westhuyzen, C. W.; Pelly, S. C.; Steenkamp, P. A.; Hoppe, H. C.; Khan, T.; Nkabinde, L. A. *Bioorganic & Medicinal Chemistry* **2011**, *19*, 4227.
- (93) Biffis, A.; Centomo, P.; Del Zotto, A.; Zecca, M. *Chemical Reviews* **2018**, *118*, 2249.
- (94) Li, X.; Ma, Y.; Hu, Q.; Jiang, B.; Wu, Q.; Yuan, Z. *Catalysis Communications* **2018**, *117*, 57.
- (95) Tahmasbi, B.; Ghorbani-Choghamarani, A. *New Journal of Chemistry* **2019**, *43*, 14485.
- (96) Scheuermann, G. M.; Rumi, L.; Steurer, P.; Bannwarth, W.; Mülhaupt, R. *Journal of the American Chemical Society* **2009**, *131*, 8262.

- (97) Keller, L.; Sanchez, M. V.; Prim, D.; Couty, F.; Evano, G.; Marrot, J. *Journal of Organometallic Chemistry* **2005**, *690*, 2306.
- (98) Rao, M. L. N.; Banerjee, D.; Dhanorkar, R. J. *Tetrahedron Letters* **2010**, *51*, 6101.
- (99) Wang, M.; Wang, L. *Chinese Journal of Chemistry - CHINESE J CHEM* **2008**, *26*, 1683.
- (100) Juma, W. P.; Chhiba, V.; Brady, D.; Bode, M. L. *Tetrahedron: Asymmetry* **2017**, *28*, 1169.
- (101) Coelho, F.; Veronese, D.; Pavam, C. H.; de Paula, V. I.; Buffon, R. *Tetrahedron* **2006**, *62*, 4563.
- (102) Mendoza-Espinosa, D.; González-Olvera, R.; Osornio, C.; Negrón-Silva, G. E.; Santillan, R. *New Journal of Chemistry* **2015**, *39*, 1587.
- (103) Chhiba, V.; Bode, M. L.; Mathiba, K.; Kwezi, W.; Brady, D. *Journal of Molecular Catalysis B: Enzymatic* **2012**, *76*, 68.
- (104) Pradhan, D. R.; Pattanaik, S.; Kishore, J.; Gunanathan, C. *Organic Letters* **2020**, *22*, 1852.
- (105) Guo, B.; de Vries, J. G.; Otten, E. *Chemical Science* **2019**, *10*, 10647.
- (106) Kamble, A.; Banoth, L.; Meena, V.; Chisti, Y.; Banerjee, U. *3 Biotech* **2012**, *3*.
- (107) Brock, C. *Journal of Research of the National Institute of Standards and Technology* **1996**, *101*, 321.
- (108) Faltin, C.; Fleming, E. M.; Connon, S. J. *The Journal of Organic Chemistry* **2004**, *69*, 6496.
- (109) Kim, E. S.; Lee, H. S.; Kim, J. N. *Tetrahedron Letters* **2009**, *50*, 6286.
- (110) Aggarwal, V. K.; Emme, I.; Fulford, S. Y. *The Journal of Organic Chemistry* **2003**, *68*, 692.
- (111) Ghorbani-Vaghei, R.; Amiri, M. *Journal of Heterocyclic Chemistry* **2014**, *51*, E372.
- (112) Tao, B.; Boykin, D. W. *The Journal of Organic Chemistry* **2004**, *69*, 4330.
- (113) Yin, W.; Pan, X.; Leng, W.; Chen, J.; He, H. *Green Chemistry* **2019**, *21*, 4614.
- (114) Wang, Y.-W.; Zheng, L.; Jia, F.-C.; Chen, Y.-F.; Wu, A.-X. *Tetrahedron* **2019**, *75*, 1497.
- (115) Ma, C.; Fan, G.; Wu, P.; Li, Z.; Zhou, Y.; Ding, Q.; Zhang, W. *Organic & Biomolecular Chemistry* **2017**, *15*, 9889.
- (116) Solaiman Hamed, A.; Mohammad Ali, E. *Research on Chemical Intermediates* **2020**, *46*, 701.

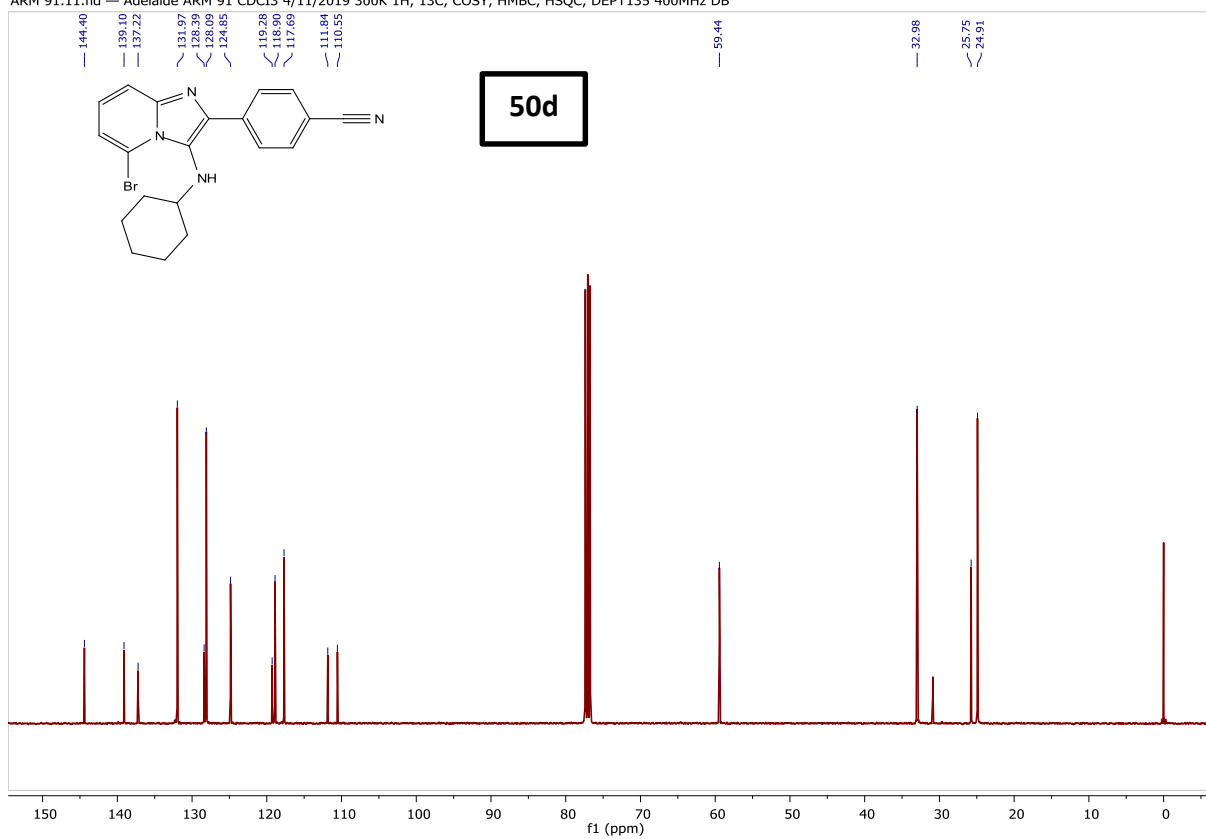
- (117) Prakash, G. K. S.; Munoz, S. B.; Papp, A.; Masood, K.; Bychinskaya, I.; Mathew, T.; Olah, G. A. *Asian Journal of Organic Chemistry* **2012**, *1*, 146.
- (118) Zhang, H.; Liu, H.; Luo, X.; Wang, Y.; Liu, Y.; Jin, H.; Liu, Z.; Yang, W.; Yu, P.; Zhang, L.; Zhang, L. *European Journal of Medicinal Chemistry* **2018**, *152*, 235.
- (119) Rotondi, G.; Guglielmi, P.; Carradori, S.; Secci, D.; Monte, C.; de filippis, B.; Maccallini, C.; Amoroso, R.; Cirilli, R.; Akdemir, A.; Angeli, A.; Supuran, C. *Journal of Enzyme Inhibition and Medicinal Chemistry* **2019**, *34*, 1400.

Appendix: ^1H & ^{13}C NMR spectra

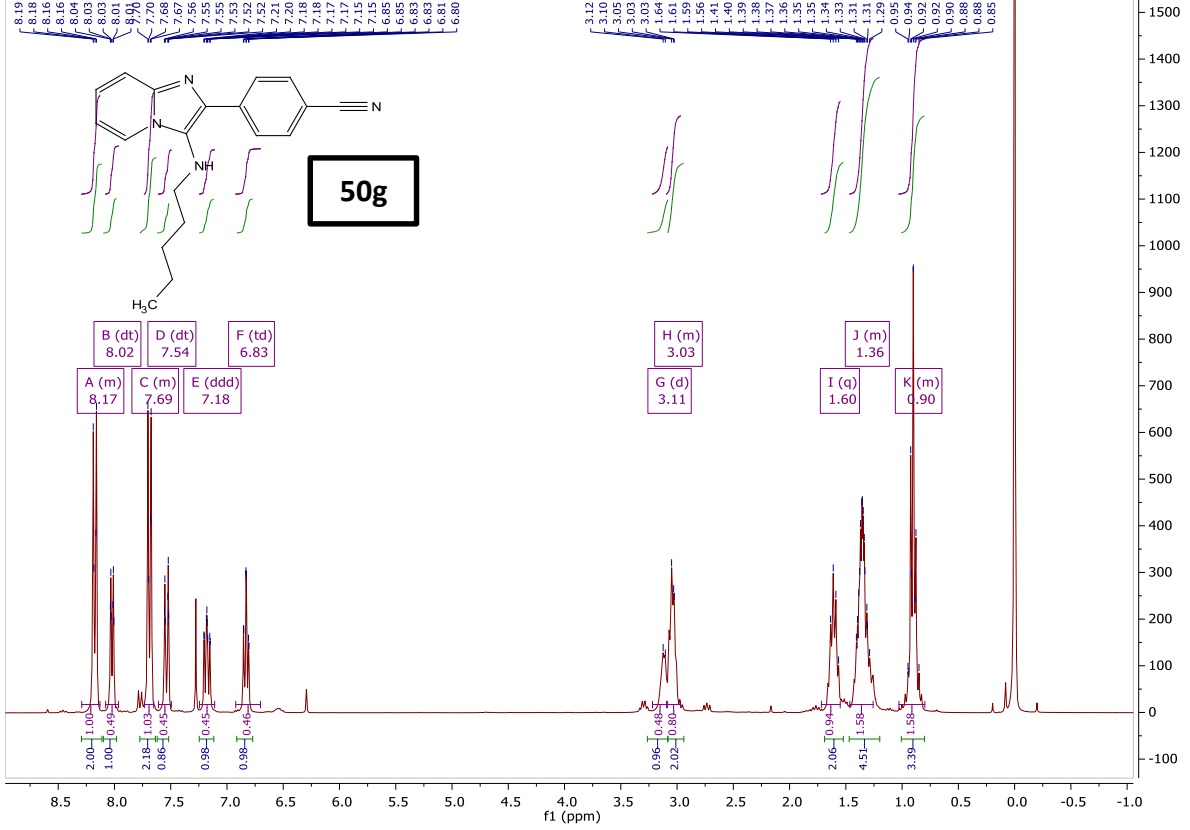
ARM 91.10.fid — Adelaide ARM 91 CDCl₃ 4/11/2019 300K 1H, 13C, COSY, HMBC, HSQC, DEPT135 400MHz DB



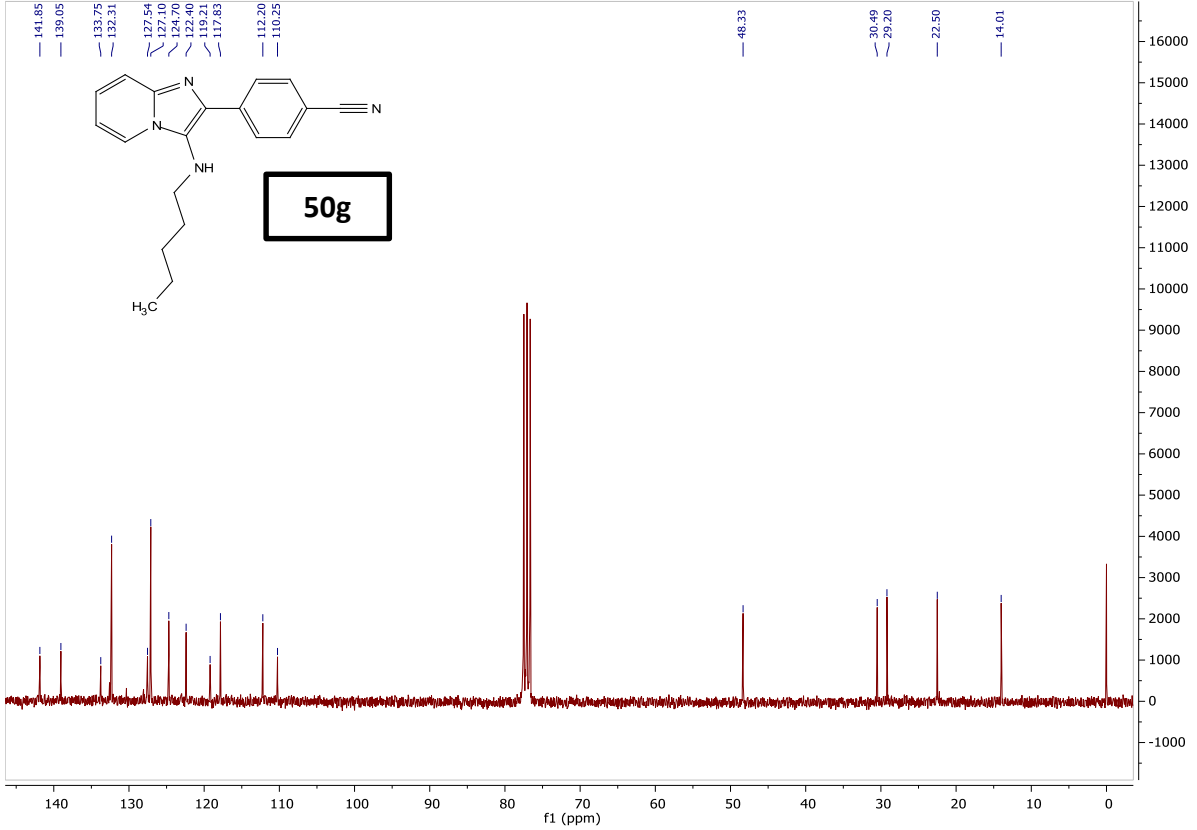
ARM 91.11.fid — Adelaide ARM 91 CDCl₃ 4/11/2019 300K 1H, 13C, COSY, HMBC, HSQC, DEPT135 400MHz DB



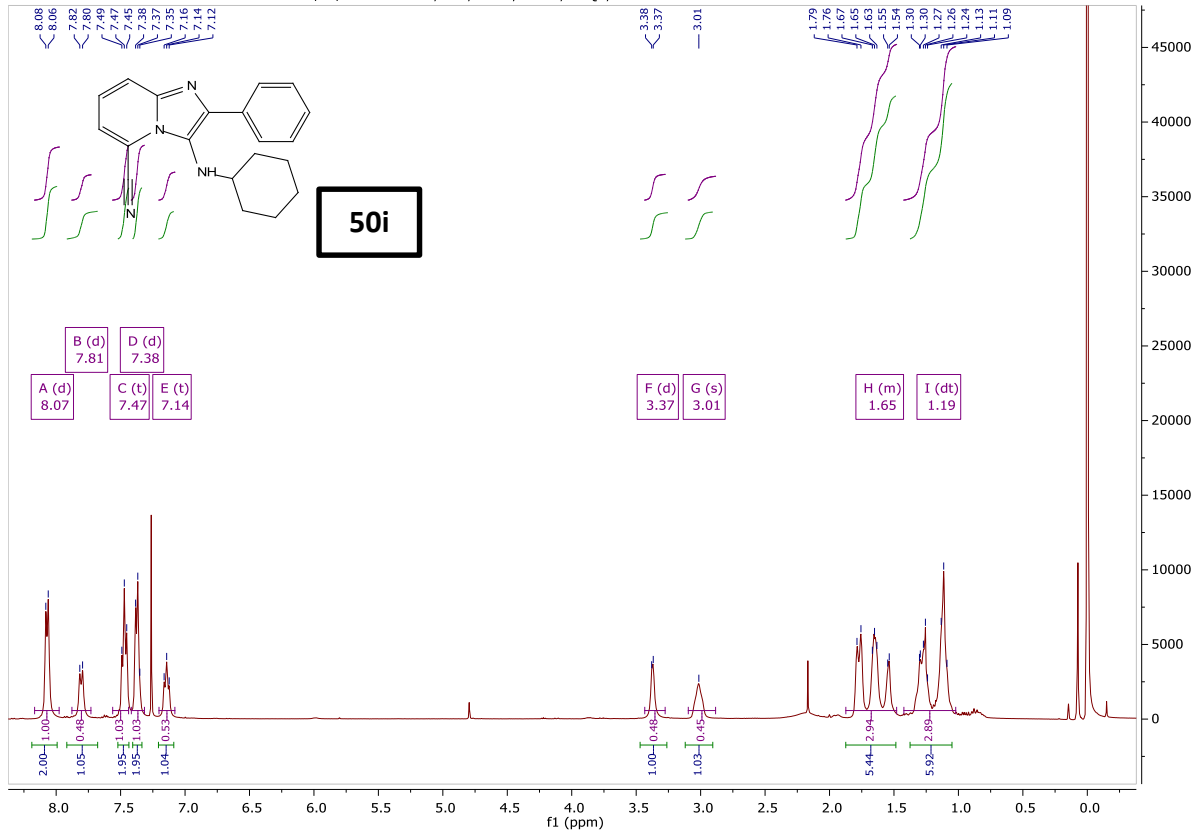
ARM 111.10.fid — Adelaide ARM 111 CDCl3 12/09/2018 H,13C,DEPT,COSY, HSQC, HMBC DB



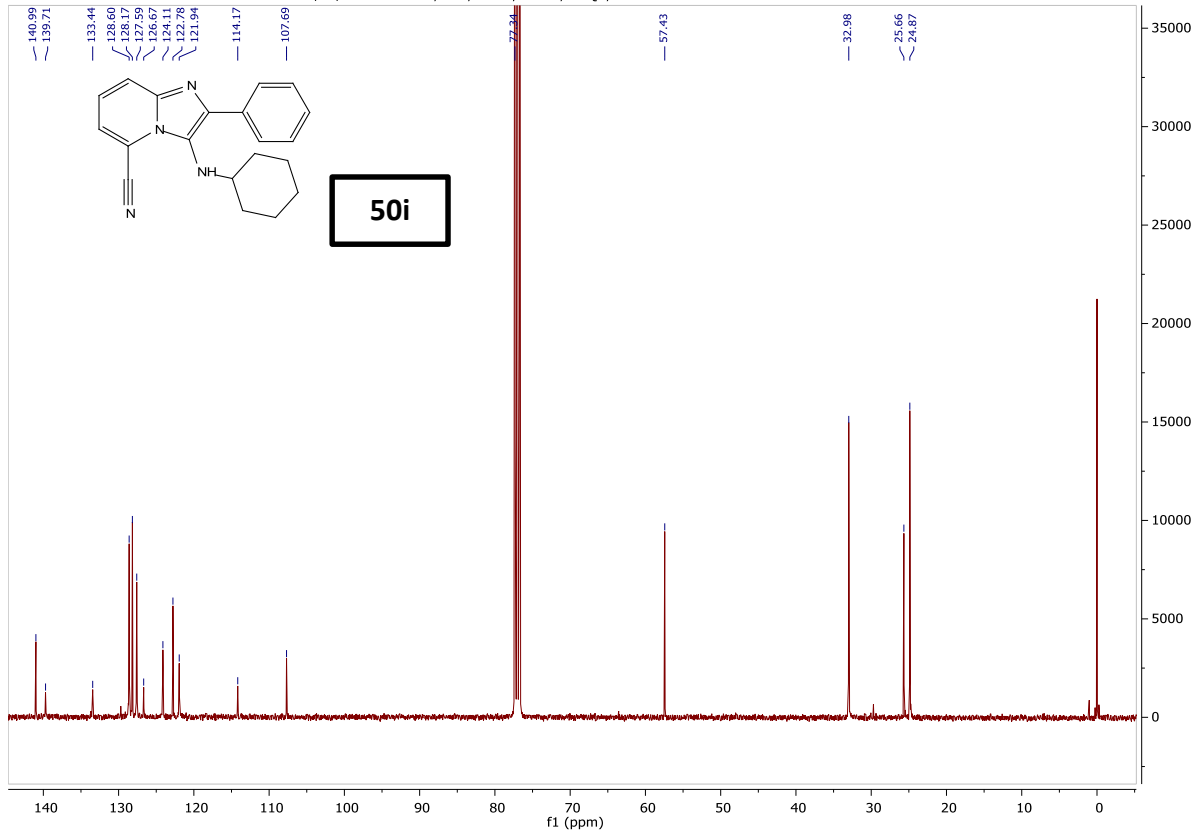
ARM 111.11.fid — Adelaide ARM 111 CDCl3 12/09/2018 H,13C,DEPT,COSY, HSQC, HMBC DB

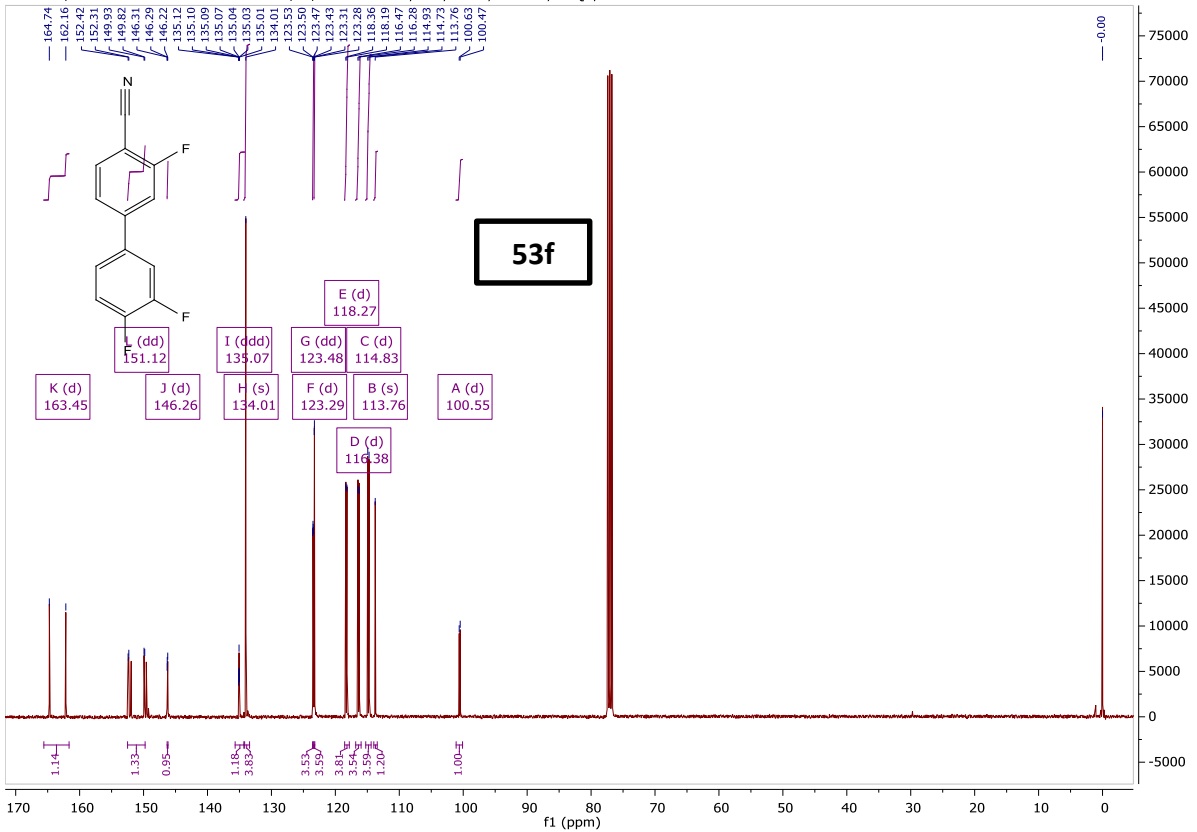
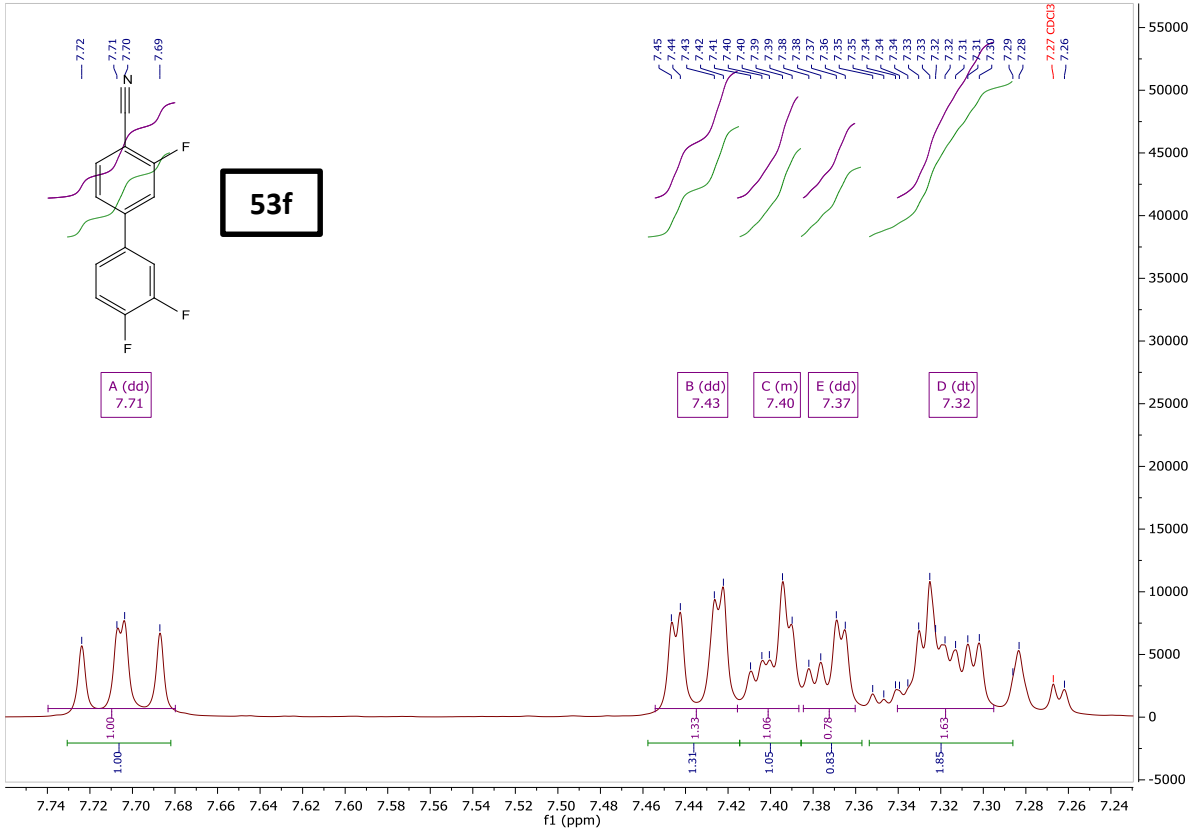


ARM 108.10.fid — Adelaide ARM 108 CDCl3 16/11/2019 300K 1H, 13C, COSY, HMBC, HSQC, DEPT135 400MHz DB

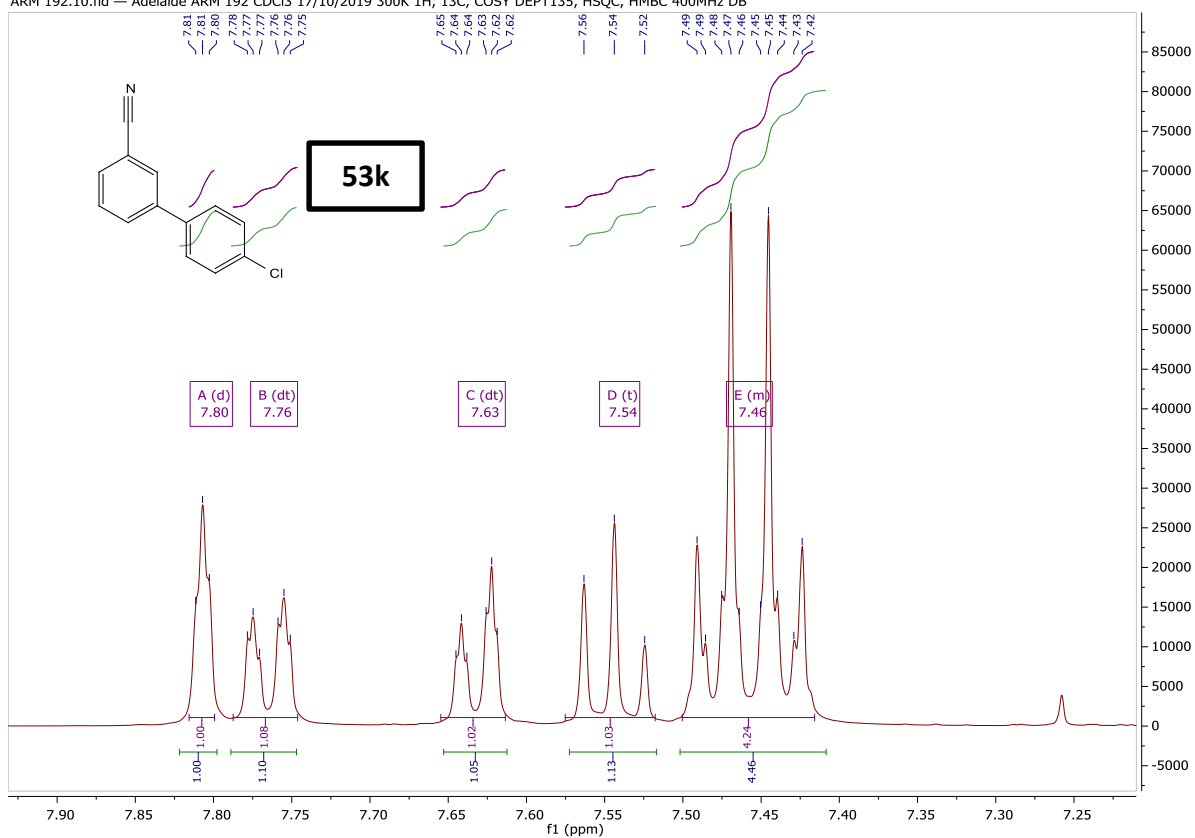


ARM 108.11.fid — Adelaide ARM 108 CDCl3 16/11/2019 300K 1H, 13C, COSY, HMBC, HSQC, DEPT135 400MHz DB

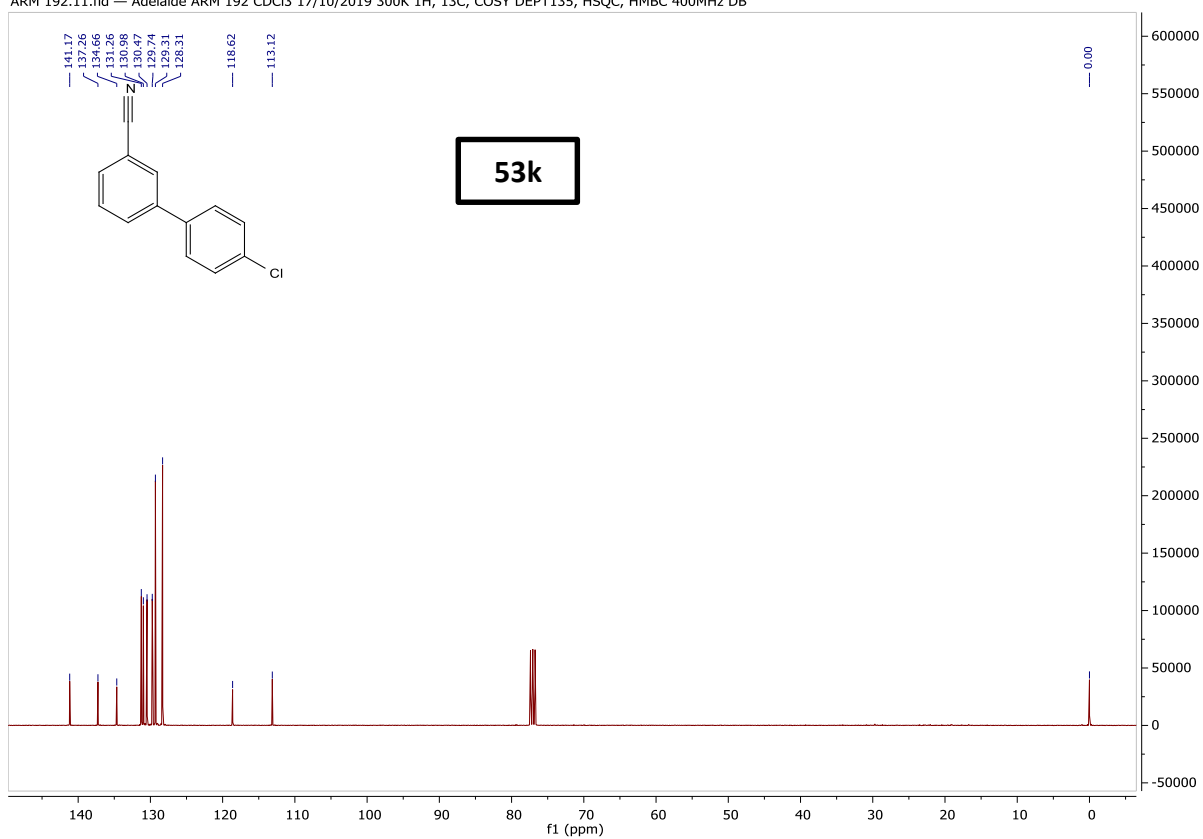


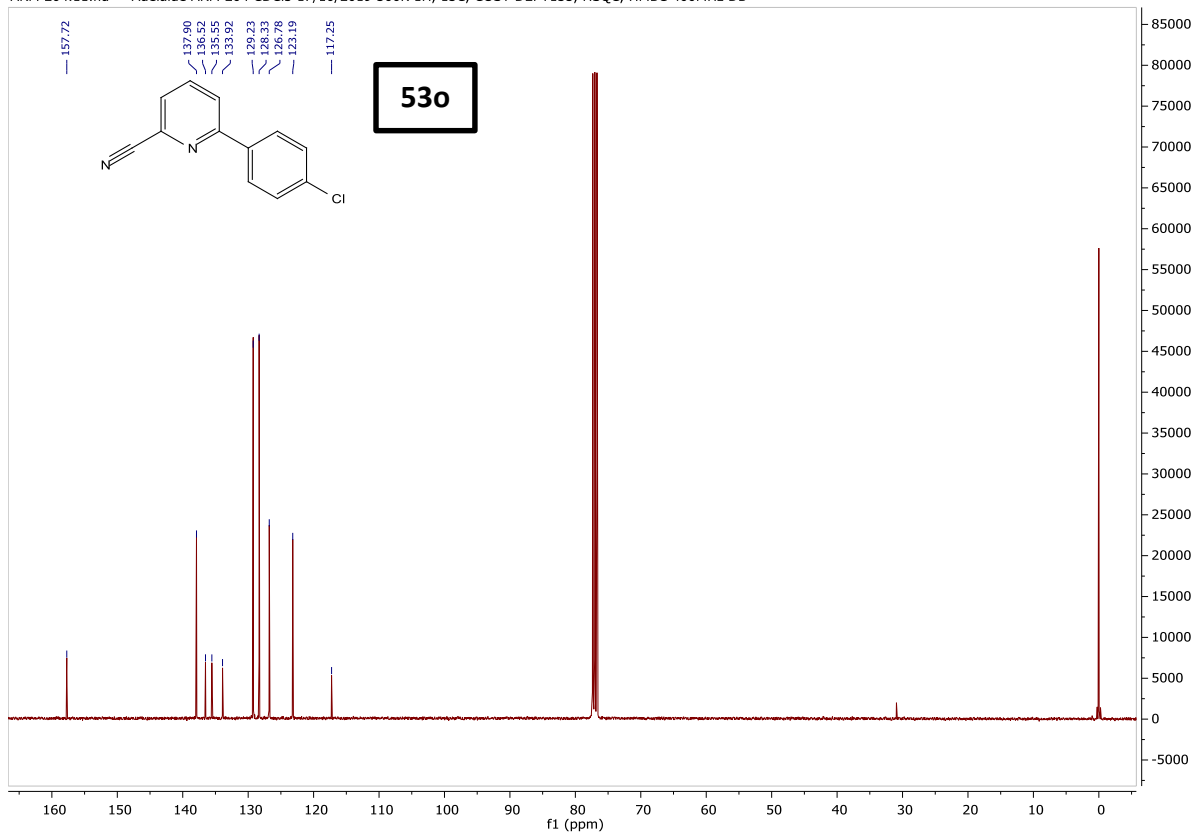
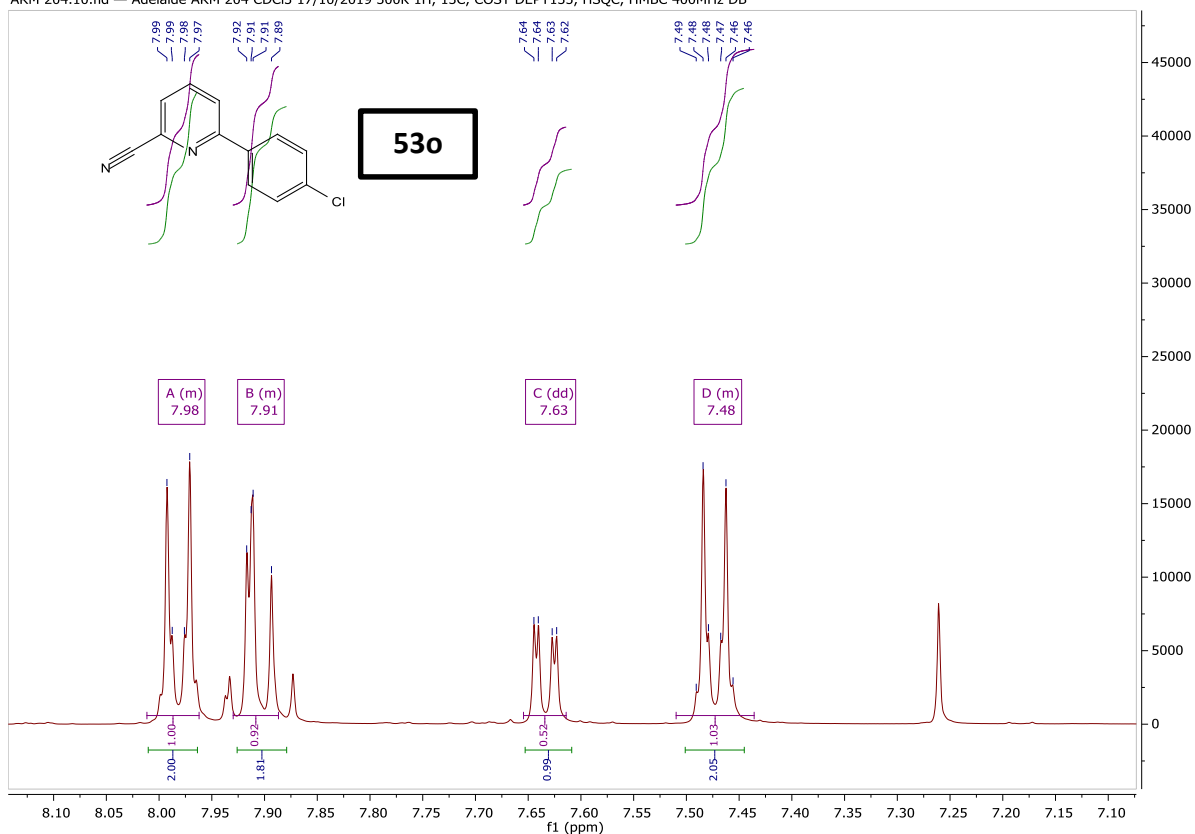


ARM 192.10.fid — Adelaide ARM 192 CDCl3 17/10/2019 300K 1H, 13C, COSY DEPT135, HSQC, HMBC 400MHz DB

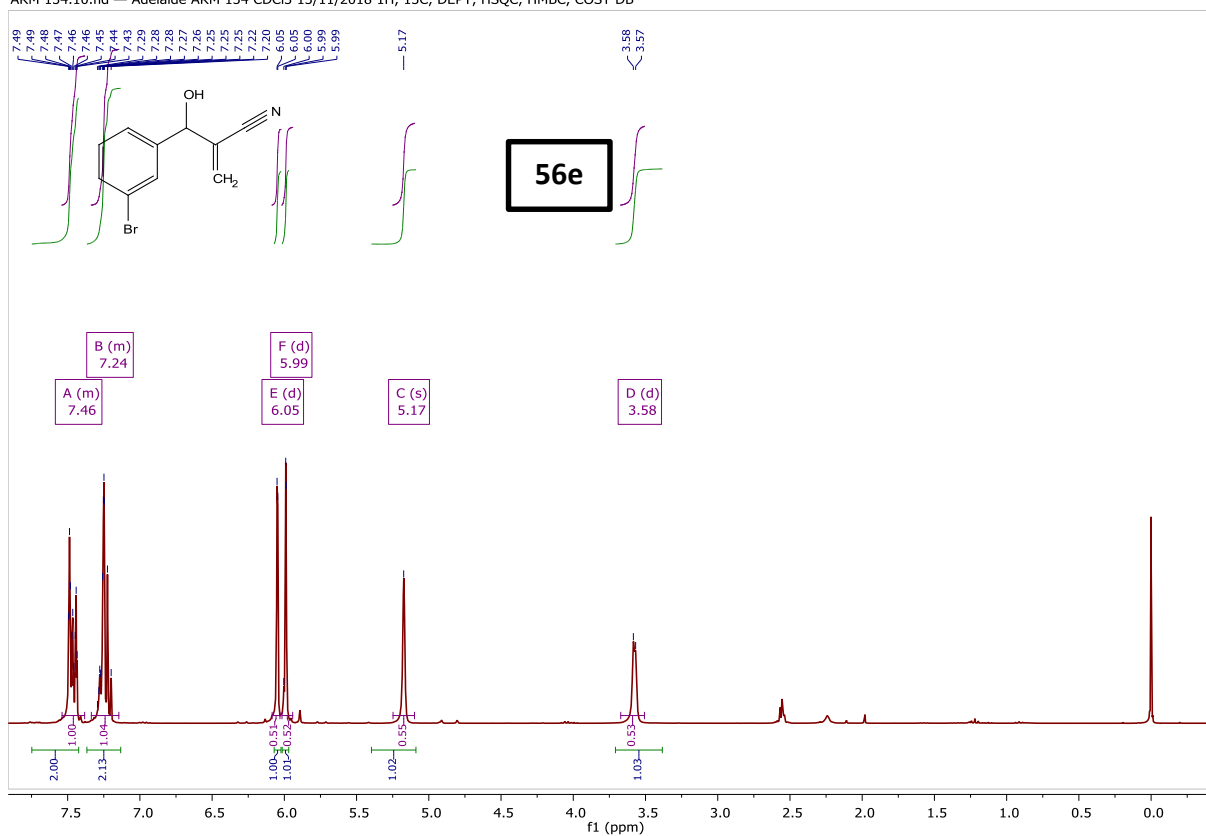


ARM 192.11.fid — Adelaide ARM 192 CDCl3 17/10/2019 300K 1H, 13C, COSY DEPT135, HSQC, HMBC 400MHz DB

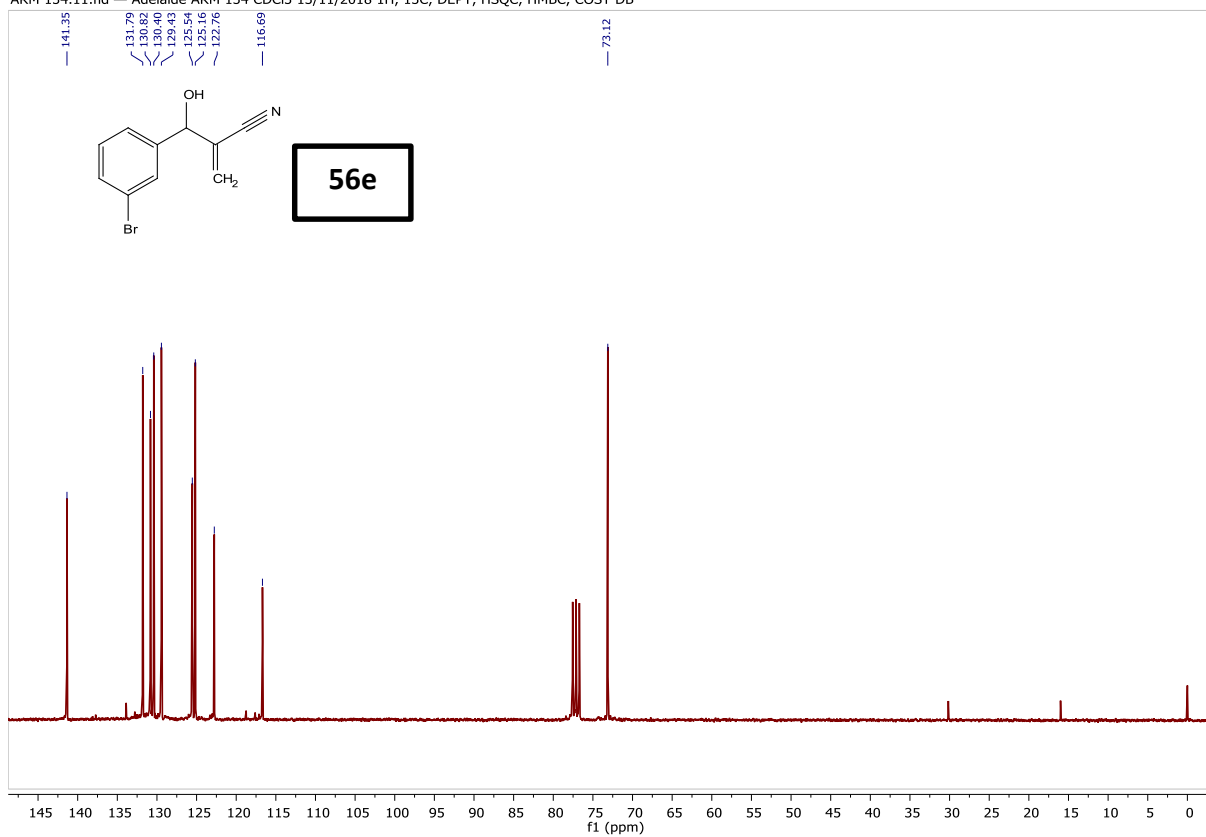




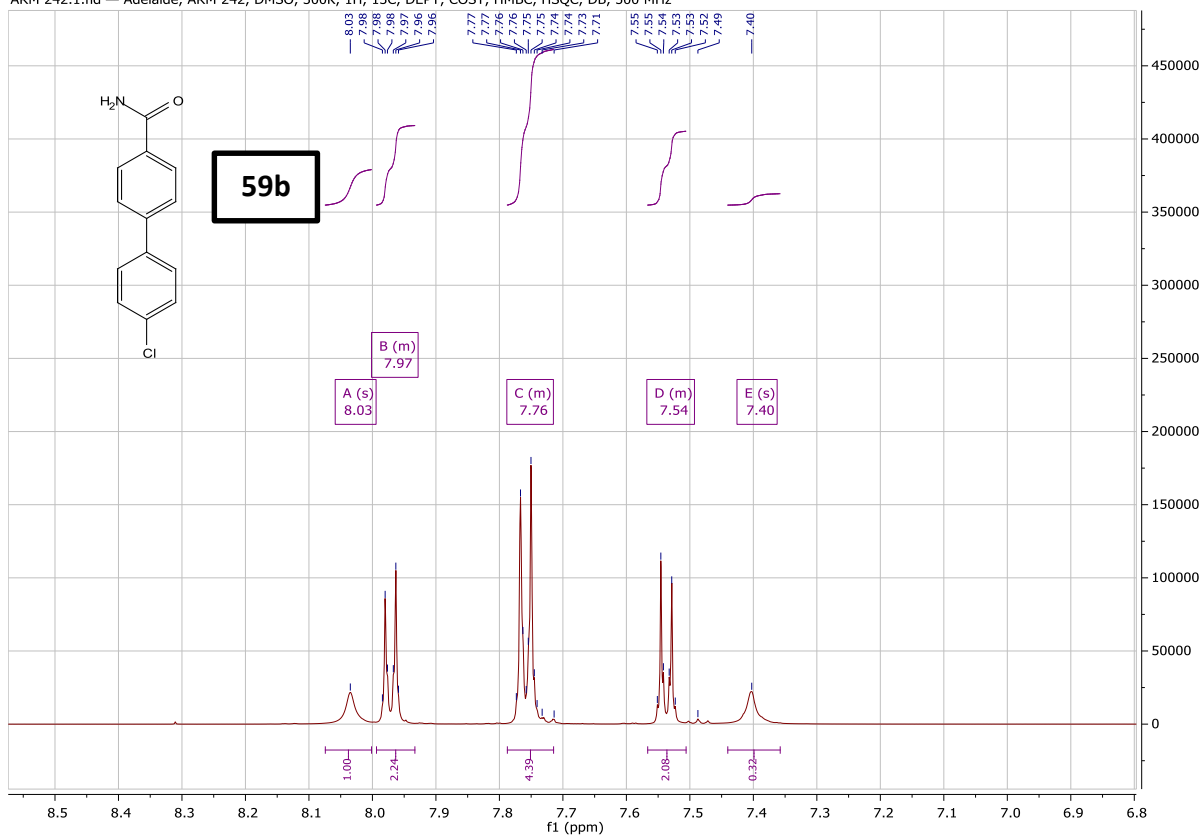
ARM 134.10.fid — Adelaide ARM 134 CDCl3 13/11/2018 1H, 13C, DEPT, HSQC, HMBC, COSY DB



ARM 134.11.fid — Adelaide ARM 134 CDCl3 13/11/2018 1H, 13C, DEPT, HSQC, HMBC, COSY DB



ARM 242.1.fid — Adelaide, ARM 242, DMSO, 300K, 1H, 13C, DEPT, COSY, HMBC, HSQC, DB, 500 MHz



ARM 242.2.fid — Adelaide, ARM 242, DMSO, 300K, 1H, 13C, DEPT, COSY, HMBC, HSQC, DB, 500 MHz

